

**UCLA**

**UCLA Electronic Theses and Dissertations**

**Title**

Targeting transcriptional and post-transcriptional gene regulation in MLL-AF4 leukemia

**Permalink**

<https://escholarship.org/uc/item/85k3694z>

**Author**

Lin, Tasha Lotus

**Publication Date**

2022

Peer reviewed|Thesis/dissertation

UNIVERSITY OF CALIFORNIA  
Los Angeles

Targeting transcriptional and post-transcriptional gene regulation in MLL-AF4 leukemia

A dissertation submitted in partial satisfaction of the requirements for the degree of Doctor of  
Philosophy in Molecular Biology

by

Tasha Lotus Lin

2022

© Copyright by

Tasha Lotus Lin

2022

## ABSTRACT OF THE DISSERTATION

Targeting transcriptional and post-transcriptional gene regulation in MLL-AF4 leukemia

by

Tasha Lotus Lin

Doctor of Philosophy in Molecular Biology

University of California, Los Angeles, 2022

Professor Dinesh Subba Rao, Chair

MLL-rearranged (MLL-r) leukemias are a clinically challenging and biologically unique subtype of leukemias associated with a poor prognosis and are characterized by their MLL-fusion proteins (MLL-FPs) that drive leukemia through epigenetic dysregulation and cooperation with downstream regulatory mechanisms. While novel therapeutic strategies for MLL-rearranged leukemias have been primarily directed at epigenetic dysregulation and concurrent downstream activating mutations or kinases, post-transcriptional gene regulation mechanisms have recently emerged as important mediators in MLL-FP leukemogenesis and have the potential to be potent combinatorial therapeutic targets. Our group has previously identified and studied the RNA binding protein, insulin-like growth factor 2 binding protein 3 (IGF2BP3) as a critical regulator of MLL-AF4 leukemogenesis. The goal of this dissertation is to investigate the mechanisms by which IGF2BP3 supports MLL-AF4 leukemogenesis and to explore its therapeutic potential by investigating combined inhibition of menin-MLL and IGF2BP3 in models of MLL-AF4 driven leukemia, in a novel combinatorial therapeutic strategy of targeting leukemia at the transcriptional and post-transcriptional level.

We studied the combined effects of targeting menin-MLL and IGF2BP3 in MLL-AF4 leukemia using human B-acute lymphoblastic leukemia (B-ALL) cell lines and murine

hematopoietic stem and progenitor (HSPCs) immortalized by MLL-Af4 expression *in vitro* and *in vivo*. In our studies, we harnessed the versatility of these immortalized HSPCs, derived from bone marrow of Cas9-EGFP mice, using their abilities to be readily modified by single-guide RNA introduction and to provide functional readouts on leukemic initiating cell function and number *in vitro* and *in vivo* using endpoint colony formation assays and transplantation. We found that IGF2BP3 knockdown via CRISPR/Cas9-mediated deletion sensitized human B-ALL cells with MLL-AF4 fusion and murine MLL-Af4 HSPCs to treatment with multiple commercially available menin-MLL inhibitors, showing anti-leukemic effects of decreased cell growth and increased apoptosis *in vitro* and negative effects on leukemic initiating cells by decreased colony formation in endpoint colony formation assays *in vitro* and by decreased leukemic engraftment in transplantation experiments *in vivo*. With regards to possible underlying mechanism, detailed evaluation of colony morphologies, histopathology, and RNA sequencing data all showed a consistent shift towards increased differentiation with IGF2BP3 knockdown and menin-MLL inhibition. While additional gene expression analyses and molecular studies are ongoing, we have noted significant overlap in the differentially expressed genes with MI-503 treatment and IGF2BP3 knockdown, in biologically relevant pathways, confirming that IGF2BP3 and MLL-Af4 closely interact and functionally cooperate to regulate gene expression in MLL-AF4 driven leukemia. Lastly, in our *in vivo* MLL-Af4 leukemia model, IGF2BP3 depletion demonstrated a greater effect on increasing survival and delaying leukemia progression than *ex vivo* MI-503 treatment at the chosen micromolar dose, highlighting IGF2BP3 as a potent and promising therapeutic target.

In summary, our studies confirm a role for IGF2BP3 as an oncogenic amplifier of MLL-AF4 driven leukemia, with open questions regarding molecular mechanisms and role in leukemic stem cell function, and highlight its therapeutic potential, while suggest a promising and novel combinatorial approach to targeting leukemia at the transcriptional and post-transcriptional level.

The dissertation of Tasha Lotus Lin is approved.

Douglas L. Black

Gay M. Crooks

Kenneth A. Dorshkind

John M. Timmerman

Dinesh Subba Rao, Committee Chair

University of California, Los Angeles

2022

## DEDICATION

This dissertation is dedicated to my family and patients.

## TABLE OF CONTENTS

ABSTRACT OF THE DISSERTATION.....	ii
DEDICATION.....	v
ACKNOWLEDGEMENTS.....	ix
VITA.....	xii
CHAPTER I.....	1
Introduction: “Transcriptional and Post-Transcriptional Mechanisms of MLL and Their Disruption in MLL-rearranged Leukemias” .....	2
References .....	16
CHAPTER II.....	26
“Combined inhibition of transcriptional and IGF2BP3-driven post-transcriptional gene regulation in MLL-AF4 leukemogenesis” .....	27
Abstract .....	28
Introduction.....	29
Results .....	32
Materials and Methods .....	38
Discussion .....	43
Figures .....	48
Figure Legends .....	60
Supplemental Tables.....	68
References .....	71
CHAPTER III.....	75



Conclusions.....	76
Future Directions.....	79
References.....	85
APPENDICES .....	88
I. “The RNA-binding protein IGF2BP3 is critical for MLL-AF4-mediated leukemogenesis” (reprint ).....	89
II. “Focused CRISPR-Cas9 genetic screening reveals USO1 as a vulnerability in B-cell acute lymphoblastic leukemia” (reprint) .....	102

## FIGURES AND TABLES

### CHAPTER II

Figure 2.1	IGF2BP3 knockdown increases sensitivity of MLL-r leukemia cells to menin-MLL inhibition .....	48
Figure 2.2	Combined IGF2BP3 knockdown and menin inhibition increases differentiation of MLL-Af4 leukemia .....	49
Figure 2.3	Increased upregulation of genes involved in differentiation with IGF2BP3 knockdown and menin-MLL inhibition in MLL-Af4 leukemia .....	50
Figure 2.4	Increased upregulation of genes involved in differentiation with IGF2BP3 knockdown and menin-MLL inhibition in MLL-Af4 leukemia, validated by RT-qPCR.....	52
Figure 2.5	Combinatorial inhibition of menin-MLL and IGF2BP3 decreases leukemic engraftment and burden and increases survival <i>in vivo</i> .....	53
Supplemental Figure 2.1.....		55
Supplemental Figure 2.2.....		56
Supplemental Figure 2.3.....		57
Supplemental Figure 2.4.....		58
Supplemental Figure 2.5.....		59
Supplemental Table 2.1 .....		68
Supplemental Table 2.2.....		69

## ACKNOWLEDGMENTS

First and foremost, I would like to thank my advisor, Dr. Dinesh Rao, for taking me on in his laboratory and supporting me in my development as a physician-scientist. He has served as an inspiration and role model in his brilliance, persistence, and optimism, as an independent investigator and physician-scientist. He has always been honest about the ups and downs of science and research, but forever encouraging me to savor the journey of challenging oneself and the boundaries of scientific and biomedical knowledge and to cherish the exciting moments of new discoveries! He has also been a wonderful clinical colleague, painstakingly reviewing difficult patient cases and diagnostic dilemmas and sharing his insights as an expert hematopathologist.

I also want to thank my thesis committee members, Douglas Black, Gay Crooks, Kenneth Dorshkind, and John Timmerman. They were all incredibly supportive and encouraging throughout my PhD, whether it was asking insightful questions, providing helpful criticism, or sharing equipment and reagents when in a bind! They all pushed me to think and develop as a scientist and have provided practical career advice on how to navigate the ups and downs of academia.

I want to express my gratitude to the STAR program at UCLA and the Division of Hematology and Oncology. I could not have pursued this PhD without their support, both in terms of protected research time and financial support. It is truly a unique opportunity to be able to pursue additional advanced training with and after fellowship. I hope that I have made the best of the opportunity in diving deep into bench research and asking questions with answers that will hopefully translate into a better understanding of hematologic malignancies and novel treatment strategies.

I want to thank the present and former members of the Rao Lab, as well as the Chen Lab. When I first started, I did not even know how to run a gel but was taught and brought up to speed

in molecular biology techniques and flow cytometry by my lab mates with their patience and time. I also greatly appreciate the friendships: being reminded that there is always time for food and boba, even when your experiment is failing!

The work presented in this dissertation was supported by the Hematology Training Grant (NIH T32 5T32HL066992), by the Tumor Immunology Training Grant (2T32CA009120-41A1, 5T32CA009120-42), and the UCLA Specialty Training and Advanced Training Program. Additional support was provided by Research Project Grant (NIH R01CA264986 to Dinesh S. Rao and Jeremy R. Sanford and Small Research Grant (NIH R03CA251854 to Dinesh S. Rao) from the National Institutes of Health.

The work presented in Chapter II is a version of Lin et al “Combined inhibition of transcriptional and IGF2BP3-driven post-transcriptional gene regulation in MLL-AF4 leukemogenesis,” and is currently a manuscript in preparation. The research was completed under the direction of PI Dinesh Rao. I designed the study, performed the experiments, analyzed the data, and wrote the manuscript. Completion of the manuscript was made possible by the experimental contributions from Amit Kumar Jaiswal, Alexander George, Zachary Neeb, Jenna Reppas, Tiffany Tran, and Sol Katzman. Contributions to experimental design, interpretation of the results and preparation of the manuscript were made by Jeremy Sanford and Dinesh Rao.

The works included in the appendices are reprints of Tran et al “The RNA binding IGF2BP3 is critical for MLL-AF4-mediated leukemogenesis” published in *Leukemia* in July 2021 and Jaiswal et al “Focused CRISPR-Cas9 genetic screening reveals USO1 as a vulnerability in B-cell acute lymphoblastic leukemia” published in *Scientific Reports* in June 2021. The authors retain copyright within these open access journals. I contributed to the experimentation, data analysis, and preparation of these manuscripts in Appendices I and II.

Lastly, I want to thank my family and patients for providing the extra motivation and support that I greatly needed when feeling tired or bleak. To Jeff, I thank my lucky stars we met at the NIH

11 years ago and that we have always supported each other in pursuing our careers, even with the sacrifices of long distance and time. To my mom, I thank you for your unconditional love, encouragement, and numerous sacrifices you made without me ever asking or knowing. To my dad, you always told me that your PhD years were the best of your life, even if it meant working 20-hour days or being mistaken for a homeless man in Berkeley. I miss you very much, and it is your memory and your battle with cancer that motivates me to push harder as a scientist and a physician. Your unwavering dedication to your family, pursuit of truth and belief in progress as a scientist, and above all, simple goodness as a person continue to inspire me every day.

VITA  
Tasha Lotus Lin

**EDUCATION**

- 2017 – current      University of California, Los Angeles, Los Angeles, CA  
Ph.D. Candidate in Molecular Biology Interdepartmental Program
- 2008- 2013          University of Michigan Medical School, Ann Arbor, MI  
Doctor of Medicine
- 2004-2008          Stanford University, Stanford, CA  
B.S., Biological Sciences (with distinction and departmental honors)

**PROFESSIONAL EXPERIENCE**

- 2021 – current      Clinical Instructor, Division of Hematology/Oncology  
David Geffen School of Medicine at University of California, Los Angeles
- 2017 – current      Fellow, Specialty Training and Advanced Research Program  
Department of Medicine, University of California, Los Angeles, Los Angeles, CA
- 2016 – 2021          Fellow Physician, Division of Hematology/Oncology  
UCLA Health System, Los Angeles, CA
- 2013 – 2016          Resident Physician, Department of Internal Medicine  
Mayo Clinic, Rochester, MN
- 2011 – 2012          Research Fellow, Clinical Research Training Program  
Pediatric Oncology Branch, National Institutes of Health, Bethesda, MD

**PUBLICATIONS**

1. Meissner GW, Manoli DS, Chavez JF, Knapp JM, **Lin TL**, Mellert DJ, Stevens RJ, Tran DH, Baker BS. Functional dissection of the neural substrates for sexual behaviors in *Drosophila melanogaster*. *Genetics*. 2011 Sep; 189(1): 195-211.
2. Tumaini B, Lee DW, **Lin T**, Castiello L, Stroncek DF, Mackall C, Wayne A, Sabatino M. Simplified process for the production of anti-CD19-CAR-engineered T cells. *Cytotherapy*. 2013 Nov; 15(11): 1406-15.
3. Chinn SB, Spector ME, Bellile EL, Rozek LS, **Lin T**, Teknos TN, Prince ME, Bradford CR, Urba SG, Carey TE, Eisbruch A, Wolf GT, Worden FP, Chepeha DB. Efficacy of induction selection chemotherapy vs primary surgery for patients with advanced oral cavity carcinoma. *JAMA Otolaryngol Head Neck Surg*. 2014 Feb; 140(2): 134-42.

4. Jaiswal AK, Truong H, Tran TM, **Lin TL**, Casero D, Alberti MO, Rao DS. Focused CRISPR-Cas9 genetic screening reveals USO1 as a vulnerability in B-cell acute lymphoblastic leukemia. *Sci Rep*. 2021 Jun 23;11(1):13158.
5. Tran TM, Philipp J, Bassi JS, Nibber N, Draper JM, **Lin TL**, Palanichamy JK, Jaiswal AK, Silva O, Paing M, King J, Katzman S, Sanford JR, Rao DS. The RNA-binding protein IGF2BP3 is critical for MLL-AF4-mediated leukemogenesis. *Leukemia*. 2021 Jul 29.

**CHAPTER I:**

**Introduction:**

“Transcriptional and Post-Transcriptional Mechanisms of MLL and Their Disruption in  
MLL-rearranged Leukemias”



We begin with a brief introduction into leukemias with translocations in the MLL1/KMT2A gene, a subset of leukemias with unique pathologic features and association with poor prognosis. Next, we will discuss how MLL-fusion proteins, resulting from these translocations, drives leukemia through gene dysregulation. Then, we will discuss the emerging evidence for post-transcriptional mechanisms for leukemogenesis, focusing on RNA-based mechanisms, including our group's work on implicating the RNA binding protein insulin-like growth factor 2 binding protein 3 (IGF2BP3) in MLL-Af4 driven leukemia and insights into IGF2BP3's biochemical function as an RNA binding protein. Lastly, we will summarize the current novel therapeutic approaches for treating MLL-rearranged leukemia, as background to our work of exploring the therapeutic potential of targeting IGF2BP3 and post-transcriptional gene dysregulation as a novel approach.

### **MLL-rearranged leukemias**

Leukemia is a clonal, malignant disease of hematopoietic tissues that results from somatic mutations in a primitive hematopoietic progenitor cell and is characterized by accumulation of leukemic blasts in the bone marrow and peripheral blood, resulting in impairment of normal hematopoiesis and leading to life-threatening cytopenias. Leukemias with chromosomal rearrangements of the mixed-lineage leukemia (*MLL*, also known as histone-lysine N-methyltransferase 2A or *KMT2A*) gene represent an important subset of leukemias due to their poor prognosis, lineage infidelity, and unique characteristics that make it a model disease to study transcriptional dysregulation in cancer.

MLL-rearranged leukemias account for more than 70% of leukemias in infants less than 1 year of age and are associated with a relatively poor prognosis with an overall five-year survival rate of approximately 35-50% in infants with MLL-rearranged B-cell acute lymphoblastic leukemia (B-ALL), compared to an overall five-year survival rate of > 85% in all pediatric patients with B-ALL [1-6]. MLL rearrangements are also seen in approximately of 5-10% of adults with acute

leukemia and can be seen in therapy-related leukemias following treatment with topoisomerase II inhibitors, which carry a very poor prognosis [7-10]. These leukemias can present as acute myeloid leukemia (AML), B-ALL, or mixed phenotype acute leukemia (MPAL) with ambiguous lineage and co-expression of myeloid and lymphoid markers. Cases of MPAL, as well as evidence of phenotypic lineage switching following treatment, demonstrate the lineage infidelity seen in MLL-rearranged leukemias, creating a mechanism for relapse and therapeutic challenge [11-14].

## **MLL in Normal Hematopoiesis and MLL-rearranged leukemias**

### *MLL Protein Structure and Function*

Wild-type MLL1 is encoded by the MLL/KMT2A gene located at the 11q23 and is structurally and functionally homologous to the *Drosophila melanogaster* trithorax protein, which serve as important epigenetic regulators of homeotic gene expression in embryonic development [15-17]. The role of MLL1 in embryogenesis and hematopoiesis has been well-studied, establishing MLL1 as essential for proper segment identity and homeotic transformation during embryogenesis, embryonic hematopoietic stem cell development, and maintenance of adult hematopoietic stem and progenitor cells, through regulation of homeobox (HOX) cluster gene expression [18-22].

The structure of the MLL1 protein has been carefully dissected through numerous studies, reviewed, and will be briefly summarized here [23, 24]. The MLL gene encodes a large 3969 amino acid protein that is cleaved post-translationally by taspase-1 into an N-terminal fragment (MLL-N) and C-terminal fragment (MLL-C). MLL-N contains a menin-binding domain, three DNA-binding AT-hook motifs, two speckled nuclear localization signals, SNL1 and SNL2, and two repression domains, RD1 with a CxxC domain and RD2. The middle portion contains four plant homology domains (PHD fingers) that mediate protein-protein interactions, including binding to H3K4me2/3, and a bromodomain that recognizes acetylated lysine residues. MLL-C contains a

transcriptional activation domain and a SET T (Su(var)3-9, enhancer of zeste, trithorax) domain with histone 3 lysine 4 (H3K4) methyltransferase activity and is responsible for Hox gene activation [25].

MLL-N and MLL-C associate with each other as part of a large multiprotein complex that regulates chromatin modification and gene expression, including histone deacetylases and members of the SWI/SNF chromatin remodeling complex, while association with menin helps recruit MLL to the chromatin-binding protein lens epithelium-derived growth factor (LEDGF) and promoters of certain cell-cycle regulatory proteins [26-28]. Interestingly, the chromosomal rearrangements with the MLL gene that result in MLL-fusion proteins typically retain the N-terminal portion, but not the middle or C-terminal portions. Therefore, the association of MLL with menin/LEDGF is thought to be crucial to the function of MLL-fusion proteins, which will be detailed later as an important therapeutic strategy, in addition to the mechanisms of transcriptional activation due to the translocation partner.

#### *Translocations underlying MLL-rearranged leukemia*

Chromosomal rearrangements with the MLL gene have been reported to occur with more than 90 different partners, but only 9 specific partners (AF4, AF9, AF10, ENL, AF10, ELL, PTD, AF6, EPS15) account for more than 90% of these fusions, with AF9 being the most common fusion partner in patients with AML and AF4 in patients with ALL [29]. Multiple fusion partners are nuclear proteins involved in transcriptional elongation, interacting with positive transcription elongation factor b (pTEFb), RNA polymerase II, and the histone 3 lysine 79 (H3K79) methyltransferase DOT1L [30-33]. The recruitment of these proteins involved in transcriptional elongation to MLL fusion proteins is thought to result in increased transcriptional activation and H3K79 methylation of key target genes, including Hox cluster genes, causing the aberrant gene expression underlying leukemogenesis through dysregulation of the normal transcriptional

machinery in hematopoietic cells. We will now focus on one of the most common fusion partners, AF4, as the current model systems in our lab focus on MLL-AF4 leukemia.

### **MLL-AF4 Leukemia**

The MLL-AF4 fusion is the most common fusion protein seen in MLL-rearranged leukemia, occurring in approximately 40-45% of infant and adult MLL-rearranged leukemias [29]. Patients typically present with acute B-cell lymphoblastic leukemia and have a generally poor prognosis, as previously noted [1-6]. The MLL-AF4 protein is the result of an in-frame fusion due to a t(4;11)(q21,q23) translocation. AF4 is a nuclear protein encoded by the *AF4/AFF1* gene and is part of the ALF family proteins that share a region known to confer transcriptional activation activity that is conserved in MLL1 fusions [34]. It has been shown to be a positive regulator of transcription, by interacting with the super elongation complex, pTEFb and DOT1L [26, 30, 32, 35]. The gene expression profile of MLL-AF4 leukemia has been shown to include stem-cell associated genes, including the late *HOXA* cluster genes, *FLT3*, *MEIS1*, *PROM1*, and *RUNX1*, with increased H3K79 methylation and other genes associated with cell cycle progression, apoptosis and cellular transformation, including *MYC* and *BCL2* [36-39]. This unique gene expression program suggests that MLL-AF4 directly activates a hematopoietic stem cell-like transcriptional program found in leukemic stem cells, as well as key oncogenic signaling pathways that are crucial to leukemogenesis [40, 41].

### **Post-transcriptional mechanisms of leukemogenesis**

Much research has been dedicated towards the underlying transcriptional and epigenetic mechanisms that are dysregulated in MLL-rearranged leukemias, as detailed above, given the biology of MLL-fusion proteins. However, post-transcriptional regulation of gene expression through RNA-based mechanisms by various cis- and trans-acting regulatory elements, such as

RNA modifications, microRNAs, long non-coding RNAs, and RNA binding proteins (RBPs), has emerged as an important part of gene regulation underlying development and normal physiologic processes. Growing research has shown that these post-transcriptional mechanisms are dysregulated in cancer and can be hijacked by tumor cells to regulate the fate and function of oncogenic RNA transcripts and their subsequent protein expression, driving oncogenesis, including in leukemias [42-47].

Our group has taken a particular interest in RBPs as there is emerging evidence that aberrant RBP expression and function is associated with acquisition of cancer stem cell phenotypes, which drive aggressive leukemia, resistance to therapy, minimal residual disease, and relapse [47-49]. RBPs have the potential to be powerful mediators of oncogenesis and potent therapeutic targets, as they can regulate multiple targets throughout different post-transcriptional steps, including splicing, polyadenylation, stability, localization, translation, and degradation, thereby causing large-scale disruption of downstream regulatory networks [50, 51]. Our group has been studying the RBP, insulin-like growth factor 2 binding protein 3, over the last several years and its role and function in MLL-AF4 leukemia. Below we will summarize what is known about its role in the pathogenesis of leukemia and its biochemical function as an RBP.

### **The RNA binding protein insulin-like growth factor 2 binding protein 3 in MLL-AF4 leukemia**

Insulin-like growth factor 2 binding protein 3 (IGF2BP3) is an oncofetal RNA binding protein that is part of the IGF2BP family of proteins, a group that has been found to be involved in a number of various cellular functions, primarily in metabolism and development, and to be overexpressed and dysregulated across various cancers [52-55]. This family consists of three structurally and functionally related paralogs, IGF2BP1, IGF2BP2, and IGF2BP3, and were identified as post-transcriptional regulators of the fetal growth factor IGF2 [56]. IGF2BP3 is expressed during embryogenesis and is mostly absent in mature adult tissues, with the exception

of reproductive tissues, although its exact physiologic effects remain difficult to elucidate due to lack of available knockout *in vivo* models. In humans, IGF2BP3 has been found to be expressed at higher levels in fetal hematopoietic progenitors compared to their adult counterparts and is needed to maintain the molecular and phenotypic features of fetal type cells [57]. Overexpression of IGF2BP3 have been found in multiple solid tumors, first in pancreatic cancer, and hematologic malignancies and has been correlated with more aggressive disease and poor prognosis [58-60].

Our group has previously identified and reported the overexpression of IGF2BP3 in MLL-rearranged B-ALL and showed that enforced expression of IGF2BP3 increased cell proliferation *in vitro* and *in vivo* and led to a pathologic expansion of hematopoietic stem and progenitor cells in a murine hematopoietic system, with features similar to those seen early in leukemogenesis [61]. Furthermore, our group found that MLL-Af4 transcriptionally induces IGF2BP3 and tested the requirement of IGF2BP3 in a bona-fide model of MLL-Af4 leukemogenesis and found that it was required for the efficient initiation of MLL-Af4 leukemia *in vivo*, using a murine knockout for IGF2BP3 (I3KO/MLL-Af4). I3KO/MLL-Af4 mice were found to have increased latency of leukemia and survival and decreased leukemic burden [62]. Further characterization of I3KO/MLL-Af4 leukemia cells showed decrease in leukemic initiating cell number (LIC), as defined as CD11b+c-kit+ cells, and functionally, decreased reconstitution in secondary transplants, consistent with reduction in the effective number of LICs [62]. Altogether, these results strongly implicate IGF2BP3 in the pathogenesis of MLL-Af4 leukemia.

With regards to IGF2BP3's biochemical function as an RNA binding protein, IGF2BP3 has been found to regulate RNA stability and alternative splicing, but the exact molecular mechanisms of these processes are of great interest and are still being investigated. Huang et al identified IGF2BP3 and other members of the IGF2BP family as readers of N<sup>6</sup>-methyladenosine (m<sup>6</sup>A) modified RNAs that promote the stability, and therefore, expression of their target mRNAs, including oncogenic transcripts such as *MYC* [63]. Direct targets of IGF2BP3 were found to be

enriched for m<sup>6</sup>A modifications, with loss of binding upon knockdown of METTL14, an enzyme that catalyzes N<sup>6</sup>-adenosine methylation [63]. IGF2BP3 was found to stabilize its mRNA targets in an m<sup>6</sup>A-dependent manner, with accelerated mRNA decay seen in high-confidence IGF2BP3 targets in HepG2 cells knocked down for IGF2BP3, METTL3 or METTL14 [63].

Multiple groups, including ours, have contributed to findings that suggest that IGF2BP3 has a complex interaction with the microRNA machinery and RNA-induced silencing complex (RISC), providing another underlying mechanism for its role in RNA stability, in addition to RNA modifications as noted above [61, 64, 65]. In Jonson et al, IGF2BP3 was found to act as a potential safehouse against let-7 microRNA-mediated decay of oncogenic mRNAs, *HMGA2* and *LIN28B*, by segregating these transcripts and other let-7 targets in cytoplasm RNP granules that do not contain RISC [64]. In Palanichamy et al, our group observed that in human B-ALL cell lines, REH and RS4;11, IGF2BP3 binding sites on target mRNAs, including oncogenic transcripts such as *MYC* and *CDK6*, were enriched at the 3'UTR near microRNA binding sites [61]. In Ennajdaoui et al, another group observed a similar pattern in the position of IGF2BP3 binding sites at the 3'UTR of target transcripts in pancreatic cancer cell lines, PANC1 and PL45 [65]. Their work also found that IGF2BP3 may modulate the association between RISC and its target transcripts to support oncogenesis. IGF2BP3-dependent changes in mRNA expression were inversely correlated with Ago2-mRNA association, suggesting that IGF2BP3 may interact with RISC to protect target transcripts from microRNA-mediated decay [65]. These targets included *HMGA2*, a known oncogene in human leukemia. The convergence of binding sites of RBPs and microRNAs at the 3'UTR of these target oncogenic mRNAs strongly suggest a shared physical and regulatory interaction among IGF2BP3, RISC, and microRNAs, but additional work remains to determine the exact biochemical and molecular actions of these combinatorial mechanisms of post-transcriptional gene regulation.

Lastly, our group implicated a possible role for IGF2BP3 in alternative splicing, a known mechanism of RBP function in biological processes including leukemogenesis [66, 67]. In Tran et al, IGF2BP3 binding sites were found in intronic regions and the 3' splice-sites of its target transcripts, in addition to within the 3'UTR, in bulk leukemic CD11b+ cells from MLL-Af4 mice and MLL-Af4 transformed hematopoietic stem and progenitors cells (abbreviated as Lin-) [62]. Using Mixture of Isoforms Bayesian inference model (MISO) analysis of RNA-sequencing data from WT or *Igf2bp3* KO CD11b+ or Lin- cells, we identified hundreds of transcripts with IGF2BP3-dependent changes in alternative splicing, which were found to have significant overlap with IGF2BP3 binding sites [62]. These results provide indirect evidence that IGF2BP3 may also regulate leukemogenesis through alternative splicing, but additional work is needed to test this hypothesis and elucidate its molecular mechanisms.

### **Treatments for MLL-rearranged leukemias**

Therapy for MLL-rearranged leukemias typically consists of the standard-of-care treatments based on the type of leukemia, acute myeloid leukemia (AML) or acute lymphoblastic leukemia (ALL), and presence of other molecular or cytogenetic features that can be targeted, such as presence of BCR-ABL rearrangement, or mutations in FLT3 or IDH1/2. Broadly, treatment options include combination chemotherapy, targeted agents against known concurrent activating mutations, molecular features or signaling pathways known to be important in the disease pathogenesis, such as FLT3 inhibitors, IDH1/2 inhibitors, and BCL-2 inhibitors, hematopoietic stem cell transplantation, and immune-based therapies directed against B-cell antigens, CD19 and CD20, in B-acute lymphoblastic leukemia. Standard-of-care treatment options have also grown to include targeted therapy against epigenetic mechanisms, including DNA methylation and histone acetylation, with hypomethylating agents and histone deacetylase inhibitors, respectively and are used widely in the treatment of hematologic malignancies. Targeting



epigenetic dysregulation in MLL-rearranged leukemias has been an area of great interest, given increased understanding of how MLL-fusion proteins associate and function with epigenetic modifiers, as detailed earlier. Novel treatment approaches for MLL-rearranged leukemias have been directed at targeting these MLL-fusion proteins and their known associated epigenetic network, which we will review below.

#### *DOT1L inhibitors*

Disruptor of telomeric silencing 1-like (DOT1L), a histone 3 lysine 79 methyltransferase has been shown to be necessary for MLL fusion-mediated leukemogenesis in a number of experimental models and has been explored as a potential therapeutic target in MLL-rearranged leukemias [68-73]. Several small molecule inhibitors against DOT1L have been developed, including EPZ-5676 (pinometostat) and EPZ0004777, and have shown promising pre-clinical activity with downregulation of MLL target genes, tumor regression, and prolonged survival in animal models for MLL-rearranged leukemia [73-75]. However, in a phase 1 clinical study of EPZ-5676, modest single-agent activity was seen, and ongoing pre-clinical and clinical studies are exploring combinatorial approaches that may potentiate the effect of DOT1L inhibition in MLL-rearranged leukemias [74, 76].

#### *Bromodomain inhibitors*

Bromodomain-containing proteins are a family of chromatin adaptor proteins that recognize and bind to N-acetylated lysines on histones and have been found to regulate the transcription of important cancer-related genes in MLL-rearranged leukemia. For example, BRD4, a member of the bromodomain and extra terminal (BET) family of proteins, was found to interact with polymerase-associated factor complex (PAFc), the super elongation complex, and MLL-fusion proteins and was identified as a possible target in MLL-rearranged leukemia [77]. Treatment with the bromodomain inhibitor I-BET151 displaced BRD4 and led to downregulation of important oncogenic transcripts *BCL2*, *CDK6* and *MYC* and anti-leukemic effects *in vitro* and

*in vivo* in MLL-r leukemia models [77]. Another member of the BET family, BRD9, is part of the SWI/SNF chromatin remodeling complex and was found to be important for sustaining MYC expression in a number of MLL-rearranged leukemia cell lines [78]. Small molecule inhibition of BRD9 with BI-7273 led to inhibition of cell growth and induction of cell differentiation in MLL-AF9 AML cells through downregulation of *MYC* [78].

#### *Menin-MLL inhibitors*

Menin is a protein encoded by the *MEN1* gene and was first characterized as a tumor suppressor, as germline mutations in the *MEN1* gene were found to result in multiple endocrine neoplasia 1, a syndrome in which patients develop tumors of the endocrine glands. However, in MLL-rearranged leukemias, it has been found to interact with the N-terminal end of MLL-fusion proteins and is essential for leukemogenesis in MLL-rearranged leukemias [79-81]. While its mechanism of action is not fully understood either in solid tumors or leukemias, it is known to act as a molecular adaptor that interacts with epigenetic regulators and cell signaling molecules [82]. Identification of the MLL binding pocket on menin led to the development of small molecule inhibitors, targeting this menin-MLL interaction that is known to be essential for MLL-fusion protein leukemogenesis [83]. Pharmacologic inhibition of the menin-MLL interaction has been found to be an effective in multiple pre-clinical models of MLL-rearranged leukemia, as well as NPM1c mutated leukemia, in which there is an upregulation of *HOXA* and *MEIS1* expression, genes known to be important in leukemogenesis, including self-renewal and maintenance of leukemic stem cells [84-86].

Borkin et al reported the discovery and activity of MI-503, MI-463, and MI-538 and showed that menin-MLL inhibition downregulated expression of MLL-fusion targets, including *HOXA9* and *MEIS1*, increased differentiation of leukemic blasts as shown by increased CD11b and decreased c-kit expression, and prolonged survival in mouse models of MLL-rearranged leukemia [84]. Krivstov et al reported the discovery and activity of VTP50469, a highly selective and orally

bioavailable small molecule inhibitor, which induced loss of MLL binding at a specific subset of genes and was found to have anti-leukemic effects with prolonged survival in patient-derived xenograft (PDX) models of MLL-rearranged AML and ALL [86]. Klossowski et al used the structure of MI-503 as a starting point to develop new analogs with increased inhibitory activity and improved drug-like properties and reported the discovery and activity of MI-3454 as a highly potent inhibitor with subnanomolar activity in PDX models of MLL-rearranged and NPM1 mutant AML [85]. VTP50469 and MI-3454 have been developed into clinical grade compounds, as SNDX-613 and KO-539 respectively, and have entered clinical trials for patients with relapsed/refractory acute leukemias with MLL gene rearrangement or NPM1 mutation.

#### *Combined therapeutic strategies against MLL-rearranged leukemias*

While the development of these novel therapeutic approaches is exciting, combinatorial strategies remain a cornerstone of cancer therapy to combat mechanisms of relapse and resistance that cancer cells exploit to maintain their survival. Menin-MLL inhibitors are the newest class of drugs to enter clinical trials with promising pre-clinical data for treatment of MLL-rearranged leukemias and AML with NPM1c mutation. Of note, while AML with NPM1c mutation is not characterized by MLL-rearrangements, it is a frequent genetic abnormality in AML seen in about 20-30% of patients [87, 88]. Kuhn et al showed that NPM1-mutant AML has a leukemogenic expression program similar to those seen in MLL-r leukemias, with overexpression of HOX, MEIS1, FLT3 and PBX and a dependency on the menin-MLL interaction for growth based on experiments using CRISPR/Cas9 deletion and pharmacologic inhibition of menin-MLL1 [89].

Two phase 1 clinical trials, AUGMENT-101 and KOMET-001, are currently evaluating the safety and efficacy of the menin-MLL inhibitors, SNDX-5613 and KO-539, respectively. Data from the AUGMENT-101 trial reported in April 2020 at the American Association Cancer Research Annual Meeting included 3 patients with MLL-rearranged leukemia, with 2 achieving a response

(complete response and partial response with incomplete count recovery), while the third had no response and progressive disease [90]. Data from the KOMET-001 trial reported in December 2020 at the American Society of Hematology Annual Meeting included 12 patients (8 evaluable for response) with relapsed/refractory AML. One patient with MLL-r leukemia had stabilization of peripheral blood counts, while two heavily pre-treated patients with NPM1-mutated AML achieved a complete response [91, 92]. These early results demonstrate clinical activity in patients who were heavily pre-treated but suggest room for improvement and need for combination therapy given limited response rates. We will review the specific combinatorial strategies that have been reported in MLL-rearranged leukemias, as we aim to highlight the novelty of our approach in targeting transcriptional and post-transcriptional gene regulation in MLL-rearranged leukemia.

Several combination strategies with DOT1L inhibitors for the treatment of MLL-rearranged leukemia have been investigated and are likely needed given modest single agent activity seen in clinical trials [93]. SIRT1, an NAD<sup>+</sup>-dependent deacetylase, in a genome-wide RNA interference screen, was identified as necessary for establishing a heterochromatin-like state after DOT1L inhibition [94]. SRT1720, a potent activator of SIRT1, was found to synergize with EPZ004777, a DOT1L inhibitor and enhance anti-proliferative activity against MLL-r leukemia cells [94]. DOT1L and BRD4, which had both been previously found to be important transcriptional activators in MLL-FP leukemogenesis, were found to cooperate functionally to regulate transcription of a subset of genes near super enhancers that are important for maintaining MLL-FP leukemia [95]. Combined targeting of DOT1L and BRD4 using SGC0946 and I-BET respectively led to synergistic efficacy against human MV4;11 cells and primary patient samples with MLL-rearranged AML [95]. Dafflon et al performed an shRNA sensitizer screen in DOT1L inhibitor treated cells and identified that the MLL gene itself or known components of MLL-fusion complexes were most enriched in their dropout screen [96]. Combined inhibition DOT1L and menin-MLL using EPZ004777 and MI 2-2, respectively, was tested and showed enhanced

downregulation of known MLL-FP targets, *HOXA9*, *MEIS1*, *MYC*, and *CDK6* and anti-proliferative effects in human MLL-rearranged leukemia cell lines *in vitro*, as well as decreased leukemogenic potential *in vitro* and *ex vivo* in MLL-AF9 transformed mouse cells, compared to either inhibitor alone [96].

In addition to combination treatment with DOT1L inhibitors as described above, inhibition of menin-MLL has been rationally combined with multiple other targets, including FLT3 inhibitors (for leukemia with concurrent FLT3 mutation) [97], BCL-2 inhibitors [98, 99], and CDK6 inhibitors [99], and most recently, against IKAROS [100], in the treatment of MLL-rearranged leukemia and AML with NPM1c mutation. Fiskus et al observed in menin KO AML MOLM13 cells a reduction in MEIS1, FLT3, HOXA9, CDK6, and BCL2 expression, prompting them to see if menin depletion would sensitize these cells to treatment with the BCL2 inhibitor venetoclax or CDK6 inhibitor abemaciclib. Menin was depleted using multiple methods including CRISPR/Cas9-mediated knockout, dTAG-13-induced degradation, and treatment with menin-MLL inhibitors, SNDX-50469 and SNDX-5613. Co-treatment with SNDX-50469 and venetoclax or abemaciclib showed enhanced killing effects compared to single-agent treatment in human-cultured and patient-derived AML cells expressing MLL-r or NPM1-mutant *in vitro*. Co-treatment with SNDX-5613 and venetoclax *in vivo* showed decreased leukemic burden and increased survival in cell line and patient-derived AML xenografts *in vivo*, compared to single inhibition. And most recently, Aubrey et al used a genome-wide CRISPR/Cas9-based functional genomic screen to look for potential resistance mechanisms and synthetic lethal interactions in MLL-r AML MOLM 13 cells treated with DOT1L or menin-inhibitors (with VTP-50469 and EPZ-5676, respectively) [100]. While they identified IKZF1 (IKAROS), MTA2, and HOAX10 as synthetic lethal targets, they further characterized the chromatin co-occupancy and shared protein-protein interactions between IKAROS and MENIN and demonstrated synergistic effects with combined targeting of IKAROS and MENIN, given readily available drugs that induce IKAROS protein degradation [100]. Their

findings suggest that IKAROS, a known critical transcription factor and regulator in various processes throughout normal hematopoiesis, functionally cooperates with MENIN to regulate gene expression in MLL-r AML and is a potent combinatorial therapeutic target in combination with menin-MLL inhibition [100].

In summary, while there has been a lot of work characterizing the underlying mechanisms of leukemogenesis in MLL-rearranged leukemia, including how MLL-FPs drive leukemia through interaction with epigenetic cofactors, causing dysregulation of key transcriptional networks and aberrant gene expression in hematopoietic stem and progenitor cells, post-transcriptional gene regulation mechanisms are emerging to be equally important players that mediate and potentially amplify this transcriptional dysregulation upstream. We have demonstrated this paradigm in the characterization of the role and function of the RNA binding protein IGF2BP3 in MLL-AF4 mediated leukemogenesis, as a transcriptional target of MLL-AF4 and critical regulator of MLL-Af4-mediated leukemogenesis, and have suggested potential molecular mechanisms, including enhancing RNA stability and affecting alternative splicing, of key MLL-AF4 and IGF2BP3 targets. The work in this dissertation investigates the combined targeting of MLL-AF4 and IGF2BP3 through chemical and genetic inhibition with menin-MLL inhibitor treatment and CRISPR/Cas9-mediated depletion of IGF2BP3 and its effects on leukemic growth, differentiation, and gene expression. This work aims to further develop IGF2BP3 as a potential therapeutic target, introduce a novel therapeutic approach of targeting transcriptional and post-transcriptional gene regulation, and further explore the mechanisms by which IGF2BP3 and MLL-AF4 interact to dysregulate gene expression in leukemia.

## References

1. Chen, C.S., et al., *Molecular rearrangements on chromosome 11q23 predominate in infant acute lymphoblastic leukemia and are associated with specific biologic variables and poor outcome*. Blood, 1993. **81**(9): p. 2386-93.
2. Biondi, A., et al., *Biological and therapeutic aspects of infant leukemia*. Blood, 2000. **96**(1): p. 24-33.
3. Hunger, S.P., et al., *Improved survival for children and adolescents with acute lymphoblastic leukemia between 1990 and 2005: a report from the children's oncology group*. J Clin Oncol, 2012. **30**(14): p. 1663-9.
4. Nguyen, K., et al., *Factors influencing survival after relapse from acute lymphoblastic leukemia: a Children's Oncology Group study*. Leukemia, 2008. **22**(12): p. 2142-50.
5. Rheingold, S.R., et al., *Prognostic factors for survival after relapsed acute lymphoblastic leukemia (ALL): A Children's Oncology Group (COG) study*. Journal of Clinical Oncology, 2019. **37**(15\_suppl): p. 10008-10008.
6. Pui, C.H., et al., *Treating childhood acute lymphoblastic leukemia without cranial irradiation*. N Engl J Med, 2009. **360**(26): p. 2730-41.
7. Muntean, A.G. and J.L. Hess, *The pathogenesis of mixed-lineage leukemia*. Annu Rev Pathol, 2012. **7**: p. 283-301.
8. Blanco, J.G., et al., *Molecular emergence of acute myeloid leukemia during treatment for acute lymphoblastic leukemia*. Proc Natl Acad Sci U S A, 2001. **98**(18): p. 10338-43.
9. Super, H.J., et al., *Rearrangements of the MLL gene in therapy-related acute myeloid leukemia in patients previously treated with agents targeting DNA-topoisomerase II*. Blood, 1993. **82**(12): p. 3705-11.
10. Felix, C.A., et al., *ALL-1 gene rearrangements in DNA topoisomerase II inhibitor-related leukemia in children*. Blood, 1995. **85**(11): p. 3250-6.

11. Mirro, J., et al., *Acute mixed lineage leukemia: clinicopathologic correlations and prognostic significance*. Blood, 1985. **66**(5): p. 1115-23.
12. Stass, S., et al., *Lineage switch in acute leukemia*. Blood, 1984. **64**(3): p. 701-6.
13. Rayes, A., R.L. McMasters, and M.M. O'Brien, *Lineage Switch in MLL-Rearranged Infant Leukemia Following CD19-Directed Therapy*. Pediatr Blood Cancer, 2016. **63**(6): p. 1113-5.
14. Gardner, R., et al., *Acquisition of a CD19-negative myeloid phenotype allows immune escape of MLL-rearranged B-ALL from CD19 CAR-T-cell therapy*. Blood, 2016. **127**(20): p. 2406-10.
15. Kassis, J.A., J.A. Kennison, and J.W. Tamkun, *Polycomb and Trithorax Group Genes in Drosophila*. Genetics, 2017. **206**(4): p. 1699-1725.
16. Schuettengruber, B., et al., *Genome Regulation by Polycomb and Trithorax: 70 Years and Counting*. Cell, 2017. **171**(1): p. 34-57.
17. Tkachuk, D.C., S. Kohler, and M.L. Cleary, *Involvement of a homolog of Drosophila trithorax by 11q23 chromosomal translocations in acute leukemias*. Cell, 1992. **71**(4): p. 691-700.
18. Yu, B.D., et al., *Altered Hox expression and segmental identity in Mll-mutant mice*. Nature, 1995. **378**(6556): p. 505-8.
19. Hess, J.L., et al., *Defects in yolk sac hematopoiesis in Mll-null embryos*. Blood, 1997. **90**(5): p. 1799-806.
20. Yagi, H., et al., *Growth disturbance in fetal liver hematopoiesis of Mll-mutant mice*. Blood, 1998. **92**(1): p. 108-17.
21. Ernst, P., et al., *Definitive hematopoiesis requires the mixed-lineage leukemia gene*. Dev Cell, 2004. **6**(3): p. 437-43.



22. Jude, C.D., et al., *Unique and independent roles for MLL in adult hematopoietic stem cells and progenitors*. Cell Stem Cell, 2007. **1**(3): p. 324-37.
23. Winters, A.C. and K.M. Bernt, *MLL-Rearranged Leukemias-An Update on Science and Clinical Approaches*. Front Pediatr, 2017. **5**: p. 4.
24. Chan, A.K.N. and C.W. Chen, *Rewiring the Epigenetic Networks in MLL-Rearranged Leukemias: Epigenetic Dysregulation and Pharmacological Interventions*. Front Cell Dev Biol, 2019. **7**: p. 81.
25. Milne, T.A., et al., *MLL targets SET domain methyltransferase activity to Hox gene promoters*. Mol Cell, 2002. **10**(5): p. 1107-17.
26. Nakamura, T., et al., *ALL-1 is a histone methyltransferase that assembles a supercomplex of proteins involved in transcriptional regulation*. Mol Cell, 2002. **10**(5): p. 1119-28.
27. Hughes, C.M., et al., *Menin associates with a trithorax family histone methyltransferase complex and with the hoxc8 locus*. Mol Cell, 2004. **13**(4): p. 587-97.
28. Milne, T.A., et al., *Menin and MLL cooperatively regulate expression of cyclin-dependent kinase inhibitors*. Proc Natl Acad Sci U S A, 2005. **102**(3): p. 749-54.
29. Meyer, C., et al., *The MLL recombinome of acute leukemias in 2013*. Leukemia, 2013. **27**(11): p. 2165-76.
30. Luo, Z., C. Lin, and A. Shilatifard, *The super elongation complex (SEC) family in transcriptional control*. Nat Rev Mol Cell Biol, 2012. **13**(9): p. 543-7.
31. Cucinotta, C.E. and K.M. Arndt, *SnapShot: Transcription Elongation*. Cell, 2016. **166**(4): p. 1058-1058 e1.
32. Mueller, D., et al., *A role for the MLL fusion partner ENL in transcriptional elongation and chromatin modification*. Blood, 2007. **110**(13): p. 4445-54.

33. Biswas, D., et al., *Function of leukemogenic mixed lineage leukemia 1 (MLL) fusion proteins through distinct partner protein complexes*. Proc Natl Acad Sci U S A, 2011. **108**(38): p. 15751-6.
34. Prasad, R., et al., *Domains with transcriptional regulatory activity within the ALL1 and AF4 proteins involved in acute leukemia*. Proc Natl Acad Sci U S A, 1995. **92**(26): p. 12160-4.
35. Lin, C., et al., *AFF4, a component of the ELL/P-TEFb elongation complex and a shared subunit of MLL chimeras, can link transcription elongation to leukemia*. Mol Cell, 2010. **37**(3): p. 429-37.
36. Benito, J.M., et al., *MLL-Rearranged Acute Lymphoblastic Leukemias Activate BCL-2 through H3K79 Methylation and Are Sensitive to the BCL-2-Specific Antagonist ABT-199*. Cell Rep, 2015. **13**(12): p. 2715-27.
37. Wilkinson, A.C., et al., *RUNX1 is a key target in t(4;11) leukemias that contributes to gene activation through an AF4-MLL complex interaction*. Cell Rep, 2013. **3**(1): p. 116-27.
38. Guenther, M.G., et al., *Global and Hox-specific roles for the MLL1 methyltransferase*. Proc Natl Acad Sci U S A, 2005. **102**(24): p. 8603-8.
39. Gaussmann, A., et al., *Combined effects of the two reciprocal t(4;11) fusion proteins MLL.AF4 and AF4.MLL confer resistance to apoptosis, cell cycling capacity and growth transformation*. Oncogene, 2007. **26**(23): p. 3352-63.
40. Barabe, F., et al., *Modeling human MLL-AF9 translocated acute myeloid leukemia from single donors reveals RET as a potential therapeutic target*. Leukemia, 2017. **31**(5): p. 1166-1176.
41. Krivtsov, A.V., et al., *Transformation from committed progenitor to leukaemia stem cell initiated by MLL-AF9*. Nature, 2006. **442**(7104): p. 818-22.
42. Peng, Y. and C.M. Croce, *The role of MicroRNAs in human cancer*. Signal Transduct Target Ther, 2016. **1**: p. 15004.

43. Bhan, A., M. Soleimani, and S.S. Mandal, *Long Noncoding RNA and Cancer: A New Paradigm*. *Cancer Res*, 2017. **77**(15): p. 3965-3981.
44. Pereira, B., M. Billaud, and R. Almeida, *RNA-Binding Proteins in Cancer: Old Players and New Actors*. *Trends Cancer*, 2017. **3**(7): p. 506-528.
45. Barbieri, I. and T. Kouzarides, *Role of RNA modifications in cancer*. *Nat Rev Cancer*, 2020. **20**(6): p. 303-322.
46. Hodson, D.J., M. Screen, and M. Turner, *RNA-binding proteins in hematopoiesis and hematological malignancy*. *Blood*, 2019. **133**(22): p. 2365-2373.
47. Elcheva, I.A. and V.S. Spiegelman, *Targeting RNA-binding proteins in acute and chronic leukemia*. *Leukemia*, 2021. **35**(2): p. 360-376.
48. Park, S.M., et al., *Musashi2 sustains the mixed-lineage leukemia-driven stem cell regulatory program*. *J Clin Invest*, 2015. **125**(3): p. 1286-98.
49. Elcheva, I.A., et al., *RNA-binding protein IGF2BP1 maintains leukemia stem cell properties by regulating HOXB4, MYB, and ALDH1A1*. *Leukemia*, 2020. **34**(5): p. 1354-1363.
50. Glisovic, T., et al., *RNA-binding proteins and post-transcriptional gene regulation*. *FEBS Lett*, 2008. **582**(14): p. 1977-86.
51. Lukong, K.E., et al., *RNA-binding proteins in human genetic disease*. *Trends Genet*, 2008. **24**(8): p. 416-25.
52. Yaniv, K. and J.K. Yisraeli, *The involvement of a conserved family of RNA binding proteins in embryonic development and carcinogenesis*. *Gene*, 2002. **287**(1-2): p. 49-54.
53. Bell, J.L., et al., *Insulin-like growth factor 2 mRNA-binding proteins (IGF2BPs): post-transcriptional drivers of cancer progression?* *Cell Mol Life Sci*, 2013. **70**(15): p. 2657-75.

54. Degrauwe, N., et al., *IMPs: an RNA-binding protein family that provides a link between stem cell maintenance in normal development and cancer*. *Genes Dev*, 2016. **30**(22): p. 2459-2474.
55. Dai, N., *The Diverse Functions of IMP2/IGF2BP2 in Metabolism*. *Trends Endocrinol Metab*, 2020. **31**(9): p. 670-679.
56. Nielsen, J., et al., *A family of insulin-like growth factor II mRNA-binding proteins represses translation in late development*. *Mol Cell Biol*, 1999. **19**(2): p. 1262-70.
57. Elagib, K.E., et al., *Neonatal expression of RNA-binding protein IGF2BP3 regulates the human fetal-adult megakaryocyte transition*. *J Clin Invest*, 2017. **127**(6): p. 2365-2377.
58. Lederer, M., et al., *The role of the oncofetal IGF2 mRNA-binding protein 3 (IGF2BP3) in cancer*. *Semin Cancer Biol*, 2014. **29**: p. 3-12.
59. Mancarella, C. and K. Scotlandi, *IGF2BP3 From Physiology to Cancer: Novel Discoveries, Unsolved Issues, and Future Perspectives*. *Front Cell Dev Biol*, 2019. **7**: p. 363.
60. Kapoor, S., *IMP3: a new and important biomarker of systemic malignancies*. *Clin Cancer Res*, 2008. **14**(17): p. 5640; author reply 5640-1.
61. Palanichamy, J.K., et al., *RNA-binding protein IGF2BP3 targeting of oncogenic transcripts promotes hematopoietic progenitor proliferation*. *J Clin Invest*, 2016. **126**(4): p. 1495-511.
62. Tran, T.M., et al., *The RNA-binding protein IGF2BP3 is critical for MLL-AF4-mediated leukemogenesis*. *Leukemia*, 2022. **36**(1): p. 68-79.
63. Huang, H., et al., *Recognition of RNA N(6)-methyladenosine by IGF2BP proteins enhances mRNA stability and translation*. *Nat Cell Biol*, 2018. **20**(3): p. 285-295.
64. Jonson, L., et al., *IMP3 RNP safe houses prevent miRNA-directed HMGA2 mRNA decay in cancer and development*. *Cell Rep*, 2014. **7**(2): p. 539-551.
65. Ennajdaoui, H., et al., *IGF2BP3 Modulates the Interaction of Invasion-Associated Transcripts with RISC*. *Cell Rep*, 2016. **15**(9): p. 1876-83.

66. Wang, E., et al., *Targeting an RNA-Binding Protein Network in Acute Myeloid Leukemia*. *Cancer Cell*, 2019. **35**(3): p. 369-384 e7.
67. Itskovich, S.S., et al., *MBNL1 regulates essential alternative RNA splicing patterns in MLL-rearranged leukemia*. *Nat Commun*, 2020. **11**(1): p. 2369.
68. Okada, Y., et al., *hDOT1L links histone methylation to leukemogenesis*. *Cell*, 2005. **121**(2): p. 167-78.
69. Chang, M.J., et al., *Histone H3 lysine 79 methyltransferase Dot1 is required for immortalization by MLL oncogenes*. *Cancer Res*, 2010. **70**(24): p. 10234-42.
70. Jo, S.Y., et al., *Requirement for Dot1l in murine postnatal hematopoiesis and leukemogenesis by MLL translocation*. *Blood*, 2011. **117**(18): p. 4759-68.
71. Bernt, K.M., et al., *MLL-rearranged leukemia is dependent on aberrant H3K79 methylation by DOT1L*. *Cancer Cell*, 2011. **20**(1): p. 66-78.
72. Nguyen, A.T., et al., *DOT1L, the H3K79 methyltransferase, is required for MLL-AF9-mediated leukemogenesis*. *Blood*, 2011. **117**(25): p. 6912-22.
73. Deshpande, A.J., et al., *Leukemic transformation by the MLL-AF6 fusion oncogene requires the H3K79 methyltransferase Dot1l*. *Blood*, 2013. **121**(13): p. 2533-41.
74. Daigle, S.R., et al., *Potent inhibition of DOT1L as treatment of MLL-fusion leukemia*. *Blood*, 2013. **122**(6): p. 1017-25.
75. Chen, L., et al., *Abrogation of MLL-AF10 and CALM-AF10-mediated transformation through genetic inactivation or pharmacological inhibition of the H3K79 methyltransferase Dot1l*. *Leukemia*, 2013. **27**(4): p. 813-22.
76. Klaus, C.R., et al., *DOT1L inhibitor EPZ-5676 displays synergistic antiproliferative activity in combination with standard of care drugs and hypomethylating agents in MLL-rearranged leukemia cells*. *J Pharmacol Exp Ther*, 2014. **350**(3): p. 646-56.

77. Dawson, M.A., et al., *Inhibition of BET recruitment to chromatin as an effective treatment for MLL-fusion leukaemia*. Nature, 2011. **478**(7370): p. 529-33.
78. Hohmann, A.F., et al., *Sensitivity and engineered resistance of myeloid leukemia cells to BRD9 inhibition*. Nat Chem Biol, 2016. **12**(9): p. 672-9.
79. Yokoyama, A., et al., *The menin tumor suppressor protein is an essential oncogenic cofactor for MLL-associated leukemogenesis*. Cell, 2005. **123**(2): p. 207-18.
80. Chen, Y.X., et al., *The tumor suppressor menin regulates hematopoiesis and myeloid transformation by influencing Hox gene expression*. Proc Natl Acad Sci U S A, 2006. **103**(4): p. 1018-23.
81. Caslini, C., et al., *Interaction of MLL amino terminal sequences with menin is required for transformation*. Cancer Res, 2007. **67**(15): p. 7275-83.
82. Matkar, S., A. Thiel, and X. Hua, *Menin: a scaffold protein that controls gene expression and cell signaling*. Trends Biochem Sci, 2013. **38**(8): p. 394-402.
83. Grembecka, J., et al., *Menin-MLL inhibitors reverse oncogenic activity of MLL fusion proteins in leukemia*. Nat Chem Biol, 2012. **8**(3): p. 277-84.
84. Borkin, D., et al., *Pharmacologic inhibition of the Menin-MLL interaction blocks progression of MLL leukemia in vivo*. Cancer Cell, 2015. **27**(4): p. 589-602.
85. Klossowski, S., et al., *Menin inhibitor MI-3454 induces remission in MLL1-rearranged and NPM1-mutated models of leukemia*. J Clin Invest, 2020. **130**(2): p. 981-997.
86. Krivtsov, A.V., et al., *A Menin-MLL Inhibitor Induces Specific Chromatin Changes and Eradicates Disease in Models of MLL-Rearranged Leukemia*. Cancer Cell, 2019. **36**(6): p. 660-673 e11.
87. Tyner, J.W., et al., *Functional genomic landscape of acute myeloid leukaemia*. Nature, 2018. **562**(7728): p. 526-531.

88. Papaemmanuil, E., et al., *Genomic Classification and Prognosis in Acute Myeloid Leukemia*. N Engl J Med, 2016. **374**(23): p. 2209-2221.
89. Kuhn, M.W., et al., *Targeting Chromatin Regulators Inhibits Leukemogenic Gene Expression in NPM1 Mutant Leukemia*. Cancer Discov, 2016. **6**(10): p. 1166-1181.
90. McGeehan, J. *A first-in-class Menin-MLL1 antagonist for the treatment of MLL-r and NPM1 mutant leukemias*. in *111th Annual Meeting of the American Association for Cancer Research*. 2020.
91. Wang, E.S., et al., *Preliminary Data on a Phase 1/2A First in Human Study of the Menin-KMT2A (MLL) Inhibitor KO-539 in Patients with Relapsed or Refractory Acute Myeloid Leukemia*. Blood, 2020. **136**.
92. Issa, G.C., et al., *Therapeutic implications of menin inhibition in acute leukemias*. Leukemia, 2021. **35**(9): p. 2482-2495.
93. Stein, E.M., et al., *The DOT1L inhibitor pinometostat reduces H3K79 methylation and has modest clinical activity in adult acute leukemia*. Blood, 2018. **131**(24): p. 2661-2669.
94. Chen, C.W., et al., *DOT1L inhibits SIRT1-mediated epigenetic silencing to maintain leukemic gene expression in MLL-rearranged leukemia*. Nat Med, 2015. **21**(4): p. 335-43.
95. Gilan, O., et al., *Functional interdependence of BRD4 and DOT1L in MLL leukemia*. Nat Struct Mol Biol, 2016. **23**(7): p. 673-81.
96. Dafflon, C., et al., *Complementary activities of DOT1L and Menin inhibitors in MLL-rearranged leukemia*. Leukemia, 2017. **31**(6): p. 1269-1277.
97. Dzama, M.M., et al., *Synergistic targeting of FLT3 mutations in AML via combined menin-MLL and FLT3 inhibition*. Blood, 2020. **136**(21): p. 2442-2456.
98. Carter, B.Z., et al., *Menin inhibition decreases Bcl-2 and synergizes with venetoclax in NPM1/FLT3-mutated AML*. Blood, 2021. **138**(17): p. 1637-1641.

99. Fiskus, W., et al., *Effective Menin inhibitor-based combinations against AML with MLL rearrangement or NPM1 mutation (NPM1c)*. Blood Cancer J, 2022. **12**(1): p. 5.
100. Aubrey, B.J., et al., *IKAROS and MENIN coordinate therapeutically actionable leukemogenic gene expression in MLL-r acute myeloid leukemia*. Nat Cancer, 2022. **3**(5): p. 595-613.



## **CHAPTER II:**

“Combined inhibition of transcriptional and IGF2BP3-driven post-transcriptional gene regulation  
in MLL-AF4 leukemogenesis”

**Combined inhibition of transcriptional and IGF2BP3-driven post-transcriptional gene regulation in MLL-AF4 leukemogenesis**

Tasha L. Lin<sup>1</sup>, Amit K. Jaiswal<sup>2</sup>, Alexander J. George<sup>3</sup>, Jenna Reppas<sup>1,2</sup>, Tiffany M. Tran<sup>1,2</sup>, Zachary Neeb<sup>3</sup>, Sol Katzman<sup>4</sup>, Jeremy R. Sanford<sup>3</sup>, Dinesh S. Rao<sup>2,5,6</sup>

<sup>1</sup>*Department of Medicine, University of California Los Angeles, Los Angeles, CA, USA.*

<sup>2</sup>*Department of Pathology and Laboratory Medicine, University of California, Los Angeles, Los Angeles, CA, USA.*

<sup>3</sup>*Department of Molecular, Cell and Developmental Biology and Center for Molecular Biology of RNA, University of California, Santa Cruz, Santa Cruz, CA, USA.*

<sup>4</sup>*Center for Biomolecular Science & Engineering, University of California, Santa Cruz, Santa Cruz, CA.*

<sup>5</sup>*Jonsson Comprehensive Cancer Center, University of California Los Angeles, Los Angeles, CA, USA .*

<sup>6</sup>*Broad Stem Cell Research Center, University of California Los Angeles, Los Angeles, CA, USA.*

**Corresponding Author:**

Dinesh S. Rao, M.D., Ph.D.

Associate Professor

Department of Pathology and Laboratory Medicine

David Geffen School of Medicine at UCLA

650 Charles E Young Drive, 12-272 Factor

Los Angeles, CA 90095

Tel. 310-825-1675

Fax. 310-825-0814

Email [drao@mednet.ucla.edu](mailto:drao@mednet.ucla.edu)

## Abstract

RNA binding proteins are emerging as a novel class of therapeutic targets in cancer, including in leukemia, given their important role in post-transcriptional gene regulation, and have the unexplored potential to be combined with existing therapies. The RNA binding protein insulin-like growth factor 2 binding protein 3 (IGF2BP3) has been found to be a critical regulator of MLL-AF4 leukemogenesis and represents a promising therapeutic target. Here, we study the combined effects of targeting IGF2BP3 and the menin-MLL interaction in MLL-AF4 driven leukemia *in vitro* and *in vivo*, using genetic inhibition with CRISPR-Cas9 mediated deletion of *Igf2bp3* and pharmacologic inhibition of the menin-MLL interaction with multiple commercially available inhibitors. Depletion of *Igf2bp3* sensitized MLL-AF4 leukemia to the effects of menin-MLL inhibition on cell growth and leukemic initiating cells *in vitro*. Mechanistically, we found that both *Igf2bp3* depletion and menin-MLL inhibition led to increased differentiation *in vitro* and *in vivo*, seen in functional readouts and by gene expression analyses. IGF2BP3 knockdown had a greater effect on increasing survival and attenuating disease than pharmacologic menin-MLL inhibition with MI-503 alone and showed enhanced anti-leukemic effects in combination. Our work shows that IGF2BP3 is an oncogenic amplifier of MLL-AF4 mediated leukemogenesis and is a potent therapeutic target and provides a paradigm for targeting leukemia at both the transcriptional and post-transcriptional level.

## Introduction

Leukemias driven by translocations in the mixed-lineage leukemia 1 gene (*MLL1/KMT2A*) represent a subgroup of particular interest due to their unique clinical and biological characteristics and poor prognosis. *MLL1* is a H3K4 histone methyltransferase that mediates the expression of critical homeobox (*HOX*) cluster genes in normal hematopoietic stem and progenitor cells (HSPCs) and is necessary for definitive hematopoiesis [1, 2]. Chromosomal rearrangements in the *MLL1* gene result in fusion proteins, with several partners that are part of the super elongation complex, leading to aberrant gene expression [3-5]. Comprehensive genomic studies of patient-derived *MLL*-rearranged leukemia cells show that these leukemias have very few genetic alterations [6, 7], suggesting that epigenetic dysregulation driven by the fusion proteins are largely responsible for leukemogenesis. This is further borne out by demonstration of the sufficiency of *MLL* fusion protein overexpression, e.g., *MLL-AF9* and *MLL-Af4*, to drive leukemia in both murine and human HSPCs [8-10]. Critical features to *MLL*-fusion protein leukemogenesis include the interaction of the N-terminal end of the *MLL*-fusion with menin, a molecular adaptor protein that interacts with epigenetic regulators and cell signaling molecules, in addition to its interactions with downstream chromatin modifiers such as disruptor of telomeric silencing 1-like (*DOT1L*) and the super elongation complex [11-13].

However, in recent years, the importance of post-transcriptional regulation of gene expression by factors such as microRNAs and RNA binding proteins (RBPs) has been increasingly appreciated. Our group implicated the oncofetal RBP insulin like growth factor 2 mRNA binding protein 3 (*IGF2BP3*) as a critical regulator of *MLL-AF4*-mediated leukemogenesis [14, 15]. We found that *MLL-AF4* transcriptionally induced *IGF2BP3* and that *IGF2BP3* targets and regulates important leukemogenic transcripts, amplifying the aberrant gene expression initiated by *MLL-AF4* [15]. Further, *IGF2BP3* is required for the efficient initiation of *MLL-Af4* driven leukemia and function of leukemic initiating cells (LICs), thereby establishing a critical role of

IGF2BP3 in the pathogenesis of MLL-AF4 driven leukemia and its potential as a promising therapeutic target.

Existing strategies for treating MLL-rearranged leukemia include chemotherapy, small molecule inhibitors, and CD19-directed therapies (in the case of MLL-rearranged B-acute lymphoblastic leukemia). Novel therapeutic strategies for MLL-rearranged leukemia have been directed towards targeting the menin-MLL interaction, H3K79 methyltransferase DOTL1, the chromatin epigenetic reader BRD4, and epigenetic modifications [16, 17]. Multiple potent inhibitors have been developed to target the menin-MLL1 interaction, including MI-503, MI-463, MI-3454, VTP-50469, and have demonstrated impressive single-agent activity in preclinical studies, with derivatives entering phase I-II clinical trials [18-22]. However, combinatorial strategies remain a cornerstone of cancer-directed therapy to combat issues with dose-limiting toxicities and drug resistance from single-agent therapy. Therefore, we sought to explore a novel therapeutic strategy of combinatorial targeting of leukemia at the transcriptional and post-transcriptional level. Our approach was to combine the pharmacologic inhibition of the menin-MLL interaction with genetic inhibition of IGF2BP3.

Here, we tested the combined effects of IGF2BP3 knockdown via CRISPR/Cas9-mediated deletion and menin-MLL inhibition using commercially available menin-MLL inhibitors in human B-ALL cell lines and a murine model for MLL-Af4 driven leukemia [8]. Depletion of *Igf2bp3* sensitized MLL-AF4 leukemia to the effects of menin-MLL inhibition on cell growth and leukemic initiating cells. Mechanistically, we found that both knockdown of IGF2BP3 and menin-MLL inhibition with the drug MI-503 led to increased differentiation of MLL-Af4 leukemia, with a more dramatic effect seen in the combination approach. Concordantly, gene expression analyses demonstrated an upregulation of differentiation genes with MI-503 treatment and IGF2BP3 knockdown. Lastly, we found decreased leukemic engraftment and significantly increased survival with IGF2BP3 knockdown in comparison to MI-503 treatment and enhanced anti-

leukemic effects with combined MI-503 and IGF2BP3 depletion in our *in vivo* model for MLL-Af4 leukemia. Together, our work supports the idea that IGF2BP3 is an oncogenic amplifier of MLL-AF4 mediated leukemogenesis and that IGF2BP3 represents an exciting therapeutic target. Our data also supports a novel combinatorial therapeutic strategy of targeting leukemia at both the transcriptional and post-transcriptional level.

## Results

### **IGF2BP3 knockdown increases sensitivity of MLL-r leukemia cells to menin-MLL inhibition *in vitro***

Here, we sought to assess the effects of combining menin-MLL inhibition with IGF2BP3 knockdown in human B-ALL cell lines and murine immortalized HSPCs transformed with MLL-Af4 (which we will refer to in this paper as MLL-Af4 Lin<sup>-</sup> as an abbreviation) as a means of inhibiting MLL-AF4 leukemogenesis at the transcriptional and post-transcriptional level. To knockdown IGF2BP3 in human B-ALL cell lines, we used a two-vector lentiviral system as previously described to deliver Cas9 and single-guide RNA (sgRNA) targeting *Igf2bp3* (I3KO) or non-targeting (NT), in two MLL-AF4-expressing human B-ALL cell lines, RS4;11 and SEM, and an additional human B-ALL cell line without MLL-AF4 translocation, NALM6 [23]. To deplete IGF2BP3 in MLL-Af4 Lin<sup>-</sup> cells, MLL-Af4 Cas9-GFP Lin<sup>-</sup> cells were transduced with a retroviral vector containing a sgRNA targeting *Igf2bp3* (I3KO or I3-TL1) after MLL-Af4 transformation of Lin<sup>-</sup> cells isolated from bone marrow of Cas9-GFP mice (Figure S1B), in two serial retroviral transductions, as previously described [15, 23]. Both guides targeting *Igf2bp3* (I3KO or I3-TL1) caused decreased IGF2BP3 expression, in comparison to non-targeting controls (NT or NT-TL) by Western blot analysis (Figure 1A, S2A). MLL-Af4 Lin<sup>-</sup> cells treated with menin-MLL inhibitor, MI-503, for 4 days showed a dose-dependent decrease in IGF2BP3 expression, consistent with our prior findings that MLL-Af4 drives expression of *Igf2bp3* [15] (Figure 1B).

IGF2BP3 knockdown resulted in dramatically enhanced menin-MLL inhibition of cell growth in SEM and RS4;11 cells treated with MI-503, MI-463 and MI-538 for 4 days in luminescent-based cell viability assays (Figure 1C-D). In contrast, there was no difference in sensitivity to effects of menin-MLL inhibition on cell growth in NALM6, a human B-ALL cell line without MLL-AF4 translocation, and IGF2BP3 knockdown (Figure 1E). This synergistic effect of

IGF2BP3 knockdown and menin-MLL inhibition on cell growth was also seen in our murine MLL-Af4 Lin<sup>-</sup> leukemia cells across multiple menin-MLL inhibitors and two different guides targeting *Igf2bp3* (I3KO, I3-TL1) (Figure 1F, S2D). Treatment with MI-503 did not cause a significant increase in apoptosis of MLL-Af4 NT Lin<sup>-</sup> cells, by annexin V staining or caspase 3/7 activity, except at very high concentrations of 1.0 μM, consistent with its limited effect on cell growth (Figure 1F-I). MLL-Af4 Lin<sup>-</sup> cells depleted for IGF2BP3 (MLL-AF4 Lin<sup>-</sup> I3KO) showed an increased effect of MI-503 treatment on apoptosis, by caspase 3/7 activity and increased annexin V positivity (Figure 1G-J). Together, these findings highlight the sensitization of MLL-Af4 leukemia cells to menin-MLL inhibition with IGF2BP3 knockdown, with enhanced inhibition of cell growth and increased apoptosis.

#### **IGF2BP3 knockdown enhances effect of menin-MLL inhibition on LIC and differentiation.**

Our group has previously shown that leukemic initiating cells (LIC), which are thought to be critical in driving relapsed disease, require IGF2BP3 to propagate *in vitro* and *in vivo*. Menin-MLL inhibition has also been shown to decrease the LIC population, consistent with prior observations that aberrant MLL expression supports LICs [9, 24]. To further characterize the combined effects of IGF2BP3 knockdown and menin-MLL inhibition on LICs *in vitro*, we seeded MI-503 treated MLL-Af4 immortalized HSPCs depleted for IGF2BP3 (I3KO) or non-depleted (NT) into endpoint colony formation assays. IGF2BP3 knockdown more significantly reduced total colony number than MI-503 treatment (Figure 2A, B). Furthermore, MI-503 treated MLL-Af4 Lin<sup>-</sup> I3KO cells showed further reduction in total colony formation, compared to IGF2BP3 knockdown alone, suggesting that the combined inhibitory effect on LICs is at least additive (Figure 2A, B).

Both MI-503 treatment and IGF2BP3 knockdown in MLL-Af4 Lin<sup>-</sup> cells showed a shift towards more differentiated colony morphologies in endpoint methylcellulose colony formation assays (Figure 2C-E) and morphologic changes consistent with increased differentiation (Figure



2F). Decreased CFU-GM progenitor colonies and increased CFU-G and CFU-M were seen with MI-503, and in I3KO cells, with the maximal effect seen in the combination (Figure 2C-E). This pattern of increased differentiation with MI-503 treatment and IGF2BP3 knockdown, alone and together, was also seen morphologically in cytologic analysis of single cell suspension preparations (Figure 2F). The effect of MI-503 treatment is consistent with prior characterization of menin-MLL inhibitors in promoting differentiation of MLL-rearranged leukemia [20, 21]. Furthermore, the effect of IGF2BP3 depletion seen in MI-503 treated cells (versus MI-503 treated MLL-Af4 Lin- NT) show that IGF2BP3 depletion enhances the effect of menin-MLL inhibition on differentiation of MLL-Af4 leukemia cells. Together, these findings confirm that both IGF2BP3 and menin inhibition affect the number and differentiation state of LICs and that combined inhibition appears to have an additive effect in our *in vitro* assay readouts.

### **IGF2BP3 knockdown in MLL-Af4 Lin- cells impacts the global transcriptome and leads to upregulation of genes involved in differentiation**

To gain insight into how combined menin-MLL inhibition and IGF2BP3 knockdown interact and affect gene expression, we performed RNA-seq analysis in MLL-Af4 Lin- cells with the following treatment conditions: (1) MLL-Af4 Lin- cells depleted for IGF2BP3 (I3KO) and treated with MI-503 (low-dose at 0.2 $\mu$ M, high-dose at 1.0 $\mu$ M) or DMSO control, (2) MLL-Af4 Lin- cells non-depleted for IGF2BP3 (NT) and treated with MI-503 (low-dose at 0.2 $\mu$ M, high-dose at 1.0 $\mu$ M) or DMSO control. Comparison of differentially expressed genes in DMSO-treated MLL-Af4 Lin- cells depleted for IGF2BP3 (I3KO) versus non-depleted (NT) showed dramatic changes in the global transcriptome with 4346 upregulated and 1720 downregulated genes, by differential expression analysis with DESeq2 [25] (Figure 3A, S3A). In contrast, a smaller number of genes were differentially expressed in MLL-Af4 Lin- NT with MI-503 compared to DMSO control, particularly at the low-dose concentration (Figure 3A-B, S3A). In comparisons of NT and I3KO

cells, we identified a significant enrichment in pathways involved in cell differentiation and activation, particularly in leukocytes: neutrophil degranulation, regulation of cell-cell adhesion, cell activation, myeloid leukocyte differentiation, and leukocyte migration (Figure 3C). Next, we evaluated the differentially expressed genes upon MI-503 treatment in NT and I3KO. Interestingly, there is significant overlap between genes that are upregulated with IGF2BP3 knockdown and with MI-503 treatment. More than 70% of genes that are upregulated with MI-503 treatment in MLL-Af4 NT and I3KO cells are upregulated with IGF2BP3 knockdown (Figure 3G). Furthermore, we saw significant enrichment in pathways involved in cell differentiation, with MI-503 treatment in both MLL-Af4 NT and I3KO cells, similar to those affected by IGF2BP3 depletion (Figure 3D, F). Specifically, analyses on MI-503 treated-MLL-Af4 NT cells using Metascape [26] showed significant enrichment in pathways of neutrophil degranulation, oxidative stress and redox pathway, leukocyte cell-cell adhesion, myeloid cell differentiation, and regulation of cysteine-type endopeptidase activity involved in apoptotic process (Figure 3D). Similar analyses on I3KO cells showed significant enrichment in upregulation of transcripts associated with leukocyte migration, cell-cell adhesion, positive regulation of cell motility, neutrophil degranulation, and myeloid leukocyte activation (Figure 3F).

We next looked to validate the differentially expressed genes involved in differentiation using individual RT-qPCR for these genes of interest. As anticipated, we found a decrease in expression of *Igf2bp3*, and its known target mRNAs, *Myc* and *Hoxa9*, in NT cells treated with MI-503 (Figure 4A-C). Next, we focused on enriched differentially upregulated genes involved in leukocyte differentiation, *Fcnb*, *Prg2*, *Mmrn1*, *Elane*, *Ets1*, *Pram1*, *Cebpd* and *Cepbe*. A significant increase was seen in all of these genes with *Igf2bp3* depletion (Figure 4D-K). Fold change was significantly higher with I3KO than with MI-503 treatment (Figure 4D-K). For genes *Fcnb*, *Prg2*, *Mmrn1*, and *Pram1*, MI-503 treatment led to a significant increase in expression in MLL-Af4 Lin<sup>-</sup> I3KO cells, while a non-significant increase was seen with the other genes of

interest, *Elane*, *Ets1*, *Cebpd*, and *Cebpe*, suggesting a saturating effect of *Igf2bp3* depletion on upregulation of these genes involved in differentiation. Together, our analyses demonstrate that similar, but not identical, impacts on gene expression are engendered by genetic inhibition of IGF2BP3 and menin-MLL inhibition with MI-503. We propose that these impacts on gene expression underlie the phenotypic effects seen upon the co-inhibition of transcriptional and post-transcriptional gene expression regulation.

### **IGF2BP3 knockdown and MI-503 treatment decrease engraftment of MLL-Af4 leukemia cells *in vivo***

To further characterize our findings *in vivo*, we developed and validated a congenic transplantation model for the murine MLL-Af4 leukemia, using the above-described cellular systems (MLL-Af4 Lin<sup>-</sup> NT and I3KO) derived from murine bone marrow (Supplementary Fig S4). To assess the effects, we transplanted either NT or I3KO Lin<sup>-</sup> cells (derived from CD45.2<sup>+</sup> mice) into CD45.1<sup>+</sup> mice following five days of treatment with MI-503 *in vitro* (Figure 5A). Six weeks post-transplantation, evaluation of peripheral blood showed that both treatment with MI-503 and IGF2BP3 depletion led to decreased CD45.2<sup>+</sup> cells in the peripheral blood, reflective of decreased leukemic engraftment (Figure 5B). Mice in these four groups were followed for development of leukemia, and at the time of the first mouse showing clinical signs of terminal leukemia (at 8.5 weeks), all mice were sacrificed. Mice were evaluated for leukemia, as defined by increased spleen weight, and presence of increased blasts seen in bone marrow, spleen and/or peripheral blood. Depletion of IGF2BP3 led to significantly decreased proportion of mice with gross leukemia, decreased bone marrow cell counts, as well as decreased CD11b<sup>+</sup> count and CD45.2<sup>+</sup>% in both spleen and bone marrow (Figure 5C, D-I). MI-503 treatment resulted in a modest decrease in proportion of mice with gross leukemia, total cellular and CD11b<sup>+</sup> counts, and CD45.2<sup>+</sup>% in bone marrow and spleen, compared to DMSO control (Figure 5D). Interestingly,

histopathologic analysis at the time of necropsy showed morphologic changes consistent with increased differentiation in spleens of mice that were transplanted with leukemic cells that were treated with MI-503 or depleted for IGF2BP3, with the cells appearing most differentiated in mice transplanted with MI-503 treated I3KO cells (Figure 5J). Furthermore, in our bone marrow samples from these mice, we saw an upregulation in genes involved in granulocytic differentiation, *Cebpe*, *Elane*, *Fcnb*, *Prg1*, *Mmrn1*, and *Ets1*, in the same pattern, with MI-503 treatment and IGF2BP3 knockdown, by performing RT-qPCR using the differentiation genes previously identified in our evaluation of the Lin- cells *in vitro* (Figure S5D-I).

In addition to the endpoint experiments outlined above, we evaluated mice for overall survival and leukemia-free survival in a separate experiment. Mice were closely followed for any signs of morbidity, and/or leukemia, and evaluated by increased spleen weight, and presence of increased blasts seen in bone marrow, spleen and/or peripheral blood at the time of necropsy. Treatment with MI-503 showed a modest effect with a delay in leukemia progression but without improvement in overall survival in mice transplanted with MLL-Af4 leukemia (NT, comparison MI-503 vs. DMSO), in the dose used and the experimental setup deployed here (Figure 5K-L). In contrast, IGF2BP3 depletion did significantly increase both overall and leukemia-free survival in mice transplanted with MLL-Af4 leukemia (comparison NT DMSO vs. I3KO DMSO) (Figure 5C). This increase in overall and leukemia-free survival was also seen in mice transplanted with MI-503 treated MLL-Af4 leukemia cells (comparison NT MI-503 vs I3KO MI503), highlighting the therapeutic potential of targeting IGF2BP3 in addition to menin-MLL inhibition.

## **Materials and Methods**

### **Cell lines and cell culture**

All cell lines were maintained in standard conditions in incubator at 37°C and 5% CO<sub>2</sub>. Human B-ALL cell lines, RS4;11 (ATCC CRL-1873), NALM6 (ATCC CRL-3273), and SEM (DMZ-ACC 546) were cultured as previously described [23]. Immortalized MLL-Af4 transformed hematopoietic stem and progenitor cells derived from mouse bone marrow (MLL-Af4 Lin<sup>-</sup> cells) were cultured in IMDM with 15% FBS, supplemented with recombinant mouse SCF 100 ng/μL, recombinant mouse IL-6 4 ng/μL, recombinant human FLT3 50 ng/μL, and mouse TPO 50 ng/μL.

### **Plasmids and viral transduction**

The MSCV-MLL-FLAG-Af4 plasmid was generously provided by Michael Thirman (University of Chicago) through a material transfer agreement [21]. Single-guide RNAs against mouse *Igf2bp3* and non-targeting guides were cloned into an in-house MSCV-hu6-sgRNA-EFS-mCherry vector [23]. Single-guide RNAs against human *Igf2bp3* and non-targeting guides were cloned into pLKO.sgRNA.EFS.tRFP (Addgene 57823). Single guide RNA sequences are available in the Supplemental Table 1. Generation of retroviral and lentiviral supernatants and viral transduction were performed according to standard procedures.

### **CRISPR/Cas9-mediated deletion of IGF2BP3 in cell lines**

Human B-ALL cell lines, SEM, RS4;11, and NALM6 were depleted for IGF2BP3 using lentiviral delivery of CRISPR/Cas9 components in a two-vector system previously described [23]. Immortalized MLL-Af4 Lin<sup>-</sup> cells were generated by initially isolating HSPCs from bone marrow of Cas9-GFP and then transformed using retroviral transduction with MLL-Af4 retroviral supernatant, with four rounds of transduction with MLL-Af4 retroviral supernatant, followed by selection in G418 supplemented media at 400 μg/mL for 7 days, as previously described [23]. Cells were then stably

transduced with lentiviral supernatant containing sgRNA against *Igf2bp3* (I3Cr2, I3-TL1) or non-targeting (NT-1, I3-TL1) and sorted on GFP and mCherry positivity.

### **Protein extraction and Western blot**

Cell lysates were made and electrophoresed using SDS-PAGE using standard conditions [14]. Antibodies used were IGF2BP3 anti-rabbit polyclonal (catalog #RNP009, MBL) and  $\beta$ -actin anti-mouse monoclonal (catalog A5441, Sigma-Aldrich).

### **In vitro assays for cell viability, apoptosis, and proliferation, with drug treatment**

Cells were treated with drug or dimethylsulfoxide (DMSO) carrier control at DMSO 0.1%. Commercially available menin-MLL inhibitors were obtained as follows: MI-503 (catalog SML2520, Sigma-Aldrich), MI-463 (catalog HY-19809, MedChemExpress), and MI-538 (catalog HY-19810, MedChemExpress). Cell viability assays were performed using a luminescent assay based on ATP quantitation (CellTiterGlo, Promega, catalog G7571), per manufacturer's protocol. 1500 cells/well (for 384 well format) and 6000 cells/well (for 96 well format) were plated and incubated with drug for four days at 37°C in a 5% CO<sub>2</sub> incubator, followed by endpoint assay. To measure apoptosis, annexin V staining with Annexin V BV421 (BD Biosciences, catalog BDB563873) followed by flow cytometry analysis and a luminescent assay measuring caspase-3 and -7 activities (Caspase-Glo 3/7 Assay, Promega, catalog, G8091) were performed, per manufacturer's instructions. For Ki67 intracellular staining, cells were fixed and permeabilized using intracellular fixation and permeabilization buffer (Invitrogen, catalog 88882400) and stained with PerCP/Cyanine 5.5-tagged anti-mouse Ki-67 (Biolegend, catalog 652423).

### **Flow cytometry**

For mouse experiments, peripheral blood was collected at pre-determined time points and bone marrow and spleen at time of sacrifice for endpoint analysis. Isolation of single cell suspensions and staining with fluorochrome-conjugated antibodies were performed per standard procedures [14]. A list of antibodies is provided in Supplemental Table 2. Flow cytometry was performed at the UCLA Jonsson Comprehensive Cancer Center and at the Broad Stem Cell Research Flow Cores, with subsequent analysis performed using FlowJo software.

### **Methylcellulose-based colony forming unit assays**

The assay was performed by seeding MLL-Af4 Cas9 Lin- cells after 4 days of drug treatment into Methocult colony forming media (STEMCELL Technologies, catalog M3434), at various cell seeding densities of 250-5000. Cells in Methocult media were cultured for 10-12 days and counted for total colony number and morphologic subtypes.

### **RNA isolation and qPCR**

Total RNA was extracted from cell pellets using Qiazol (Qiagen) per manufacturer's protocol. Previous protocols were adapted for RT-qPCR as standard procedures [14]. A full list of RT-qPCR primers is presented in Supplemental Table 1. For normalization to housekeeping genes, we used RT-qPCR primers for human 18S (or actin) and mouse L32.

### **RNA Sequencing**

Total RNA was extracted from cell pellets using Qiazol (Qiagen) per manufacturer's protocol with the following modification to include an additional RNA ethanol wash step: after the total RNA was solubilized in ddH<sub>2</sub>O, one overnight ethanol precipitation step was included for further purification. Libraries were prepared from 2 µg of total RNA per sample using the NEXTFLEX Rapid

Directional RNA-Seq Kit 2.0 (Perkin Elmer Applied Genomics), following Poly(A) selection and purification using the NEXTFLEX Poly(A) Beads Kit 2.0 per the manufacturer's protocol (Perkin Elmer Applied Genomics), and sequenced on Illumina NovaSeq S4 (UC Davis Genome Center, DNA Technologies, and Expression Analysis Core Laboratory), generating 150bp paired-end reads. RNA-seq reads were mapped to the mouse genome assembly mm18 using STAR 2.5.3 and Bowtie 2 [27, 28]. Differentially expressed genes were identified using DESeq2 [25]. Multiple testing correction was performed using the Benjamini–Hochberg method. Significant differentially expressed genes have adjusted  $P$  value  $\leq 0.05$  and absolute  $\log_2FC \geq 1$ . Enrichment analyses were completed with Metascape [26].

### **Mice and bone marrow transplantation**

C57BL/6J, B6.SJL-*Ptprca*<sup>a</sup> *Pepc*<sup>b</sup>/BoyJ (B6 CD45.1), and B6J.129(Cg)-Gt(ROSA)26Sor<sup>tm1.1(CAG-cas9\*,-EGFP)<sup>F<sub>0</sub>zh</sup>/J (Cas9-GFP BL/6J) mice were obtained from Jackson Laboratory. MLL-Af4 Lin- cells were transplanted into 8–10-week-old CD45.1 female recipients (or C57BL/6J in pilot experiments). Recipients were initially conditioned with busulfan 30 m/kg intraperitoneally on D-3 and D-2, followed by transplantation by retro-orbital injection of 2e5 Lin- cells with 1e5 of CD45.1 carrier marrow (with the exception of the experiment in supplemental figure S4, which used a dose of 3e5 Lin- cells with 1e5 carrier marrow from CD57Bl/6J mice).</sup>

### **Histopathology**

Cell samples were prepared for Wright staining and microscopy using Shandon Cytospin III Centrifuge. Fixation and staining of peripheral blood smears were performed using methanol and Wright staining. Fixation and sectioning of mouse tissue samples were performed per standard procedures, as previously described [29], and then subsequently processed in the UCLA



Translational Pathology Clinical Laboratory. Analysis and review were performed by a board-certified hematopathologist (DSR).

### **Statistical analysis**

Data shown represent mean  $\pm$  SD for continuous numerical data. Two-tailed student's *t* tests or one-way ANOVA followed by Bonferroni's multiple comparisons test were performed using GraphPad Prism software and conducted as described in the figure legends. Survival analyses were performed using Kaplan-Meier method with comparisons made using log-rank tests, followed by Bonferroni's correction for multiple comparisons. A *P* value less than 0.05 was considered significant.

## Discussion

In this study, we tested a novel combinatorial therapeutic strategy of targeting MLL-Af4 leukemia at the transcriptional and post-transcriptional level, using commercially available inhibitors of menin-MLL and genetic inhibition of IGF2BP3, an RNA binding protein critical to MLL-Af4 mediated leukemogenesis. The development of this approach was based on our prior work showing that IGF2BP3 is necessary for the efficient initiation of MLL-Af4 driven leukemia, and therefore, represents a promising therapeutic target [15]. We found that concomitant targeting of IGF2BP3 enhanced the therapeutic effect of pharmacologic menin-MLL inhibition in MLL-Af4 driven leukemia in our *in vitro* and *in vivo* studies. Both inhibition of IGF2BP3 and the menin-MLL interaction affect the number and function of leukemic initiating cells, as shown by functional readouts in endpoint colony formation assays. Furthermore, detailed evaluation of colony morphologies, histopathology, and RNA sequencing data all show a consistent shift towards increased differentiation with IGF2BP3 knockdown and menin-MLL inhibition, highlighting a mechanism for their combined anti-leukemic effects.

Our prior work showing the importance of the RNA binding protein IGF2BP3 as a critical regulator of MLL-Af4 leukemogenesis has added to growing evidence for the role and function of RNA binding proteins as important regulators of oncogenesis and their potential as a novel class of therapeutics. Small molecule inhibitors have been developed against a number of these RNA binding proteins, including Musashi-2, HuR, LIN28B, and MBNL1, and have been studied as single-agents, but have not been combined with therapies directed towards upstream transcriptional regulators [30-34]. In the same vein, inhibitors targeted at the menin-MLL interaction have been developed for the treatment of MLL-rearranged leukemias and NPM1c mutated acute myeloid leukemias but have not been combined with therapies targeting post-transcriptional gene dysregulation [18-22, 35, 36]. Here, we have shown a potent effect of combining genetic inhibition of the RNA binding protein IGF2BP3 and pharmacologic inhibition of

the menin-MLL interaction, in our models for MLL-Af4 leukemia, resulting in decreased cell growth *in vitro* and leukemic burden *in vivo*. These results not only support the combined targeting of menin-MLL and IGF2BP3 as a novel therapeutic approach for treatment of MLL-rearranged leukemia and highlight an essential interaction between MLL and IGF2BP3 in the gene regulation of MLL-Af4 driven leukemia, but also establish support for a novel treatment paradigm of targeting transcriptional and post-transcriptional gene regulation.

With regards to underlying mechanism of IGF2BP3 function in leukemogenesis, we have previously shown that deletion of *Igf2bp3* led to decreased number and function of MLL-Af4 leukemic-initiating cells [15]. Borkin et al showed that treatment with menin-MLL inhibitors, MI-503 and MI-563, led to decreased c-kit (CD117) expression in their MLL-r leukemia cells [20]. Because there is some disagreement over which immunophenotypic markers are expressed by and used to define leukemic stem cells depending on the model system, we used a functional readout for leukemic initiating cells to assess the combined effects of IGF2BP3 knockdown and menin-MLL inhibition with *in vitro* endpoint colony formation assays. We showed a decrease in total colony number and shift towards more differentiated colony morphologies, which is consistent with prior characterization of the pharmacologic effects of these menin-MLL inhibitors. Notably, IGF2BP3 knockdown enhanced the effect of MI-503 in these readouts of LIC function and number, suggesting that together inhibition of IGF2BP3 and menin-MLL further target the leukemic stem cell, a known critical driver of refractory and relapsed disease [37-40].

Furthermore, we tested the combined inhibition of IGF2BP3 and the menin-MLL interaction on the ability to initiate MLL-Af4 leukemia *in vivo*. We demonstrated that transformed MLL-Af4 HSPCs can efficiently engraft and initiate leukemia in both syngeneic and congenic mice, following limited amounts of time in culture and CRISPR/Cas9-mediated deletion of *Igf2bp3*. This system allows for the genetic manipulation of any gene as the mouse model carries Cas9-eGFP in its genome. We also standardized the model for *in vivo* engraftment, finding that leukemia

engraftment and terminal morbidity occur at about 4 and 8 weeks respectively. Treatment of these MLL-Af4 transformed HSPCs with menin-MLL inhibitor *in vitro* and CRISPR/Cas9-mediated deletion of *Igf2bp3* effectively reduced leukemic engraftment *in vivo*, showing that IGF2BP3 and menin-MLL inhibition reduce the number and function of leukemic initiating cells and is consistent with the results from our *in vitro* colony formation assays. Hence, this represents a single integrated system that allows for both *in vitro* and *in vivo* analyses of leukemogenesis.

In our RNA sequencing experiments, we characterized gene expression changes with menin-MLL inhibition and depletion of IGF2BP3 in MLL-rearranged leukemia. We demonstrated that both menin-MLL inhibition and IGF2BP3 upregulated genes involved in leukocyte/granulocyte differentiation, with a stronger effect seen with *Igf2bp3* depletion than pharmacologic menin-MLL inhibition alone, and an additive effect in combination with menin-MLL inhibition. The results from this gene expression data help provide a molecular explanation for the increased differentiation seen with menin-MLL inhibitor treatment, previously reported in studies of MI-503, MI-463, and VTP-50469 [18, 20, 21]. Furthermore, the pattern of upregulation of genes involved in granulocyte differentiation, seen with MI-503 treatment alone, IGF2BP3 knockdown alone, and then combined, mirror the functional and phenotypic outputs of anti-leukemic effects on cell growth, differentiation and LIC number and function.

We demonstrated that menin-MLL inhibition does in fact reduce IGF2BP3 expression, as well as expression of known IGF2BP3 targets that are important in leukemogenesis, *Hoxa9* and *Myc*, and that the addition of IGF2BP3 knockdown further reduced the expression of these important oncogenic transcripts. This effect supports our understanding of IGF2BP3 as an oncogenic amplifier of MLL-Af4 mediated leukemogenesis. Prior work from our group and others have shown the ability for IGF2BP3 and other RNA binding proteins to affect RNA splicing and RNA stability through interaction with microRNAs, the RNA-induced silencing complex, as potential molecular mechanisms underlying the RBP's role and function in oncogenesis [14, 15,

41-44]. Elucidating these molecular mechanisms remains an area of great interest and future direction for our work. This study provides possible targets of interest that can be studied to further understand the interaction between MLL-Af4 and IGF2BP3. For example, in this study, we identified *Elane* as a differentially upregulated gene with MI-503 treatment and IGF2BP3 knockdown. Interestingly, *Elane* is also a direct target of IGF2BP3, based on our data from enhanced crosslinking-immunoprecipitation experiments in MLL-Af4 Lin<sup>-</sup> cells [15]. Additional studies using functional genomic analyses in which these targets are knocked out would help define the contribution of these transcripts to MLL-Af4 leukemogenesis and help elucidate the mechanism by which IGF2BP3 contributes to leukemogenesis. Our model system for MLL-Af4 leukemia using Cas9-expressing MLL-Af4 transformed HSPCs lends itself readily to these functional genomic analyses, as multiple targets could be quickly screened using a CRISPR sgRNA library in Cas9-expressing MLL-Af4 cells depleted for IGF2BP3. Important functional targets could be identified based on their ability to restore growth in IGF2BP3 depleted leukemia cells, with *in vitro* and *in vivo* screens predicted to show relative enrichment for sgRNAs against these targets.

From the perspective of clinical translation, we look forward to methods of inhibiting IGF2BP3 in combination with existing experimental therapeutics, including menin-MLL inhibitors. One limitation of our study is that *Igf2bp3* deletion occurred prior to the functional readouts that we pursued. Hence, the role of IGF2BP3 in maintenance remains an important and unanswered question. Future studies, using a conditional knockout system and/or protein degradation system, will help us further explore the therapeutic potential of targeting IGF2BP3. While developing targeting and developing small molecule inhibitors against RNA-binding proteins remains challenging, in this study, we have shown that targeting IGF2BP3 had potent anti-leukemic effects against MLL-Af4 leukemia *in vitro* and *in vivo*, and that this results in additional, anti-leukemic effects with menin-MLL inhibitors. Our studies confirm a role for IGF2BP3 as an oncogenic

amplifier of MLL-AF4-driven leukemia and suggest a promising and novel combinatorial approach to targeting leukemia at the transcriptional and post-transcriptional level.

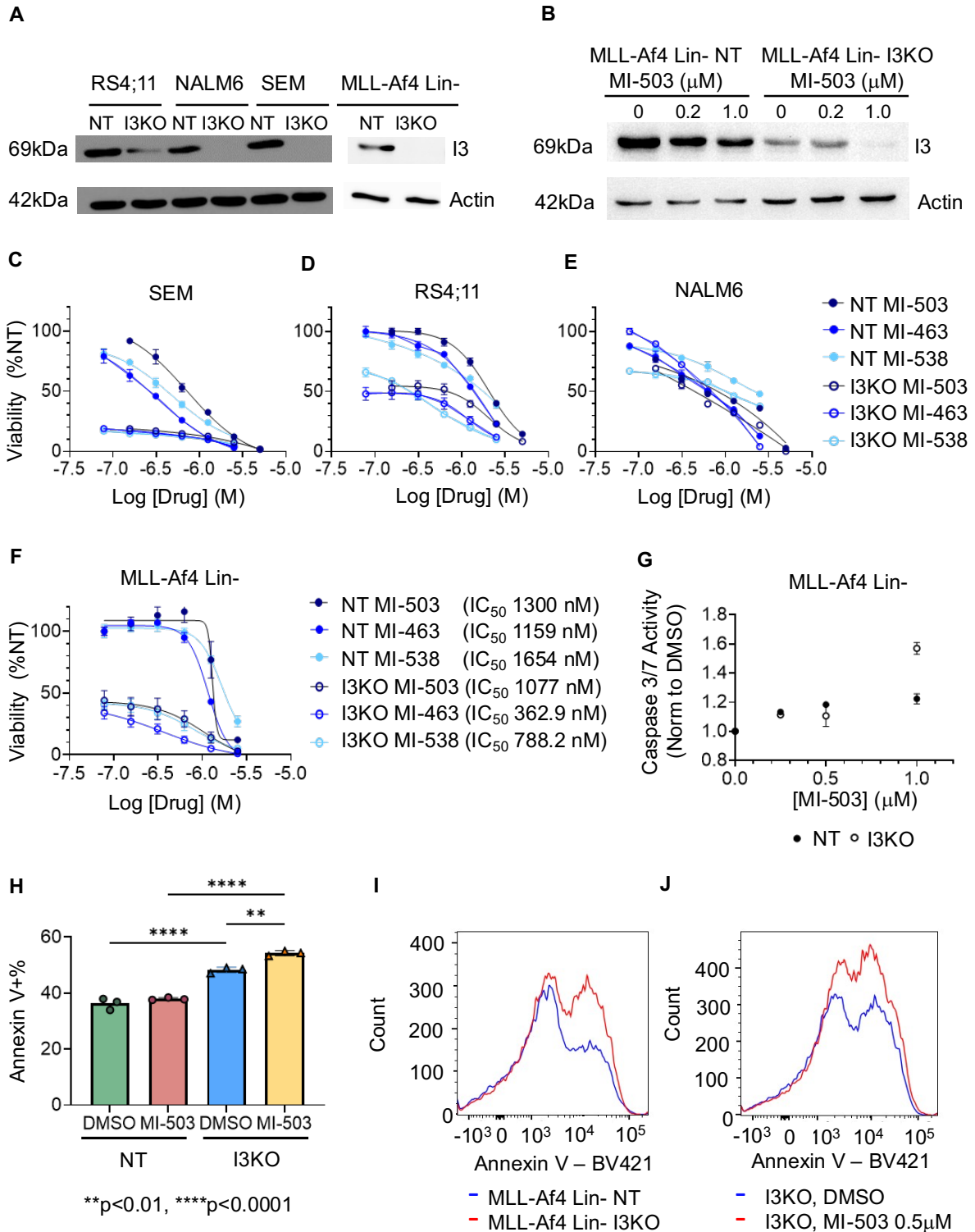


**Figure 1. IGF2BP3 knockdown increases sensitivity of MLL-r leukemia cells to menin-MLL inhibition.**

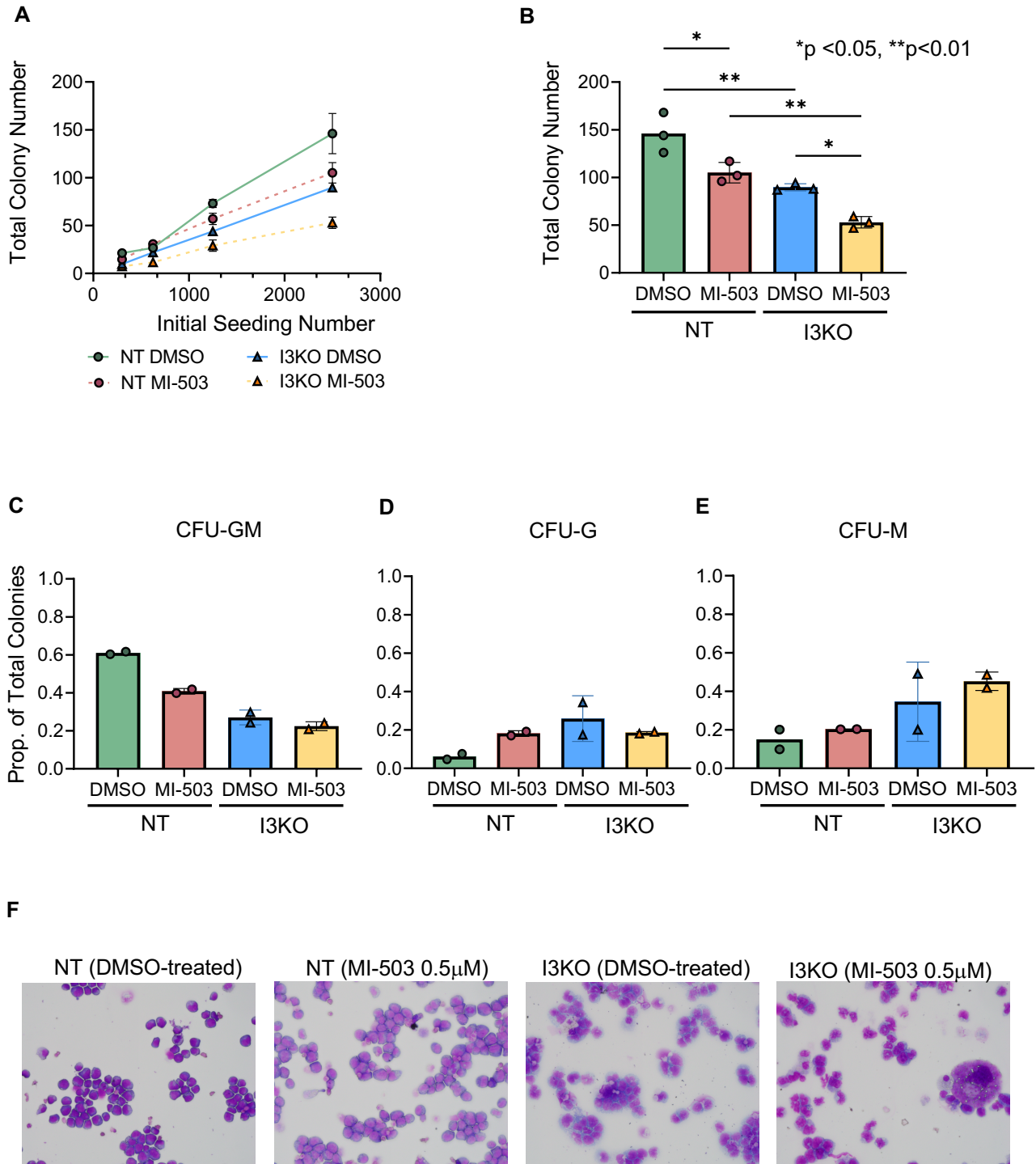


**Figure 2. Combined IGF2BP3 knockdown and menin inhibition increases differentiation of MLL-Af4 leukemia.**



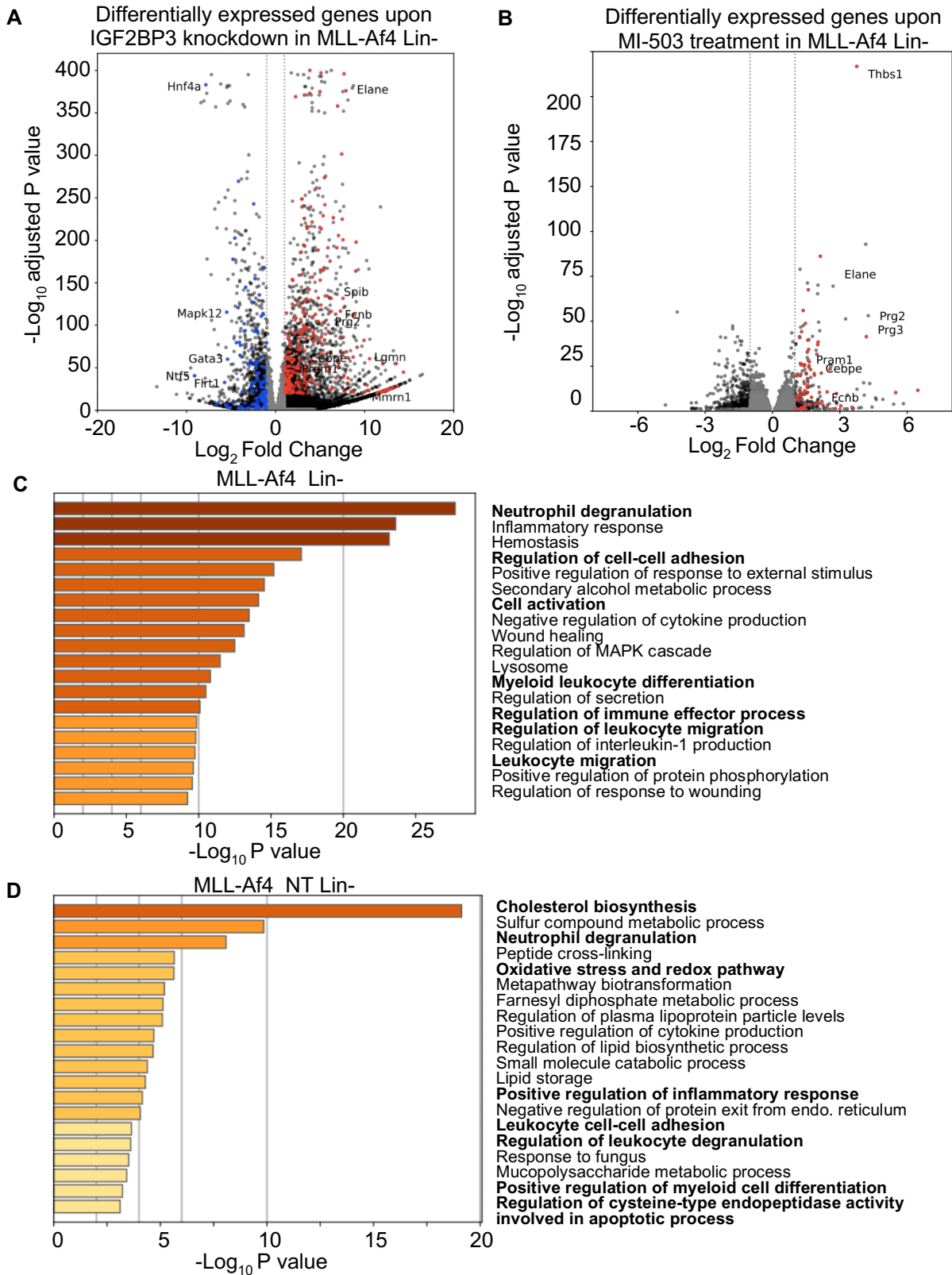
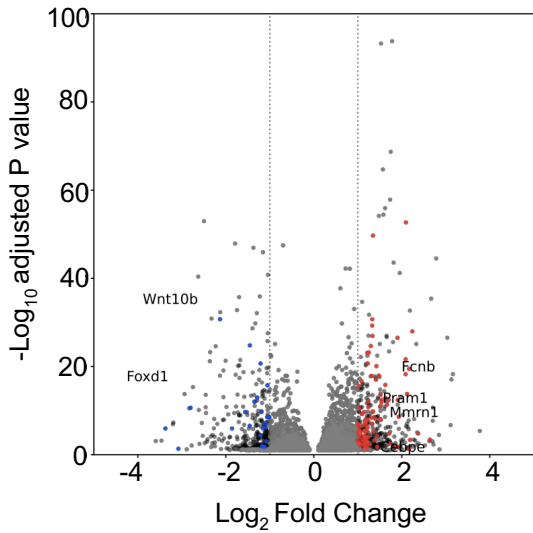


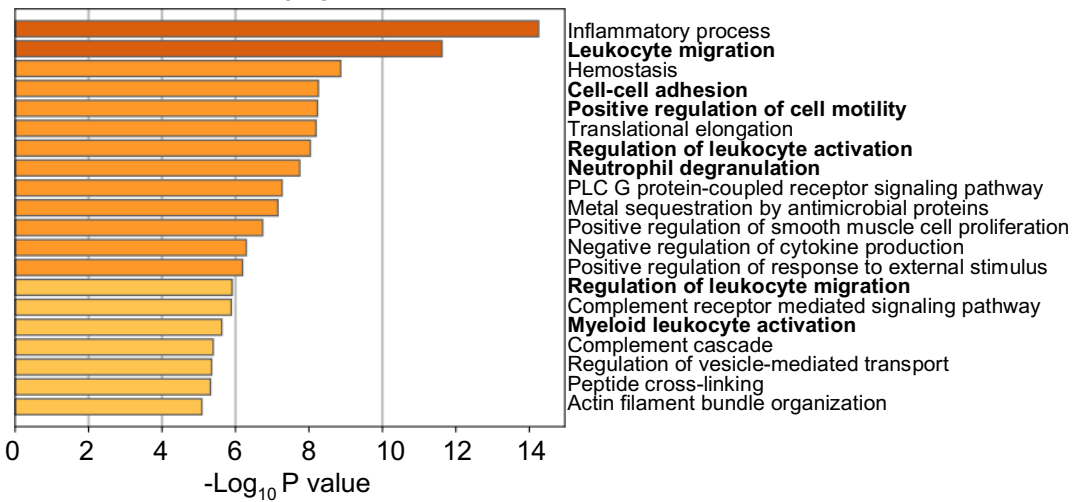
**Figure 3. Increased upregulation of genes involved in differentiation with IGF2BP3 knockdown and menin-MLL inhibition in MLL-Af4 leukemia.**

**Figure 3 (Continued). Increased upregulation of genes involved in differentiation with IGF2BP3 knockdown and menin-MLL inhibition in MLL-Af4 leukemia.**

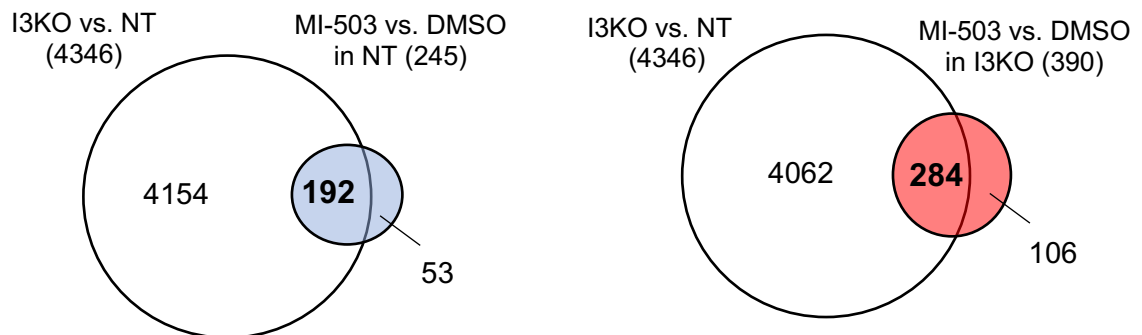
**E** Differentially expressed genes upon MI-503 treatment in MLL-Af4 I3KO Lin-



**F** MLL-Af4 I3KO Lin-



**G Shared upregulated genes with IGF2BP3 knockdown and MI-503 treatment**



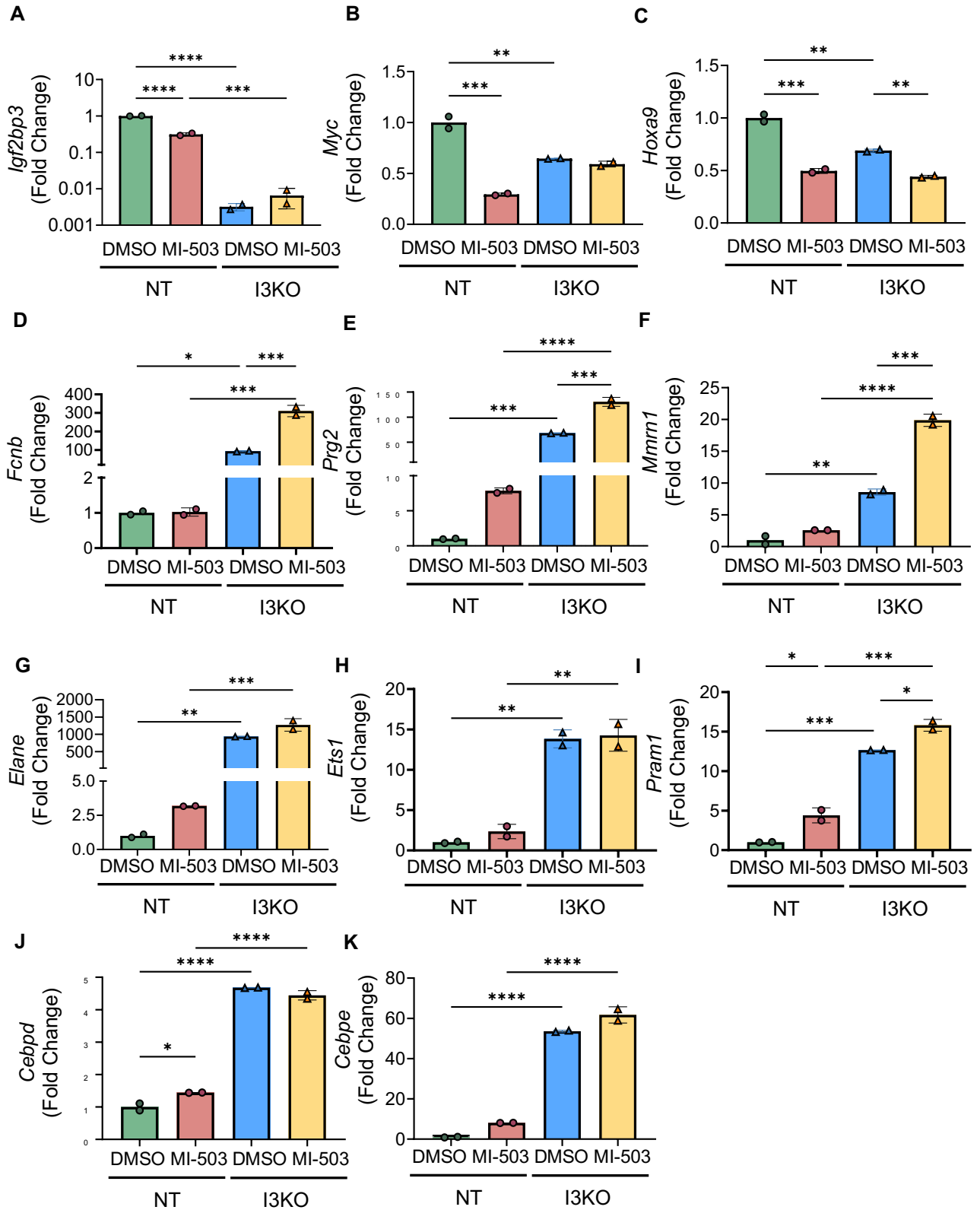


**Figure 4. Increased upregulation of genes involved in differentiation with IGF2BP3 knockdown and menin-MLL inhibition in MLL-Af4 leukemia, validated by RT-qPCR.**

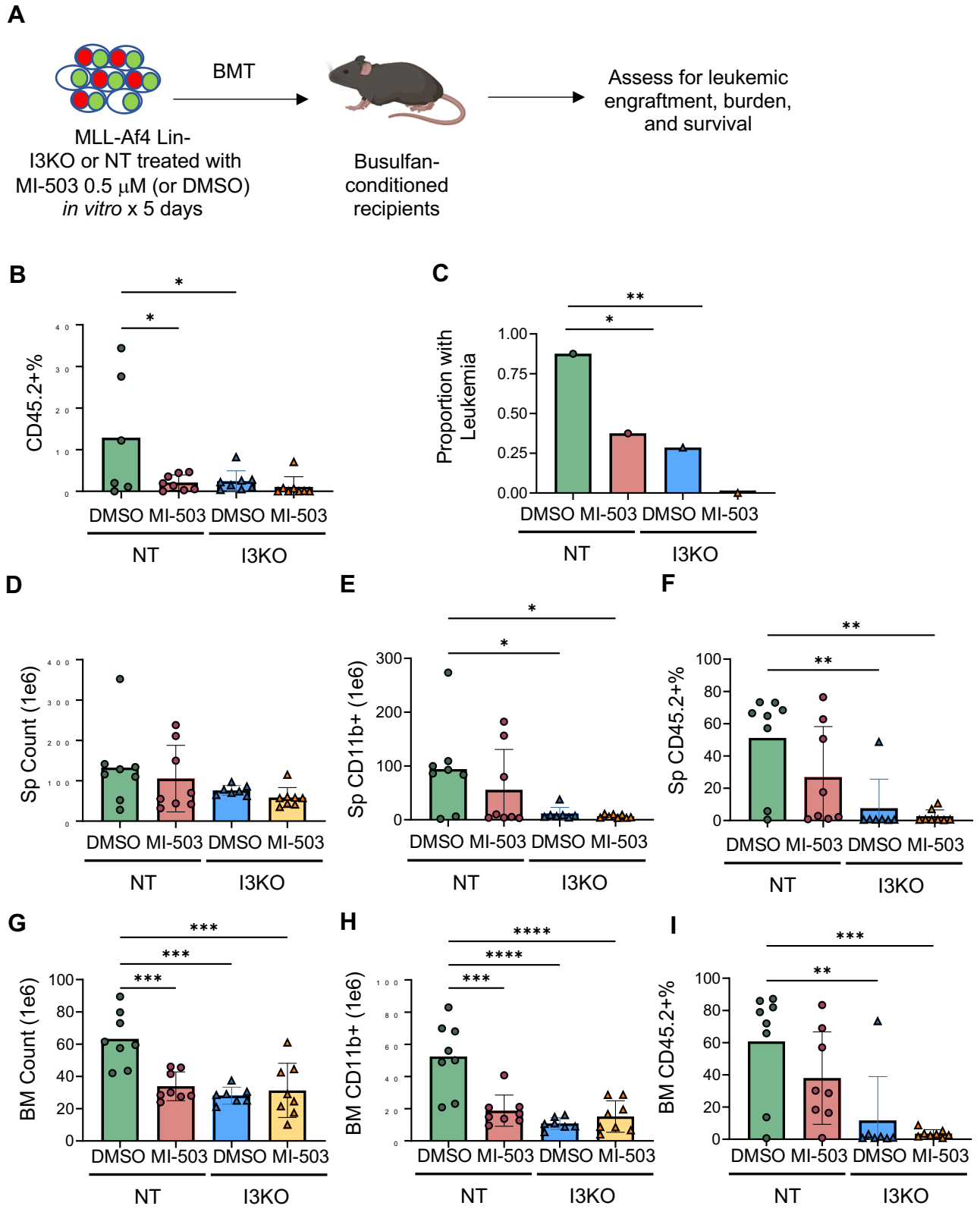
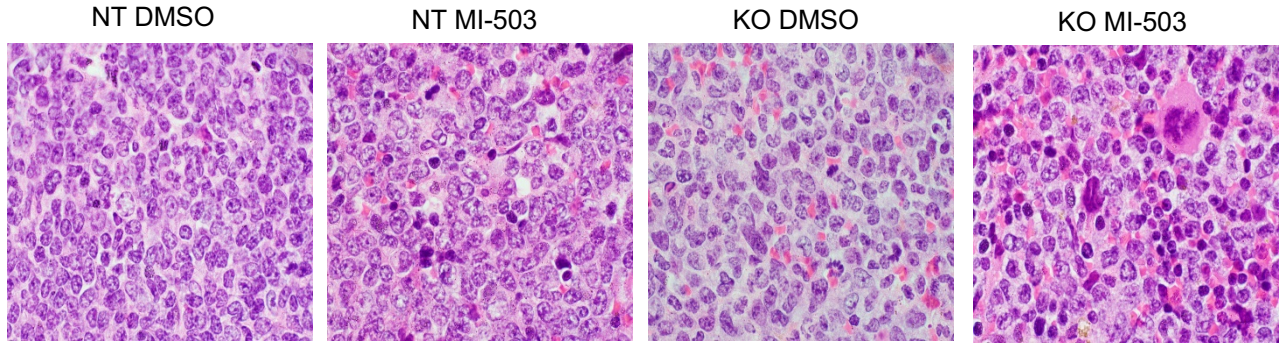


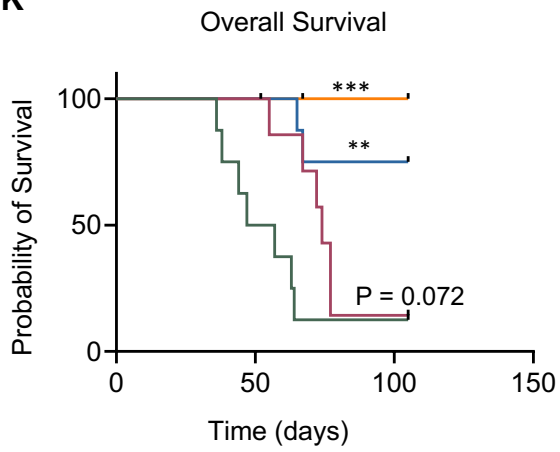
**Figure 5. Combinatorial inhibition of menin-MLL and IGF2BP3 decreases leukemic engraftment and burden and increases survival *in vivo*.**

**Figure 5 (Continued). Combinatorial inhibition of menin-MLL and IGF2BP3 decreases leukemic engraftment and burden and increases survival *in vivo*.**

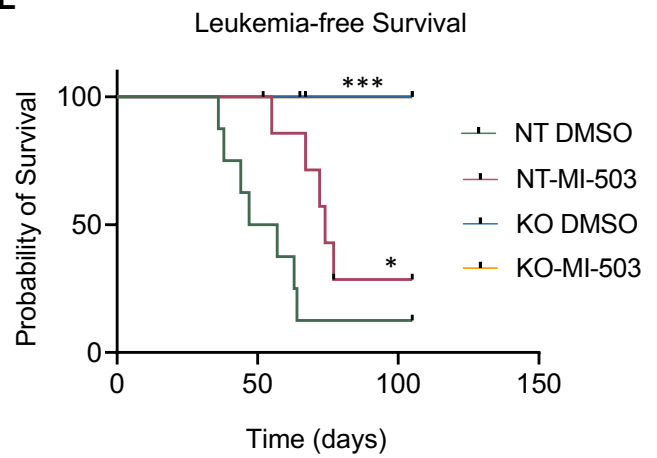
**J**

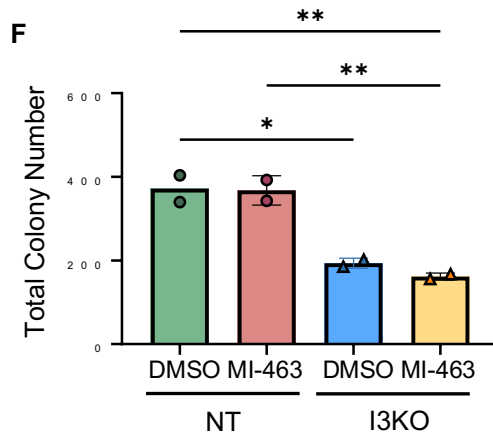
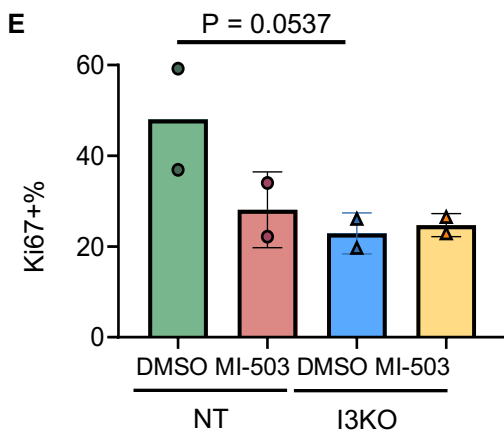
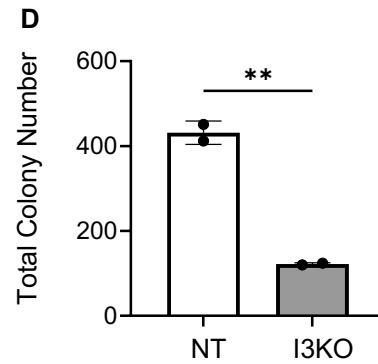
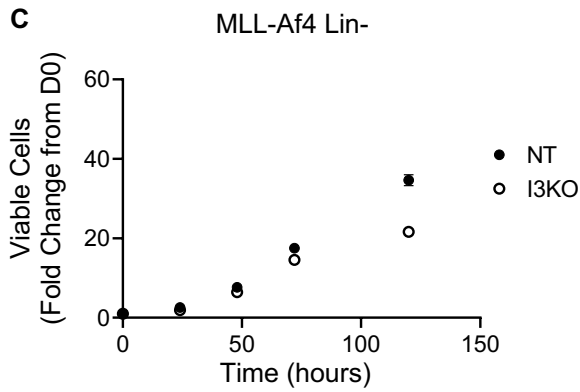
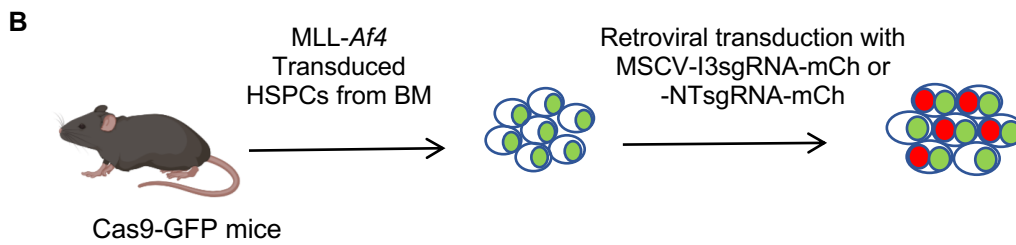
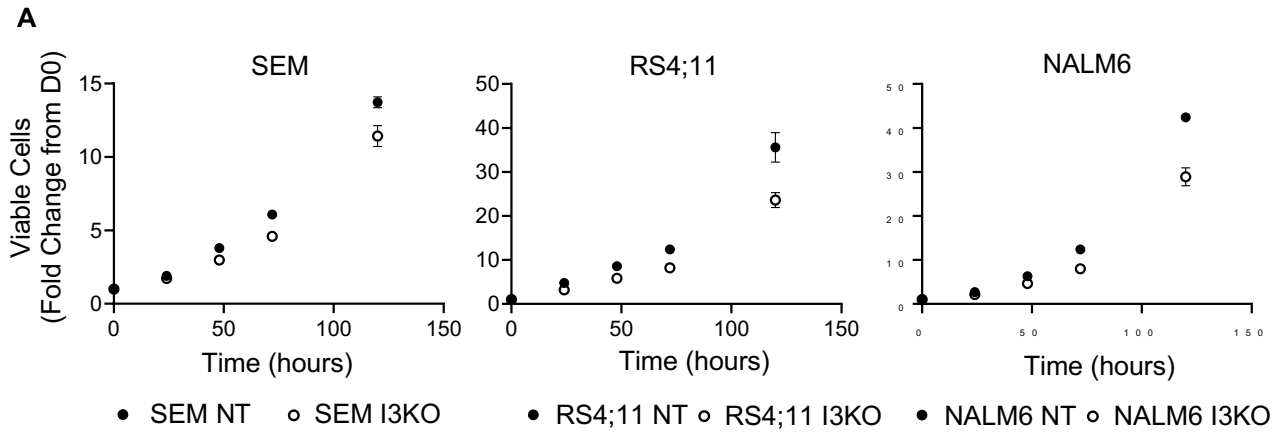


**K**

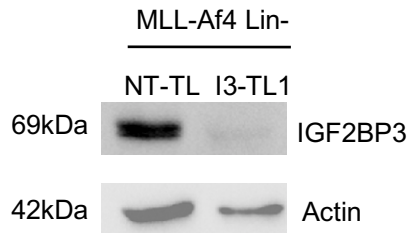
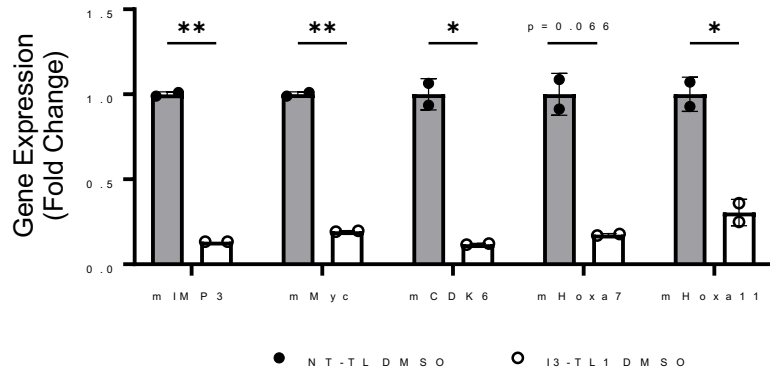
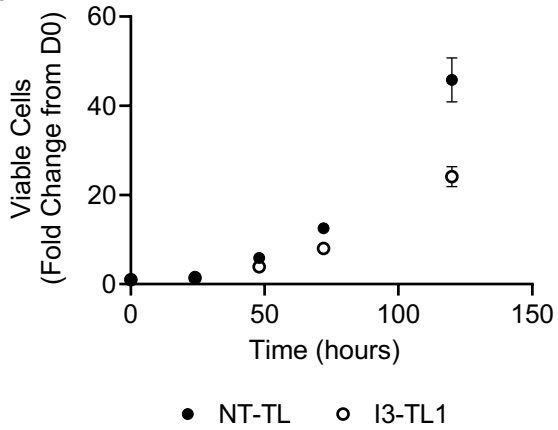
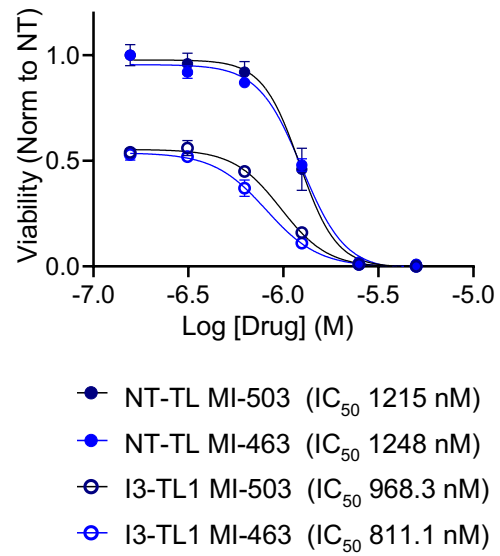


**L**





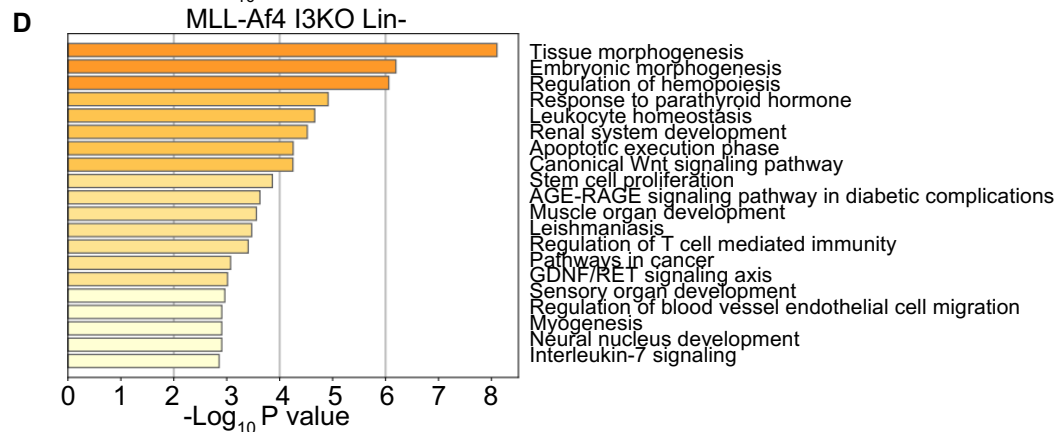
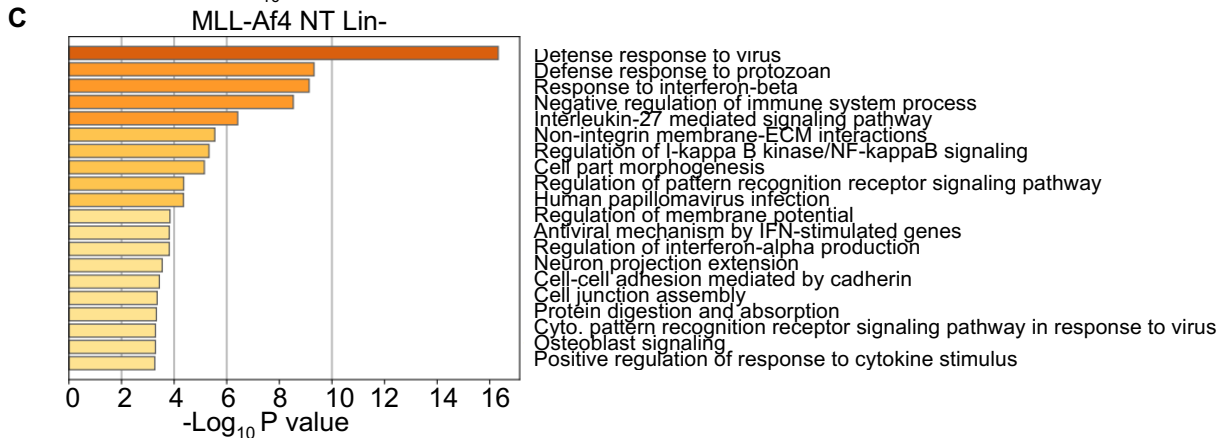
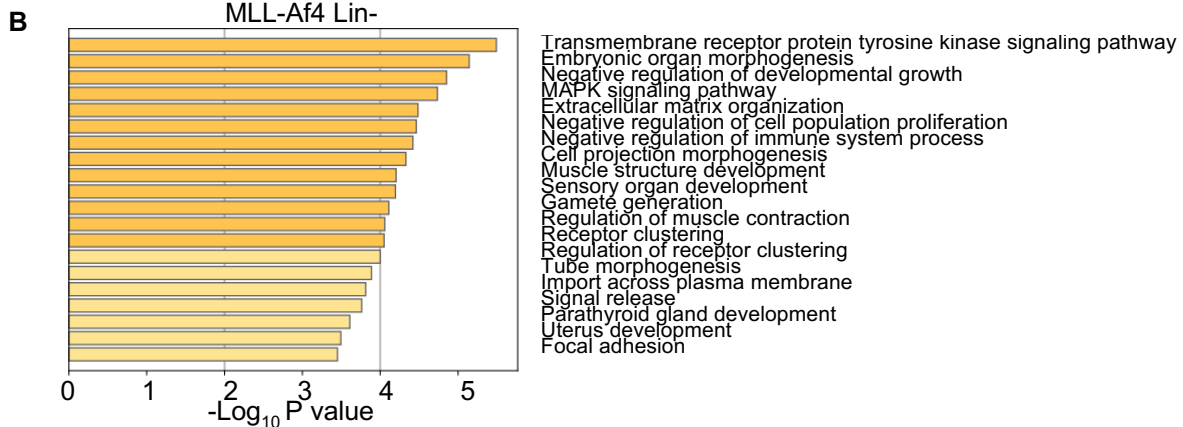
**Supplemental Figure S1. IGF2BP3 knockdown in human B-ALL cell lines and murine MLL-Af4 Lin-HSPCs decreases cell growth.**

**A****B****C****D**

**Supplemental Figure S2. IGF2BP3 depletion, using alternative guides targeting IGF2BP3, show expected changes in downregulation of known IGF2BP3 targets, decreased cell growth, and sensitization to menin-MLL inhibition.**

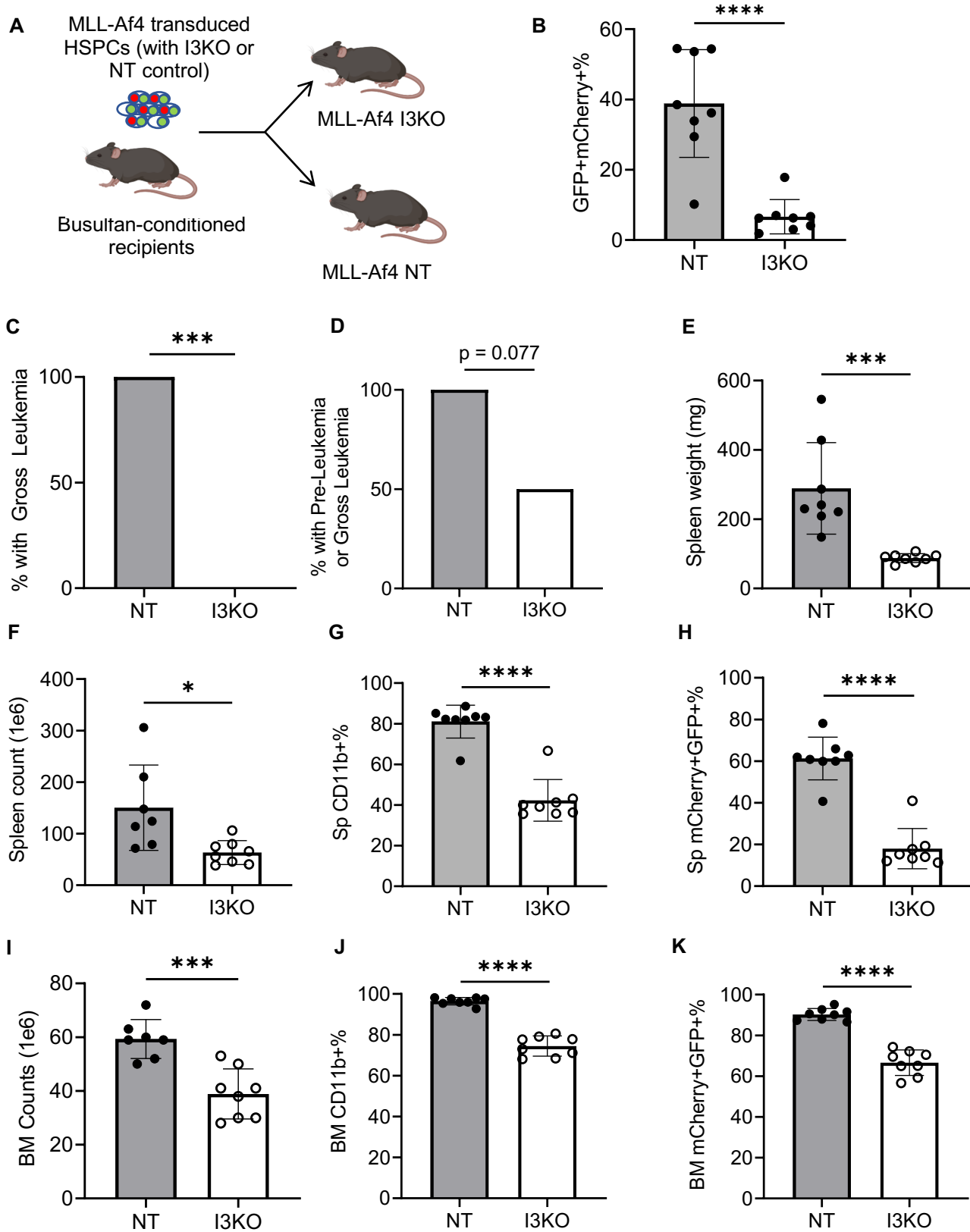
**A**

	Comparison	↑	↓	Total
I3KO vs NT	I3KO vs. NT DMSO	4346	1720	6066
MI-503 vs DMSO	NT 0.2 μM vs. DMSO	5	6	11
	NT 1.0 μM vs. DMSO	245	495	740
	I3KO 0.2 μM vs. DMSO	18	260	278
	I3KO 1.0 μM vs. DMSO	390	307	697

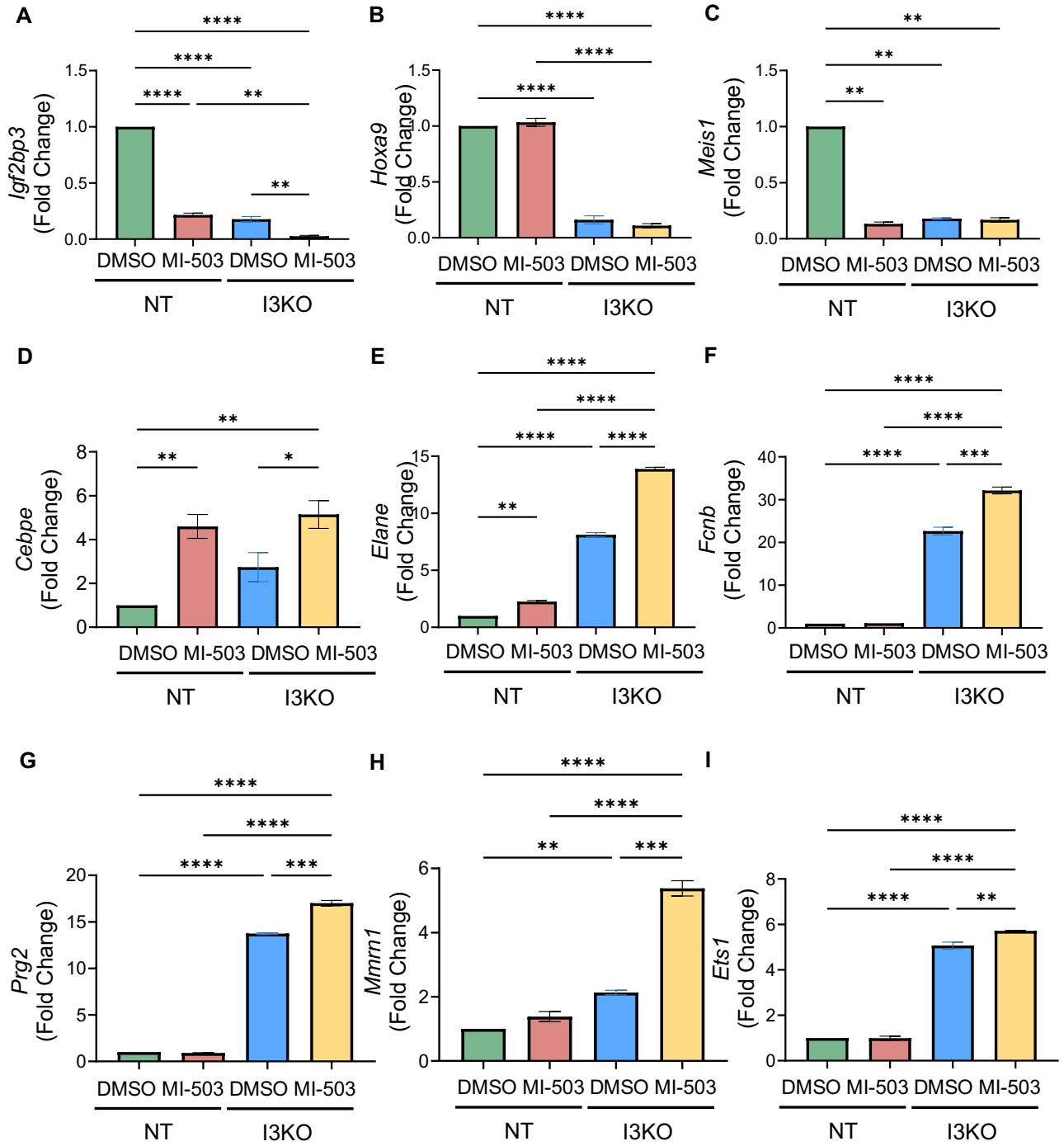


**Supplemental Figure S3. Differentially expressed genes in MLL-Af4 Lin- cells with depletion of IGF2BP3 and treatment with menin-MLL inhibitor, MI-503.**





**Supplemental Figure S4. IGF2BP3 knockdown via CRISPR/Cas9 leads to decreased leukemic burden *in vivo*.**



**Supplemental Figure S5. Validation of individual RT-qPCR genes upregulated in differentiation pathways in mice transplanted with MLL-Af4 leukemia cells, depleted for IGF2BP3 and treated with MI-503 *in vitro***

## Figure Legends

### **Figure 1. IGF2BP3 knockdown increases sensitivity of MLL-r leukemia cells to menin-MLL inhibition.**

**(A)** Western blot analysis showing IGF2BP3 knockdown in RS4;11, NALM6 and SEM cell lines and MLL-Af4 Lin<sup>-</sup> cells (using I3KO sgRNA targeting Igf2bp3 and NT, as a non-targeting guide).

**(B)** Western blot analysis showing IGF2BP3 expression in MI-503 treated MLL-Af4 Lin<sup>-</sup> cells depleted (I3KO) or non-depleted for IGF2BP3 (NT). Cells were treated with MI-503 (0.2 $\mu$ M, 1.0 $\mu$ M or DMSO control) for 4 days.

**(C-E)** Dose-response curves from cell viability assays, using CellTiterGlo, of human B-ALL cell lines, SEM, RS4;11, and NALM6, depleted (I3KO) versus non-depleted (NT) for IGF2BP3 treated with menin-MLL inhibitors (MI-503, MI-463, and MI-538) for 4 days. Viability has been normalized to DMSO control-treated cells not depleted for IGF2BP3 (NT DMSO), mean  $\pm$  SD, n = 6.

**(F)** Dose-response curves from cell viability assays, using CellTiterGlo, of MLL-Af4 Lin<sup>-</sup> cells depleted for IGF2BP3 (I3KO) versus non-depleted (NT) treated with menin-MLL- inhibitors for 4 days. Viability has been normalized to DMSO control-treated cells not depleted for IGF2BP3 (NT DMSO), mean  $\pm$  SD, n = 6.

**(G)** Increased caspase 3/7 activity of MI-503 treated MLL-Af4 Lin<sup>-</sup> cells depleted for IGF2BP3 (I3KO) versus non-depleted (NT). Cells treated with MI-503 for 4 days at various concentrations for dose-response. Caspase 3/7 activity measured using Caspase-Glo 3/7 and normalized to activity of DMSO-treated control, mean  $\pm$  SD, n = 3.

**(H)** Increased Annexin V positivity in MLL-Af4 Lin<sup>-</sup> I3KO cells (versus NT) and with MI- 503 treatment (versus DMSO control), mean  $\pm$  SD, n = 3. (One-way ANOVA with Bonferroni's multiple comparisons test, \*\*p<0.01, \*\*\*\*p<0.0001).

**(I-J)** Histograms from representative samples for Annexin V staining, analyzed by flow cytometry.

**Figure 2. Combined IGF2BP3 knockdown and menin inhibition increases differentiation of MLL-Af4 leukemia**

**(A)** Total colony numbers of MI-503 treated MLL-Af4 Lin<sup>-</sup> cells, depleted (I3KO) or non-depleted (NT) for IGF2BP3. MLL-Af4 Lin<sup>-</sup> NT and I3KO cells were treated with MI-503 0.5 $\mu$ M for 4 days and seeded in methylcellulose colony formation assays, at various initial seeding densities and cultured for 10 days.

**(B)** Total colony number was reduced with both I3KO and MI-503 treatment in methylcellulose colony formation assays, at initial seeding density of 2500, mean  $\pm$  SD, n =3, one way ANOVA with Bonferroni's multiple comparison's test (\*p <0.05, \*\*p<0.01).

**(C-E)** Proportion of CFU-GM colonies is decreased with both I3KO and MI-503 treatment with trend towards increased proportion of CFU-G and CFU-M colonies with I3KO and MI-503 treatment, mean  $\pm$  SD, n =2 (one-way ANOVA with Bonferroni's multiple comparisons test, \*\*p<0.01, \*\*\*p<0.001).

**(F)** Wright staining of cytopspins of MLL-Af4 Lin<sup>-</sup> cells depleted for IGF2BP3 (I3KO) or non-depleted (NT) treated with MI-503 0.5 $\mu$ M (or DMSO) for 4 days. Representative images shown.

**Figure 3. Increased upregulation of genes involved in differentiation with IGF2BP3 knockdown and menin-MLL inhibition in MLL-Af4 leukemia.**

**(A)** Volcano plot of differentially expressed genes with IGF2BP3 knockdown using DESeq analysis on RNA sequencing samples from MLL-Af4 Lin<sup>-</sup> NT or I3KO cells.

**(B)** Volcano plot of differentially expressed genes with MI-503 treatment using DESeq analysis on RNA sequencing samples from MLL-Af4 Lin<sup>-</sup> NT cells treated with MI-503 1.0 $\mu$ M vs DMSO.

**(C)** Pathway enrichment for upregulated genes with IGF2BP3 knockdown utilizing Metascape analysis webtool on MLL-Af4 Lin<sup>-</sup> IGF2BP3 DESeq dataset with an adjusted P < 0.05 cutoff.

**(D)** Pathway enrichment for upregulated genes with MI-503 treatment 1.0 $\mu$ M utilizing Metascape analysis webtool on MLL-Af4 Lin- NT MI-503 DESeq dataset with an adjusted P < 0.05 cutoff.

**(E)** Volcano plot of differentially expressed genes with MI-503 treatment in MLL-Af4 Lin- I3KO cells using DESeq analysis on RNA sequencing samples from MLL-Af4 Lin- I3KO cells treated with MI-503 1.0 $\mu$ M (versus DMSO control).

**(F)** Pathway enrichment for upregulated genes with MI-503 treatment at 1.0 $\mu$ M in MLL-Af4 Lin- I3KO cells utilizing Metascape analysis webtool on MLL-Af4 Lin- I3KO MI-503 DESeq dataset with an adjusted P < 0.05 cutoff.

**(G)** Venn diagram of shared upregulated genes with IGF2BP3 knockdown and MI-503 treatment in MLL-Af4 Lin- NT (blue) and I3KO (red) cells.

**Figure 4. Increased upregulation of genes involved in differentiation with IGF2BP3 knockdown and menin-MLL inhibition in MLL-Af4 leukemia, validated by RT-qPCR.**

**(A-C)** MI-503 treatment at 1.0 $\mu$ M leads to downregulation of *Igf2bp3* and known IGF2BP3 targets, *Myc*, *Hoxa9*, in MLL-Af4 Lin- cells.

**(D-K)** Upregulation of genes involved in differentiation with IGF2BP3 knockdown and MI-503 treatment.

mRNA expression was measured by RT-qPCR in MLL-Af4 Lin- cells depleted (I3KO) or non-depleted (NT) for IGF2BP3 and treated with MI-503 1.0 $\mu$ M or DMSO control. Expression shown as fold change from NT DMSO (mean  $\pm$  SD, n=2; one-way ANOVA with Bonferroni's multiple comparisons test ; \*p < 0.05, \*\* p <0.01, \*\*\*p< 0.001, \*\*\*\* p< 0.0001).

**Figure 5. Combinatorial inhibition of menin-MLL and IGF2BP3 decreases leukemic engraftment and burden and increases survival *in vivo*.**

**(A)** Schematic of BMT of MI-503 treated MLL-Af4 Lin<sup>-</sup> cells, depleted (I3KO) or non-depleted (NT) for IGF2BP3. Cells treated with MI-503 0.5 $\mu$ M (or DMSO control) for 5 days *in vitro* were transplanted into CD45.1 recipients following busulfan conditioning.

**(B)** Decreased peripheral blood engraftment of leukemic cells by CD45.2+% with MI-503 treatment and I3KO, at D42 (mean  $\pm$  SD, n = 8 mice per group; one way ANOVA with Bonferroni's multiple comparison's test, \* p < 0.05).

**(C)** Decreased proportion of mice with leukemia with MI-503 treatment and IGF2BP3 knockdown, (8 mice per group; Fisher's exact test, \* p < 0.05, \*\* p < 0.01). Mice were all evaluated at necropsy at 8.5 weeks after first mouse developed signs of terminal leukemia.

**(D-I)** Decreased leukemic burden seen with IGF2BP3 knockdown and MI-503 treatment in NT groups, based on total counts, CD11b+ counts and CD45.2+% by flow cytometry in spleen (D-F) and bone marrow (G-I) (mean  $\pm$  SD, n = 7-8 mice per group; one way ANOVA with Bonferroni's multiple comparison's test, \* p < 0.05, \*\* p < 0.01, \*\*\* p < 0.001, \*\*\*\* p < 0.0001). Mice were all evaluated at necropsy at 8.5 weeks after first mouse developed signs of terminal leukemia.

**(J)** Histopathology shows increased differentiation in spleens of mice transplanted with MLL-Af4 leukemia with IGF2BP3 depletion and MI-503 treatment, as seen by decreased nucleus-to-cytoplasm ratio and presence of mature granulocytes and megakaryocytes. Images are from representative mice in each group.

**(K-L)** Increased overall survival and leukemia survival with IGF2BP3 knockdown and MI-503 treatment in NT groups (n = 8 mice per group; Kaplan-Meier with log-rank test, \* p < 0.05, \*\* p < 0.01, \*\*\* p < 0.001). Comparisons made versus NT DMSO. Follow-up to 15 weeks with terminal sac of remaining mice.

**Supplemental Figure S1. IGF2BP3 knockdown in human B-ALL cell lines and murine MLL-Af4 Lin- HSPCs decreases cell growth.**

**(A)** Cell viability of SEM, RS4;11 and NALM6 cells depleted for IGF2BP3 (I3KO) or non-depleted (NT) was measured using CellTiterGlo, at multiple timepoints over 120 hours, and is plotted as fold change from D0, mean  $\pm$  SD, n =6.

**(B)** Schematic for generation of MLL-Af4 transformed HSPCs depleted for IGF2BP3 using CRISPR/Cas9 by harvesting HSPCs from bone marrow of Cas9-GFP mice, followed by MLL-Af4 transduction, and then retroviral transduction to introduce sgRNA targeting *Igf2bp3* or non-targeting guides.

**(C)** Cell viability of MLL-Af4 Lin- cells depleted for IGF2BP3 (I3KO) or non-depleted (NT) was measured using CellTiterGlo, at multiple timepoints over 120 hours, and is plotted as fold change from D0, mean  $\pm$  SD, n =6.

**(D)** Total colony number is reduced with IGF2BP3 knockdown in MLL-Af4 Lin- cells in methylcellulose colony formation assays. MLL-Af4 Lin- depleted for IGF2BP3 (I3KO) or non-depleted (NT) were seeded at an initial seeding density of 5000 cells, followed by 10 days in methylcellulose culture media. Mean  $\pm$  SD, n =2 (*t*- test, \*\* p < 0.01).

**(E)** Ki67 positivity by FACS staining in MLL-Af4 NT and I3KO Lin- cells treated with MI-503 0.5 $\mu$ M or DMSO control, mean  $\pm$  SD, n =2. (One-way ANOVA with Bonferroni multiple comparisons test)

**(F)** Total colony number of MI-463 treated MLL-Af4 NT and I3KO Lin- cells is reduced with IGF2BP3 knockdown in methylcellulose colony formation assays. MLL-Af4 Lin- cells depleted for IGF2BP3 (I3KO) or non-depleted (NT) were treated with MI-463 0.5 $\mu$ M or DMSO control for 5 days before seeding 500 cells into methylcellulose culture media for 12 days. Mean  $\pm$  SD, n =2 (One-way ANOVA with Bonferroni multiple comparisons test, \* p < 0.05, \*\* p < 0.01).

**Supplemental Figure S2. IGF2BP3 depletion, using alternative guides targeting IGF2BP3, show expected changes in downregulation of known IGF2BP3 targets, decreased cell growth, and sensitization to menin-MLL inhibition.**

**(A)** Western blot analysis showing IGF2BP3 knockdown in MLL-Af4 Lin<sup>-</sup> cells (using I3-TL1 sgRNA targeting *Igf2bp3* and NT-TL, as a non-targeting guide).

**(B)** Expression of *Igf2bp3* and known downstream targets was decreased, as measured by RT-qPCR (mean  $\pm$  SD, n=2; *t*-test; \**p* < 0.05, \*\* *p* < 0.01, \*\*\**p* < 0.001, \*\*\*\* *p* < 0.0001).

**(C)** Cell viability of MLL-Af4 Lin<sup>-</sup> cells depleted for IGF2BP3 (I3-TL1) and non-depleted (NT-TL) was measured using CellTiterGlo, at multiple timepoints over 120 hours, and is plotted as fold change from D0, mean  $\pm$  SD, n = 6.

**(D)** Dose-response curves from cell viability assays, using CellTiterGlo, of MLL-Af4 NT-TL and I3-TL1 Lin<sup>-</sup> cells treated with menin-MLL inhibitors, MI-503 and MI-463, for 4 days. Viability has been normalized to DMSO control-treated cells not depleted for IGF2BP3 (NT-TL DMSO), mean  $\pm$  SD, n = 6.

**Supplemental Figure S3. Differentially expressed genes in MLL-Af4 Lin<sup>-</sup> cells with depletion of IGF2BP3 and treatment with menin-MLL inhibitor, MI-503.**

**(A)** Number of differentially expressed genes with MI-503 treatment (0.2  $\mu$ M or 1.0  $\mu$ M) vs. DMSO control for 4 days and with IGF2BP3 depletion (I3KO vs. NT) in MLL-Af4 Lin<sup>-</sup> cells, by DESeq analysis on RNA sequencing samples.

**(B)** Pathway enrichment for downregulated genes with IGF2BP3 knockdown in MLL-Af4 Lin<sup>-</sup> cells utilizing Metascape analysis webtool on MLL-Af4 Lin<sup>-</sup> IGF2BP3 DESeq dataset with an adjusted *P* < 0.05 cutoff.

**(C)** Pathway enrichment for downregulated genes with MI-503 treatment (1.0  $\mu$ M) in MLL-Af4 Lin<sup>-</sup> NT utilizing Metascape analysis webtool on MLL-Af4 Lin<sup>-</sup> NT MI-503 DESeq dataset with an



adjusted  $P < 0.05$  cutoff.

**(D)** Pathway enrichment for downregulated genes with MI-503 treatment (1.0  $\mu\text{M}$ ) in MLL-Af4 Lin- I3KO utilizing Metascape analysis webtool on MLL-Af4 Lin- I3KO MI-503 DESeq dataset with an adjusted  $P < 0.05$  cutoff.

**Supplemental Figure S4. IGF2BP3 knockdown via CRISPR/Cas9 leads to decreased leukemic burden *in vivo*.**

**(A)** Schematic of bone marrow transplantation of MLL-Af4 Lin- knocked out for IGF2BP3 (I3KO) vs. control (NT), using CRISPR/Cas9 mediated knockdown.

**(B)** Decreased leukemic burden in peripheral blood with IGF2BP3 knockdown, based on GFP+mCherry+ cells by FACS at D23, mean  $\pm$ SD,  $n = 8$  mice/group ( $t$  test, \*\*\*\*  $p < 0.0001$ ).

**(C-D)** Decreased proportion of mice with gross leukemia or pre-leukemia in I3KO mice, in timed sac at D30. Leukemia defined as spleen weight  $> 150$  mg or presence of leukemic blasts in peripheral blood or bone marrow. Pre-leukemia was defined based on morphologic changes seen on histopathology.  $N = 8$  mice/group (Fisher's exact test, \*\*\*  $p < 0.001$ ).

**(E-H)** Decreased leukemic burden in spleens of I3KO mice, as shown by weights, counts, CD11b+% and mCherry+GFP+%, mean  $\pm$ SD,  $n = 8$  mice/group ( $t$  test, \*  $p < 0.05$ , \*\*\*  $p < 0.001$ , \*\*\*\*  $p < 0.0001$ ).

**(I-K)** Decreased leukemic burden in bone marrow of I3KO mice, as shown by counts, CD11b+% and mCherry+GFP+%, mean  $\pm$ SD,  $n = 8$  mice/group ( $t$  test, \*\*\*  $p < 0.001$ , \*\*\*\*  $p < 0.0001$ ).

**Supplemental Figure S5. Validation of individual RT-qPCR genes upregulated in differentiation pathways in mice transplanted with MLL-Af4 leukemia cells, depleted for IGF2BP3 and treated with MI-503 *in vitro***

Expression of genes of interest in bone marrow of mice transplanted with MI-503 treated MLL-Af4 Lin<sup>-</sup> NT or I3KO cells was measured by RT-qPCR. MLL-Af4 Lin<sup>-</sup> cells depleted (I3KO) or non-depleted (NT) for IGF2BP3 were treated with MI-503 0.5 $\mu$ M (MI-503) or carrier control (DMSO) for 5 days *in vitro* before transplantation. Mice were sacrificed at 8.5 weeks at first signs of first mouse developing terminal leukemia. Gene expression data shown from selected mice in each group. Shown as fold change from NT DMSO (mean  $\pm$  SD, n=2; one-way ANOVA with Bonferroni's multiple comparisons test ; \*p < 0.05, \*\* p <0.01, \*\*\*p< 0.001, \*\*\*\* p< 0.0001).

## Supplemental Tables

Supplemental Table 1. Single-guide RNA sequences and qPCR primer sequences

sgRNA sequences		
Name	Target	Sequence
NT	Non-targeting (human)	TAGACAACCGCGGAGAATGC
I3KO	<i>IGF2BP3</i> (human)	ATTCCAGTAAGGACCAAGCT
NT	Non-targeting (mouse)	GAGGTATTCGGCTCCGCG
I3KO	<i>Igf2bp3</i> (mouse)	GATGGCGCCAACGGACAGGG
NT-TL	Non-targeting (mouse)	GAATCCATTCAGTTTGTCTA
I3-TL1	<i>Igf2bp3</i> (mouse)	ATGTTGCAGTTCGGCTCGAT
Mouse qPCR primers		
Gene	Forward primer	Reverse primer
<i>Fcnb</i>	CACTATTCGTCTTGACCCTGAC	GGTCCAGTTGGTCCCTCTTT
<i>Prg2</i>	TGAAACTTCTGACTCCAAAAGCC	CGGCATTAGCTCTTCCCCT
<i>Mmrn1</i>	GGTCTTCAGGCTTACCAACAC	GAGTGGCCGAGAGCACTTG
<i>Ets1</i>	GGGTGATGTGGGCTGTGAAT	TGGGTAGGTAGGGTTGGCTC
<i>Cebpe</i>	GCAGCCACTTGAGTTCTCAGG	GATGTAGGCGGAGAGGTCGAT
<i>Cebpd</i>	CRACTTCAGCGCCTACATTGA	CTAGCGACAGACCCCACAC
<i>Elane</i>	AGCAGTCCATTGTGTGAACGG	CACAGCCTCCTCGGATGAAG
<i>Pram1</i>	GAAACCTTCATATCCTCAAGCCA	GCTGTGGATGCTTCTTAGGGAA
<i>Igf2bp3</i>	CCTGGTGAAGACGGGCTAC	TCAACTTCCATCGGTTTCCCA
<i>Hoxa9</i>	AAAACACCAGACGCTGGAAC	TCT TTTGCTCGGTCTTGTT
<i>Myc</i>	ATGCCCTCAACGTGAACTTC	CGCAACATAGGATGGAGAGCA
<i>Spib</i>	AGGAGTCTTCTACGACCTGGA	GAAGGCTTCATAGGGAGCGAT

<i>PML</i>	CAGGCCCTAGAGCTGTCTAAG	ATACACTGGTACAGGGTGTGC
<i>CDK6</i>	TCTCACAGAGTAGTGCATCGT	CGAGGTAAGGGCCATCTGAAAA
<i>L32</i>	AAGCGAAACTGGCGGAAAC	TAACCGATGTTGGGCATCAG
<i>Hoxa10</i>	GAAGAAACGCTGCCCTTACA	GATTCGGTTTTCTCGGTTCA
<i>Hoxa7</i>	ATGTGAACGCGCTTTTTAGC	ATTGTATAAGCCCGGCACAG
<i>Meis1</i>	CTCCCTTCAGTGCAGCAGTT	CTGTCAATCACAGGCGAGGT

*Supplemental Table 2. Antibodies for flow cytometry*

<b>Antibody</b>	<b>Vendor/Catalog Number</b>
CD45.1 APC/Cy7	Biolegend, 110716
CD45.2 APC	Biolegend 109814
CD11b PE/Cy7	Biolegend, 10216
B220 PerCP/Cy5.5	Biolegend, 103236
Annexin V BV421	BD Biosciences, B563873
Ki67 PerCP/Cy5.5	Biolegend, 652423
CD3e-Biotin	Biolegend 100304
CD4-Biotin	eBioscience 13-0041-82
CD8-Biotin	Biolegend 100704
B220-Biotin	Biolegend 103204
NK1.1-Biotin	Biolegend 108703
Ter119-Biotin	Biolegend 116204
TCR $\beta$	Biolegend 118103
TCR $\gamma\delta$	Biolegend 109203

## **Acknowledgments**

We thank members of the Rao lab for helpful discussions regarding the research. This work was supported by R01CA264986 from the National Institutes of Health (DSR, JRS) and R03CA251854 (DSR). TLL was supported by the Hematology Training Grant (T32HL066992), Tumor Immunology training Grant (NIH T32CA009120), a training grant from the Broad Stem Cell Research Center, and the UCLA Specialty Training and Advanced Research Program. TMT was supported by the Tumor Cell Biology Training Grant (NIH T32 CA009056). Flow cytometry was performed in the UCLA Jonsson Comprehensive Cancer Center (JCCC) and Center for AIDS Research Flow Cytometry Core Facility that is supported by National Institutes of Health awards AI-28697, and award number P30CA016042, the JCCC, the UCLA AIDS Institute, and the David Geffen School of Medicine at UCLA.

## References

1. Yu, B.D., et al., *Altered Hox expression and segmental identity in Mll-mutant mice*. Nature, 1995. **378**(6556): p. 505-8.
2. Hess, J.L., et al., *Defects in yolk sac hematopoiesis in Mll-null embryos*. Blood, 1997. **90**(5): p. 1799-806.
3. Luo, Z., C. Lin, and A. Shilatifard, *The super elongation complex (SEC) family in transcriptional control*. Nat Rev Mol Cell Biol, 2012. **13**(9): p. 543-7.
4. Cucinotta, C.E. and K.M. Arndt, *SnapShot: Transcription Elongation*. Cell, 2016. **166**(4): p. 1058-1058 e1.
5. Collins, C.T. and J.L. Hess, *Deregulation of the HOXA9/MEIS1 axis in acute leukemia*. Curr Opin Hematol, 2016. **23**(4): p. 354-61.
6. Mullighan, C.G., et al., *Genome-wide analysis of genetic alterations in acute lymphoblastic leukaemia*. Nature, 2007. **446**(7137): p. 758-64.
7. Radtke, I., et al., *Genomic analysis reveals few genetic alterations in pediatric acute myeloid leukemia*. Proc Natl Acad Sci U S A, 2009. **106**(31): p. 12944-9.
8. Lin, S., et al., *Instructive Role of MLL-Fusion Proteins Revealed by a Model of t(4;11) Pro-B Acute Lymphoblastic Leukemia*. Cancer Cell, 2016. **30**(5): p. 737-749.
9. Krivtsov, A.V., et al., *Transformation from committed progenitor to leukaemia stem cell initiated by MLL-AF9*. Nature, 2006. **442**(7104): p. 818-22.
10. Barabe, F., et al., *Modeling human MLL-AF9 translocated acute myeloid leukemia from single donors reveals RET as a potential therapeutic target*. Leukemia, 2017. **31**(5): p. 1166-1176.
11. Yokoyama, A., et al., *The menin tumor suppressor protein is an essential oncogenic cofactor for MLL-associated leukemogenesis*. Cell, 2005. **123**(2): p. 207-18.

12. Chen, Y.X., et al., *The tumor suppressor menin regulates hematopoiesis and myeloid transformation by influencing Hox gene expression*. Proc Natl Acad Sci U S A, 2006. **103**(4): p. 1018-23.
13. Caslini, C., et al., *Interaction of MLL amino terminal sequences with menin is required for transformation*. Cancer Res, 2007. **67**(15): p. 7275-83.
14. Palanichamy, J.K., et al., *RNA-binding protein IGF2BP3 targeting of oncogenic transcripts promotes hematopoietic progenitor proliferation*. J Clin Invest, 2016. **126**(4): p. 1495-511.
15. Tran, T.M., et al., *The RNA-binding protein IGF2BP3 is critical for MLL-AF4-mediated leukemogenesis*. Leukemia, 2022. **36**(1): p. 68-79.
16. Chan, A.K.N. and C.W. Chen, *Rewiring the Epigenetic Networks in MLL-Rearranged Leukemias: Epigenetic Dysregulation and Pharmacological Interventions*. Front Cell Dev Biol, 2019. **7**: p. 81.
17. Bernt, K.M. and S.A. Armstrong, *Targeting epigenetic programs in MLL-rearranged leukemias*. Hematology Am Soc Hematol Educ Program, 2011. **2011**: p. 354-60.
18. He, S., et al., *Menin-MLL inhibitors block oncogenic transformation by MLL-fusion proteins in a fusion partner-independent manner*. Leukemia, 2016. **30**(2): p. 508-13.
19. Kuhn, M.W., et al., *Targeting Chromatin Regulators Inhibits Leukemogenic Gene Expression in NPM1 Mutant Leukemia*. Cancer Discov, 2016. **6**(10): p. 1166-1181.
20. Borkin, D., et al., *Pharmacologic inhibition of the Menin-MLL interaction blocks progression of MLL leukemia in vivo*. Cancer Cell, 2015. **27**(4): p. 589-602.
21. Krivtsov, A.V., et al., *A Menin-MLL Inhibitor Induces Specific Chromatin Changes and Eradicates Disease in Models of MLL-Rearranged Leukemia*. Cancer Cell, 2019. **36**(6): p. 660-673 e11.
22. Klossowski, S., et al., *Menin inhibitor MI-3454 induces remission in MLL1-rearranged and NPM1-mutated models of leukemia*. J Clin Invest, 2020. **130**(2): p. 981-997.

23. Jaiswal, A.K., et al., *Focused CRISPR-Cas9 genetic screening reveals USO1 as a vulnerability in B-cell acute lymphoblastic leukemia*. *Sci Rep*, 2021. **11**(1): p. 13158.
24. Cozzio, A., et al., *Similar MLL-associated leukemias arising from self-renewing stem cells and short-lived myeloid progenitors*. *Genes Dev*, 2003. **17**(24): p. 3029-35.
25. Love, M.I., W. Huber, and S. Anders, *Moderated estimation of fold change and dispersion for RNA-seq data with DESeq2*. *Genome Biol*, 2014. **15**(12): p. 550.
26. Zhou, Y., et al., *Metascape provides a biologist-oriented resource for the analysis of systems-level datasets*. *Nat Commun*, 2019. **10**(1): p. 1523.
27. Langmead, B. and S.L. Salzberg, *Fast gapped-read alignment with Bowtie 2*. *Nat Methods*, 2012. **9**(4): p. 357-9.
28. Dobin, A., et al., *STAR: ultrafast universal RNA-seq aligner*. *Bioinformatics*, 2013. **29**(1): p. 15-21.
29. O'Connell, R.M., et al., *Lentiviral vector delivery of human interleukin-7 (hIL-7) to human immune system (HIS) mice expands T lymphocyte populations*. *PLoS One*, 2010. **5**(8): p. e12009.
30. Minuesa, G., et al., *Small-molecule targeting of MUSASHI RNA-binding activity in acute myeloid leukemia*. *Nat Commun*, 2019. **10**(1): p. 2691.
31. Muralidharan, R., et al., *HuR-targeted small molecule inhibitor exhibits cytotoxicity towards human lung cancer cells*. *Sci Rep*, 2017. **7**(1): p. 9694.
32. Ahmed, R., et al., *Molecular Targeting of HuR Oncoprotein Suppresses MITF and Induces Apoptosis in Melanoma Cells*. *Cancers (Basel)*, 2021. **13**(2).
33. Wang, L., et al., *Small-Molecule Inhibitors Disrupt let-7 Oligouridylation and Release the Selective Blockade of let-7 Processing by LIN28*. *Cell Rep*, 2018. **23**(10): p. 3091-3101.
34. Itskovich, S.S., et al., *MBNL1 regulates essential alternative RNA splicing patterns in MLL-rearranged leukemia*. *Nat Commun*, 2020. **11**(1): p. 2369.



35. Dzama, M.M., et al., *Synergistic targeting of FLT3 mutations in AML via combined menin-MLL and FLT3 inhibition*. Blood, 2020. **136**(21): p. 2442-2456.
36. Aubrey, B.J., et al., *IKAROS and MENIN coordinate therapeutically actionable leukemogenic gene expression in MLL-r acute myeloid leukemia*. Nat Cancer, 2022. **3**(5): p. 595-613.
37. Costello, R.T., et al., *Human acute myeloid leukemia CD34+/CD38- progenitor cells have decreased sensitivity to chemotherapy and Fas-induced apoptosis, reduced immunogenicity, and impaired dendritic cell transformation capacities*. Cancer Res, 2000. **60**(16): p. 4403-11.
38. Eppert, K., et al., *Stem cell gene expression programs influence clinical outcome in human leukemia*. Nat Med, 2011. **17**(9): p. 1086-93.
39. Bachas, C., et al., *The role of minor subpopulations within the leukemic blast compartment of AML patients at initial diagnosis in the development of relapse*. Leukemia, 2012. **26**(6): p. 1313-20.
40. Shlush, L.I., et al., *Tracing the origins of relapse in acute myeloid leukaemia to stem cells*. Nature, 2017. **547**(7661): p. 104-108.
41. Ennajdaoui, H., et al., *IGF2BP3 Modulates the Interaction of Invasion-Associated Transcripts with RISC*. Cell Rep, 2016. **15**(9): p. 1876-83.
42. Xueqing, H., et al., *IGF2BP3 May Contributes to Lung Tumorigenesis by Regulating the Alternative Splicing of PKM*. Front Bioeng Biotechnol, 2020. **8**: p. 679.
43. Huang, H., et al., *Recognition of RNA N(6)-methyladenosine by IGF2BP proteins enhances mRNA stability and translation*. Nat Cell Biol, 2018. **20**(3): p. 285-295.
44. Elcheva, I.A. and V.S. Spiegelman, *Targeting RNA-binding proteins in acute and chronic leukemia*. Leukemia, 2021. **35**(2): p. 360-376.

### **CHAPTER III:**

#### Conclusions and Future Directions

## Conclusions

MLL-rearranged leukemias are a subtype of leukemias associated with a poor prognosis and have unique biological features in which they are characterized by their MLL-fusion proteins (MLL-FPs) that drive leukemia through dysregulation of critical transcriptional networks and co-regulatory mechanisms. While novel therapeutic strategies for MLL-rearranged leukemias have been primarily directed at epigenetic dysregulation and concurrent downstream activating mutations or kinases, post-transcriptional gene regulation mechanisms have recently emerged as important mediators in MLL-FP leukemogenesis and have the potential to be potent combinatorial therapeutic targets. Here, we build on prior work that has shown that the RNA binding protein, IGF2BP3, is an important regulator and amplifier of MLL-AF4 leukemogenesis and a promising therapeutic target and to explore a novel therapeutic strategy of combinatorial targeting of leukemia at the transcriptional and post-transcriptional level by investigating combined inhibition of menin-MLL and IGF2BP3 in models of MLL-AF4 driven leukemia.

We found that IGF2BP3 depletion sensitized human MLL-AF4 leukemia cells and murine MLL-Af4 HSPCs to menin-MLL inhibition *in vitro*, with increased inhibition in cell growth and increased apoptosis. Mechanistically, we found that combined menin-MLL inhibition and IGF2BP3 knockdown led to increased differentiation of MLL-Af4 leukemia as seen in functional readouts. These findings were further supported by gene expression analyses showing an upregulation of differentiation genes with menin-MLL inhibition and IGF2BP3 knockdown both *in vitro* and *in vivo*. Ongoing analyses are being performed to explore potential mechanisms through which menin-MLL inhibition and IGF2BP3 knockdown lead to increased differentiation and their combined anti-leukemic effects, including curating differentially expressed genes (with MI-503 treatment or IGF2BP3 knockdown) as known MLL-Af4 (or MLL-AF4) targets and/or known IGF2BP3 targets, using published and available MLL-Af4 (MLL-AF4) chromatin-

immunoprecipitation sequencing (ChIP-seq) data [1-3] and our group's IGF2BP3 crosslinking immunoprecipitation data [4, 5].

Lastly, we studied the combined effects of menin-MLL inhibition with MI-503 treatment *ex vivo* and IGF2BP3 knockdown on the ability of treated cells to establish MLL-Af4 leukemia in mice and found decreased leukemic engraftment and burden in mice transplanted with MLL-Af4 I3KO cells, with a further decrease seen in mice transplanted with MI-503 treated MLL-Af4 I3KO cells. We also saw a survival benefit in mice transplanted with MLL-Af4 I3KO cells versus MI-503 treated MLL-Af4 NT cells but did not observe an additional survival benefit to IGF2BP3 depletion with MI-503 treatment. The lack of a combined effect on survival *in vivo* may be a limitation of our study with regards to powering the study to detect a difference in survival based on the number of animals, leukemic burden in control mice, or length of follow-up. We currently addressing these limitations with repeat experiments, but these results also highlight the potent effect of targeting IGF2BP3 alone, especially in comparison to menin-MLL inhibition, a novel therapeutic strategy that is currently in early clinical trials. Altogether, our studies confirm a role for IGF2BP3 as an oncogenic amplifier of MLL-AF4 driven leukemia and suggest a promising and novel combinatorial approach to targeting leukemia at the transcriptional and post-transcriptional level.

### **Using Cas9-expressing HSPCs transformed by retroviral introduction of oncogenes**

In addition to presenting the conclusions of our work and future directions, we would like to discuss the model system used in our studies, immortalized Cas9-expressing HSPCs following retroviral introduction of oncogenes. This has been a powerful tool for us to study MLL-Af4 leukemogenesis and has the flexibility to be a tool to model and study other types of leukemia. Lin et al made a significant advance in developing a high-titer MLL-Af4 retrovirus that contained the N-terminal sequence of human MLL with the murine homolog of the human AF4 protein that allowed for the transformation of murine HSPCs and human CD34+ HSPCs isolated from cord

blood [1]. These MLL-Af4 transformed HSPCs were immortalized in *in vitro* cell culture and reliably engrafted in sub-lethally irradiated C57BL/6 mice and manifested a leukemia with myelomonocytic morphology [1]. Interestingly, human CD34+ MLL-Af4 transformed HSPCs initiated an acute lymphoblastic leukemia when transplanted into NSG mice. While there are some limitations in using an MLL-Af4 induced AML to study MLL-AF4 leukemogenesis, as this typically gives rise to an acute lymphoblastic leukemia, this model recapitulates the molecular aspects of MLL-AF4 leukemia with significant overlap in targets, with known human MLL-AF4 targets as identified by ChIP-seq, and gene expression signatures of MLL-AF4 leukemia cells. Therefore, this model of MLL-Af4 transformed HSPCs has provided us with a powerful tool to study MLL-Af4 driven leukemia *in vitro* with functional readouts such as cell growth, proliferation, apoptosis, and colony formation and *in vivo* with leukemic engraftment in a syngeneic, immunocompetent mouse model, in addition to studying the changes in gene expression at the transcriptional, post-transcriptional and protein levels. We can subsequently attempt to validate and extend the relevance of our findings from this model of MLL-Af4 leukemia into a human ALL model, using MLL-Af4 transformed human CD34+ cells.

Furthermore, we have expanded on the utility of this system as a model by harvesting our HSPCs from Cas9 mice, which provides great flexibility to quickly knockdown genes of interest using CRISPR/Cas9 based strategies or more broadly perform CRISPR-based functional genomic screens to dissect loss-of and gain-of function phenotypes *in vitro* and *in vivo* [6]. We have also been able to generate other model systems of leukemia using retroviral vectors expression known oncogenes or fusion proteins, including MLL-AF9, AML1-ETO, MYC, NRAS<sup>G12D</sup>, NPM1c, and FLT3-ITD, highlighting the flexibility and applicability of this approach to generate novel tools.

## Future Directions

### *Role of IGF2BP3 in maintenance of leukemia*

While our work has highlighted the importance of IGF2BP3 in the initiation of MLL-Af4 leukemia through knockout models *in vitro* and *in vivo* for IGF2BP3, ongoing and future studies have been aimed at assessing the role of IGF2BP3 in maintenance of leukemia. We have attempted to develop conditional knockout systems for IGF2BP3 in hematopoietic cells using the Cre-Lox recombination system, under the control of an interferon-inducible promoter (Mx1-Cre) and tamoxifen-inducible promoter (CreERT2). As previously reported, we engineered *Igf2bp3*<sup>flox/flox</sup> mice in collaboration with the University of California Irvine Transgenic Mouse Facility [4]. To generate an inducible knockout in hematopoietic cells, we bred *Igf2bp3*<sup>flox/flox</sup> mice to Mx1-Cre mice to generate *Mx1-Cre; Igf2bp3*<sup>flox/flox</sup> mice and were successfully able to induce *Igf2bp3* deletion upon polyinosinic:polycytidylic administration. To evaluate the requirement of *Igf2bp3* in MLL-Af4 leukemia, we next looked to transform HSPCs from *Mx1-Cre; Igf2bp3*<sup>flox/flox</sup> mice by overexpression of MLL-Af4 using retroviral transduction, but unfortunately, found spontaneous deletion of *Igf2bp3* following transformation. This phenomenon is unfortunately a known issue for inducible Cre-Lox systems and has been reported in the setting of retroviral introduction of oncogenes, which is thought to induce an interferon response, the same signal for *Mx1-Cre* induction [7]. We unfortunately found similar background deletion upon MLL-Af4 retroviral transduction in *CreERT2; Igf2bp3*<sup>flox/flox</sup> HSPCs, limiting our ability to use either model as a conditional knockout system to assess the role of IGF2BP3 in maintenance of leukemia.

We are currently developing a targeted protein degradation system for the inducible deletion of IGF2BP3 upon administration of small molecule degraders based on the dTAG system [8, 9] in order to address the question of IGF2BP3's requirement in the maintenance of MLL-Af4 leukemia. We would plan to knock-in FKBP12<sup>F36V</sup> at the endogenous *Igf2bp3* locus in MLL-Af4 transformed HSPCs and first validate the ability to degrade IGF2BP3 rapidly upon dTAG-13

administration *in vitro* and confirm the inhibitory effect of IGF2BP3 degradation on leukemic cell growth *in vitro*. We would then transplant these cells into busulfan-conditioned CD45.1+ recipients following our established protocols and would expect engraftment of MLL-Af4 leukemia around 4 weeks based on our prior experience with this transplant model. Following leukemic engraftment, as confirmed by peripheral blood analysis for CD45.2+ cells, we would then treat with dTAG-13 *in vivo* to degrade IGF2BP3 quickly and assess its impact on leukemia maintenance. Leukemic burden will be monitored by serial peripheral bleeds with flow cytometric analysis for CD45.2+ and then at the time of necropsy, in peripheral blood, bone marrow, and spleen by counts, flow cytometry, and histopathology.

#### *Role of IGF2BP3 in leukemic stem cells and leukemia relapse*

Our work has implicated IGF2BP3 in supporting leukemic stem cell function (LSC) through functional readouts of the effects of *Igf2bp3* deletion *in vitro*, showing decreased colony formation in endpoint colony formation assays, and *in vivo* with decreased leukemic engraftment in bone marrow transplantation assays and in serial, secondary bone marrow transplants [5, Chapter 2]. Future experiments are aimed at identifying and better characterizing these LSCs within our model systems for MLL-Af4 leukemia with a priori defined markers, using a combination of immunophenotyping with flow cytometry analysis [10-12], enrichment using reactive-oxygen species based sorting [13-15], and single cell RNA sequencing [16-18]. Furthermore, given the difficulty of identifying such a priori markers in LSCs, single-cell RNA sequencing would give us the opportunity to better dissect and characterize the different stem/progenitor populations that are supported by IGF2BP3 and insight into the critical gene expression programs underlying leukemogenesis.

Identification of such markers or expression profile specific to LSCs would also allow us to further study the role of IGF2BP3 in the setting of relapse or drug resistance, two major clinical

scenarios in which LSCs have been implicated [19-22]. To study the role of IGF2BP3 in the relapse setting, we will utilize a leukemia relapse model in which mice with MLL-Af4 leukemia are treated with cytarabine, which causes an initial leukemic remission followed by subsequent relapse [23]. IGF2BP3 degradation would then be induced using the dTAG system described above to determine the effect of IGF2BP3 on leukemic progression in the relapse setting and on the number of leukemic stem cells. We could design similar studies in drug resistant models, in which we deplete IGF2BP3 from drug-resistant leukemic cells that have grown out *in vitro* or *in vivo* and see if loss of IGF2BP3 restores sensitivity to drug treatment and assess if there is a correlation with the number of LSCs.

#### *Molecular mechanisms of IGF2BP3*

Our work here has highlighted IGF2BP3 as an oncogenic amplifier of MLL-Af4 mediated leukemogenesis, but much remains to be answered with regards to the molecular mechanisms of its function as an RNA binding protein. In Chapter I, we briefly summarized work done by our group and others, implicating IGF2BP3's function in alternative pre-mRNA splicing [5] and RNA stability based on its probable association with the RNA-induced silencing complex (RISC) and microRNAs at the 3'UTR of oncogenic transcripts [4, 24] and interactions with m<sup>6</sup>A-modified RNAs [25]. We have postulated potential models for how IGF2BP3 is a multifunctional RNA binding protein that acts as an oncogenic m<sup>6</sup>A reader, interacts with RISC to protect oncogenic transcripts from microRNA-mediated decay, and mediates alternative splicing events at the 3' splice site, to regulate and amplify the aberrant gene expression program underlying leukemogenesis.

We will plan to investigate how alternative splicing of known oncogenic IGF2BP3 targets (such as *Hoxa7*, *Hoxa9*, *Cdk6*, and *Bcl2*) affects leukemogenesis through (1) complementation experiments with spliced isoforms in MLL-Af4/I3KO Lin<sup>-</sup> cells and (2) enforced isoform-specific expression through deletion of splice sites using CRISPR/Cas9 homology-directed repair in MLL-



Af4 Lin<sup>-</sup> cells. Functional readouts will include *in vitro* cell growth and colony formation assays and *in vivo* transplantation assays for leukemic initiation, as previously used by our group [5, 26] and within this thesis in Chapter 2 and discussion of the MLL-Af4 Lin<sup>-</sup> system in this chapter.

We are also planning to investigate, in collaboration with our colleagues in the Sanford group at UCSC, how IGF2BP3 targets and stabilizes m<sup>6</sup>A modified mRNAs and potentially modulates the interaction between RISC and its target transcripts, which are possibly enriched for m<sup>6</sup>A modifications. We would first look globally for the presence of m<sup>6</sup>A modified transcripts in our MLL-Af4 I3KO and NT Lin<sup>-</sup> cells using m<sup>6</sup>A CLIP and then overlap these with our existing RNA-Seq data from MLL-Af4 I3KO and NT Lin<sup>-</sup> cells identifying transcripts that are differentially expressed with IGF2BP3 knockdown and IGF2BP3 CLIP data identifying direct targets of IGF2BP3. This global analysis would allow us to identify m<sup>6</sup>A-modified RNAs that are likely to be regulated by IGF2BP3 and test the premise of whether IGF2BP3 acts as an oncogenic m<sup>6</sup>A reader within our MLL-Af4 leukemia model. Subsequent validation would be performed using RNA immunoprecipitation with m<sup>6</sup>A, followed by RT-qPCR to quantify RNA bound. We can further validate the specificity of IGF2BP3 binding to these m<sup>6</sup>A modified targets of interest and explore whether IGF2BP3 stabilizes m<sup>6</sup>A modified RNAs by protecting them from RISC-mediated degradation by assessing the impact of m<sup>6</sup>A loss on binding to IGF2BP3 and the RISC-associated protein AGO2, by inhibiting METTL3 and METTL14, enzymes that catalyze the N<sup>6</sup>-adenosine methylation, and performing subsequent RNA immunoprecipitations with IGF2BP3 and AGO2, followed by RT-qPCR to quantify RNA bound.

To further understand how IGF2BP3 modulates mRNA-RISC interactions, we would perform a global analysis of transcripts whose association with the RISC protein AGO2 may be regulated by IGF2BP3. We would generate MLL-Af4 I3KO and NT Lin<sup>-</sup> cells from Halo-Ago2 mice that express the endogenous Halo-Ago2 allele to facilitate AGO2 immunoprecipitation experiments [27]. AGO2-mRNA complexes would be immunoprecipitated from MLL-Af4 I3KO and

NT Lin- cells and then sequenced to assess for global changes in AGO2 binding and delineate transcripts of interest whose binding to AGO2 correlates with changes in IGF2BP3 expression. Based on our model, we would anticipate that oncogenic transcripts that are known IGF2BP3 targets, such as *Hoxa9*, might be found to be more susceptible to AGO2 binding upon IGF2BP3 knockdown and could be validated in subsequent RNA immunoprecipitations with AGO2.

#### *Development of small molecule inhibitors against IGF2BP3*

Studies, including our own work implicating IGF2BP3 in the pathogenesis of MLL-Af4 mediated leukemogenesis, have highlighted IGF2BP3 as a potential therapeutic target in multiple cancers. RNA binding proteins have emerged as a novel class of therapeutics for which small molecule inhibitors are being developed. Ongoing and future work in our group is aimed at targeting IGF2BP3 therapeutically by developing small molecule inhibitors using strategies adapted from prior large-scale screens based on inhibiting the RNA-protein interaction [28, 29]. Development of a small molecule inhibitor against IGF2BP3 is an exciting next step into developing IGF2BP3 as a therapeutic target and will also allow us to address several of the limitations of our current tools for study, using deletion of *IGF2BP3* with CRISPR/Cas9-mediated knockdown, genetic knockouts, and small-interfering or short hairpin RNAs against *IGF2BP3*.

#### *Use of menin-MLL inhibitors for the treatment of patients with leukemia*

Two menin-MLL inhibitors, SNDX-5613 and KO-539, are currently in clinical trials for patients with relapsed/refractory acute myeloid leukemia with MLL-rearrangement or NPM1c mutation, with the latter drug trial currently being active at our institution. Given our interest in developing therapies for patients with MLL-rearranged leukemia and our work in studying how targeting IGF2BP3 can enhance the anti-leukemic effects of menin-MLL inhibitors, we have an excellent opportunity to further understand how patients respond to menin-MLL inhibition by

obtaining patient samples at the time of diagnosis, response, progression, or relapse. Bulk and single-cell RNA sequencing of leukemic blasts from patient bone marrow or peripheral blood may help identify biomarkers of response, one of which may be IGF2BP3 expression, and mechanisms of relapse to menin-MLL inhibition. Understanding how these leukemias respond and relapse to treatment will help us design future combination therapeutic strategies with menin-MLL inhibition and clarify how IGF2BP3 may be a useful therapeutic target.

## References

1. Lin, S., et al., *Instructive Role of MLL-Fusion Proteins Revealed by a Model of t(4;11) Pro-B Acute Lymphoblastic Leukemia*. *Cancer Cell*, 2016. **30**(5): p. 737-749.
2. Guenther, M.G., et al., *Global and Hox-specific roles for the MLL1 methyltransferase*. *Proc Natl Acad Sci U S A*, 2005. **102**(24): p. 8603-8.
3. Wilkinson, A.C., et al., *RUNX1 is a key target in t(4;11) leukemias that contributes to gene activation through an AF4-MLL complex interaction*. *Cell Rep*, 2013. **3**(1): p. 116-27.
4. Palanichamy, J.K., et al., *RNA-binding protein IGF2BP3 targeting of oncogenic transcripts promotes hematopoietic progenitor proliferation*. *J Clin Invest*, 2016. **126**(4): p. 1495-511.
5. Tran, T.M., et al., *The RNA-binding protein IGF2BP3 is critical for MLL-AF4-mediated leukemogenesis*. *Leukemia*, 2022. **36**(1): p. 68-79.
6. Joung, J., et al., *Genome-scale CRISPR-Cas9 knockout and transcriptional activation screening*. *Nat Protoc*, 2017. **12**(4): p. 828-863.
7. Velasco-Hernandez, T., et al., *Potential Pitfalls of the Mx1-Cre System: Implications for Experimental Modeling of Normal and Malignant Hematopoiesis*. *Stem Cell Reports*, 2016. **7**(1): p. 11-8.
8. Nabet, B., et al., *The dTAG system for immediate and target-specific protein degradation*. *Nat Chem Biol*, 2018. **14**(5): p. 431-441.
9. Nabet, B., et al., *Rapid and direct control of target protein levels with VHL-recruiting dTAG molecules*. *Nat Commun*, 2020. **11**(1): p. 4687.
10. Somervaille, T.C. and M.L. Cleary, *Identification and characterization of leukemia stem cells in murine MLL-AF9 acute myeloid leukemia*. *Cancer Cell*, 2006. **10**(4): p. 257-68.
11. Somervaille, T.C., et al., *Hierarchical maintenance of MLL myeloid leukemia stem cells employs a transcriptional program shared with embryonic rather than adult stem cells*. *Cell Stem Cell*, 2009. **4**(2): p. 129-40.

12. Joseph, C., et al., *Deciphering hematopoietic stem cells in their niches: a critical appraisal of genetic models, lineage tracing, and imaging strategies*. Cell Stem Cell, 2013. **13**(5): p. 520-33.
13. Jang, Y.Y. and S.J. Sharkis, *A low level of reactive oxygen species selects for primitive hematopoietic stem cells that may reside in the low-oxygenic niche*. Blood, 2007. **110**(8): p. 3056-63.
14. Diehn, M., et al., *Association of reactive oxygen species levels and radioresistance in cancer stem cells*. Nature, 2009. **458**(7239): p. 780-3.
15. Stevens, B.M., et al., *Enriching for human acute myeloid leukemia stem cells using reactive oxygen species-based cell sorting*. STAR Protoc, 2021. **2**(1): p. 100248.
16. Moignard, V., et al., *Characterization of transcriptional networks in blood stem and progenitor cells using high-throughput single-cell gene expression analysis*. Nat Cell Biol, 2013. **15**(4): p. 363-72.
17. Wilson, N.K., et al., *Combined Single-Cell Functional and Gene Expression Analysis Resolves Heterogeneity within Stem Cell Populations*. Cell Stem Cell, 2015. **16**(6): p. 712-24.
18. Zhang, P., et al., *Single-cell RNA sequencing to track novel perspectives in HSC heterogeneity*. Stem Cell Res Ther, 2022. **13**(1): p. 39.
19. Costello, R.T., et al., *Human acute myeloid leukemia CD34<sup>+</sup>/CD38<sup>-</sup> progenitor cells have decreased sensitivity to chemotherapy and Fas-induced apoptosis, reduced immunogenicity, and impaired dendritic cell transformation capacities*. Cancer Res, 2000. **60**(16): p. 4403-11.
20. Eppert, K., et al., *Stem cell gene expression programs influence clinical outcome in human leukemia*. Nat Med, 2011. **17**(9): p. 1086-93.

21. Bachas, C., et al., *The role of minor subpopulations within the leukemic blast compartment of AML patients at initial diagnosis in the development of relapse*. *Leukemia*, 2012. **26**(6): p. 1313-20.
22. Shlush, L.I., et al., *Tracing the origins of relapse in acute myeloid leukaemia to stem cells*. *Nature*, 2017. **547**(7661): p. 104-108.
23. Zuber, J., et al., *Mouse models of human AML accurately predict chemotherapy response*. *Genes Dev*, 2009. **23**(7): p. 877-89.
24. Ennajdaoui, H., et al., *IGF2BP3 Modulates the Interaction of Invasion-Associated Transcripts with RISC*. *Cell Rep*, 2016. **15**(9): p. 1876-83.
25. Huang, H., et al., *Recognition of RNA N(6)-methyladenosine by IGF2BP proteins enhances mRNA stability and translation*. *Nat Cell Biol*, 2018. **20**(3): p. 285-295.
26. Jaiswal, A.K., et al., *Focused CRISPR-Cas9 genetic screening reveals USO1 as a vulnerability in B-cell acute lymphoblastic leukemia*. *Sci Rep*, 2021. **11**(1): p. 13158.
27. Li, X., et al., *High-Resolution In Vivo Identification of miRNA Targets by Halo-Enhanced Ago2 Pull-Down*. *Mol Cell*, 2020. **79**(1): p. 167-179 e11.
28. Wu, P., *Inhibition of RNA-binding proteins with small molecules*. *Nature Reviews Chemistry*, 2020. **4**(9): p. 441-458.
29. Julio, A.R. and K.M. Backus, *New approaches to target RNA binding proteins*. *Current Opinion in Chemical Biology*, 2021. **62**: p. 13-23.

APPENDIX I:

“The RNA-binding protein IGF2BP3 is critical for MLL-AF4-mediated leukemogenesis”(reprint)

## ARTICLE OPEN



## Acute lymphoblastic leukemia

## The RNA-binding protein IGF2BP3 is critical for MLL-AF4-mediated leukemogenesis

Tiffany M. Tran <sup>1,2</sup>, Julia Philipp<sup>3</sup>, Jaspal Singh Bassi<sup>1</sup>, Neha Nibber<sup>1</sup>, Jolene M. Draper<sup>3</sup>, Tasha L. Lin <sup>4,5</sup>, Jayanth Kumar Palanichamy <sup>1,6</sup>, Amit Kumar Jaiswal<sup>1</sup>, Oscar Silva<sup>7</sup>, May Paing<sup>1</sup>, Jennifer King<sup>8</sup>, Sol Katzman<sup>9</sup>, Jeremy R. Sanford<sup>3</sup> and Dinesh S. Rao <sup>1,2,10,11</sup>✉

© The Author(s) 2021

Despite recent advances in therapeutic approaches, patients with MLL-rearranged leukemia still have poor outcomes. Here, we find that the RNA-binding protein IGF2BP3, which is overexpressed in MLL-translocated leukemia, strongly amplifies MLL-Af4-mediated leukemogenesis. Deletion of *Igf2bp3* significantly increases the survival of mice with MLL-Af4-driven leukemia and greatly attenuates disease, with a minimal impact on baseline hematopoiesis. At the cellular level, MLL-Af4 leukemia-initiating cells require *Igf2bp3* for their function in leukemogenesis. At the molecular level, IGF2BP3 regulates a complex posttranscriptional operon governing leukemia cell survival and proliferation. IGF2BP3-targeted mRNA transcripts include important MLL-Af4-induced genes, such as those in the *Hoxa* locus, and the Ras signaling pathway. Targeting of transcripts by IGF2BP3 regulates both steady-state mRNA levels and, unexpectedly, pre-mRNA splicing. Together, our findings show that IGF2BP3 represents an attractive therapeutic target in this disease, providing important insights into mechanisms of posttranscriptional regulation in leukemia.

*Leukemia*; <https://doi.org/10.1038/s41375-021-01346-7>

## INTRODUCTION

Chromosomal rearrangements of the mixed-lineage leukemia (*MLL*, *KMT2A*) gene are recurrently found in a subset of acute lymphoblastic leukemia (ALL), acute myeloid leukemia (AML), and acute leukemia of ambiguous lineage [1]. Despite recent advances in therapeutic approaches, patients with *MLL*-rearranged leukemia have poor outcomes, high risk of relapse, and show resistance to novel targeted therapies [2, 3]. *MLL* encodes an H3K4 methyltransferase required for hematopoietic stem cell (HSC) development during both embryonic and adult hematopoiesis [4–7]. Many translocation partners for *MLL*, including *AF4* (*AFF1*), encode proteins that regulate transcriptional elongation [8–14]. Of more than 90 translocation fusion partner genes, *MLL-AF4* (*KMT2A-AFF1*) is the most common *MLL* fusion protein in patients [15]. Biologically, *MLL-AF4*-driven leukemia is a distinct entity compared to non-*MLL*-rearranged leukemias, with a unique gene expression profile showing significant overlap with stem cell programs [16–18].

At the posttranscriptional level, emerging evidence suggests a role for microRNAs, RNA-binding proteins (RBP), and other RNA-based mechanisms in regulating gene expression during leukemogenesis [19–21]. We recently identified the oncofetal RBP

Insulin like growth factor 2 mRNA binding protein 3 (IGF2BP3) as an important regulator of gene expression in *MLL*-rearranged B-ALL [22]. IGF2BP3 is expressed during embryogenesis, lowly expressed in healthy adult tissues, and strongly reexpressed in cancer cells [23]. Elevated levels of IGF2BP3 expression are correlated with diminished patient survival in many cancers and may be a marker of disease aggressiveness in B-ALL [24–26]. Previously, we determined that overexpression of IGF2BP3 in bone marrow (BM) of mice led to a pathologic expansion of hematopoietic stem and progenitor cells (HSPC). IGF2BP3 interacted with and upregulated oncogenic transcripts (e.g., MYC, CDK6) via the 3'UTR, contributing to the pathologic proliferative phenotype [22]. Together, these studies illuminated a novel role for posttranscriptional gene regulation in the pathologic proliferation of HSPCs.

Experimentally, *MLL-AF4*-driven leukemogenesis has been studied using a range of in vitro and in vivo models leading to significant progress in our understanding of *MLL*-rearranged leukemia [16, 27–31]. Here, we explicitly tested the requirement for *Igf2bp3* in a bona-fide model of *MLL-AF4*-driven leukemogenesis [32]. Deletion of *Igf2bp3* significantly increased survival of

<sup>1</sup>Department of Pathology & Laboratory Medicine, David Geffen School of Medicine, UCLA, Los Angeles, CA 90095, USA. <sup>2</sup>Molecular, Cellular, and Integrative Physiology Interdepartmental Ph.D. Program, UCLA, Los Angeles, CA 90095, USA. <sup>3</sup>Department of Molecular, Cellular and Developmental Biology, UCSC, Santa Cruz, CA 95064, USA. <sup>4</sup>Division of Hematology/Oncology, Department of Medicine, UCLA, Los Angeles, CA 90095, USA. <sup>5</sup>Molecular Biology Interdepartmental Doctoral Program, UCLA, Los Angeles, CA 90095, USA. <sup>6</sup>Department of Biochemistry, All India Institute of Medical Sciences, New Delhi 110029, India. <sup>7</sup>Department of Pathology, Stanford University School of Medicine, Stanford, CA 94305, USA. <sup>8</sup>Division of Rheumatology, Department of Medicine, UCLA, Los Angeles, CA 90095, USA. <sup>9</sup>UCSC Genomics Institute, Santa Cruz, CA 95064, USA. <sup>10</sup>Jonsson Comprehensive Cancer Center (JCCC), UCLA, Los Angeles, CA 90095, USA. <sup>11</sup>Broad Stem Cell Research Center, UCLA, Los Angeles, CA 90095, USA. ✉email: DRao@mednet.ucla.edu

Received: 19 February 2021 Revised: 25 June 2021 Accepted: 6 July 2021  
Published online: 29 July 2021



MLL-Af4 transplanted mice and decreased the numbers and self-renewal capacity of MLL-Af4 leukemia-initiating cells (LICs). Mechanistically, we found that IGF2BP3 targets and modulates the expression of transcripts encoding regulators of leukemogenesis, through multiple posttranscriptional mechanisms. Together, our findings show that IGF2BP3 is a critical regulator of MLL-AF4-mediated leukemogenesis and a potential therapeutic target in this disease.

## METHODS

### Molecular biology assays

ChIP-PCR on RS4;11 and SEM cells were performed as previously described [33]. IGF2BP3 ChIP primer sequences were kindly provided by Dr. James Mulloy (University of Cincinnati) [32]. Protein and mRNA extracts were prepared, and western blot/RT-qPCR performed as previously described [34]. Primers and antibodies are listed in Table S1.

### Plasmids, retroviral transduction and BM transplantation (BMT)

The MSCV-MLL-FLAG-Af4 plasmid was kindly provided by Michael Thirman (University of Chicago) through MTA [32]. Nontargeting (NT) or *Igf2bp3* sgRNA was cloned into an in-house MSCV-hU6-sgRNA-EFS-mCherry vector [35]. Retroviral transduction and BMT are previously described [34, 36]. 5-FU enriched BM and Lin<sup>-</sup> cells were spin-infected four times with MSCV-MLL-FLAG-Af4 virus at 30 °C for 45 min with polybrene and selected with 400 µg/ml G418 for 7 days. MLL-Af4 Cas9-GFP cells were retrovirally infected with MSCV-hU6-sgRNA-EFS-mCherry.

### Mice

C57BL/6J and B6J.129(Cg)-Gt(ROSA)26Sor<sup>tm1.1(CAG-cas9<sup>+</sup>-EGFP)<sup>Fvzh</sup>/J (Cas9-GFP BL/6J) mice were from Jackson Laboratory. The UCI Transgenic Mouse Facility utilized CRISPR-Cas9 to insert loxP sites flanking exon 2 of *Igf2bp3* to generate *Igf2bp3<sup>fl/fl</sup>* mice. To generate conditional KO, *Igf2bp3<sup>fl/fl</sup>* mice were bred with Vav1-Cre mice. Consistent with prior reports, this strategy led to “leaky” Cre expression, resulting in germline deletion [37–39]. To isolate floxed and deletion (del) alleles, mice were back-crossed onto C57BL/6 mice with successful germline, Mendelian transmission of del and floxed alleles in two successive generations (Table S2). Mice heterozygous for del allele were mated, leading to homozygous *Igf2bp3* deletion and *Igf2bp3<sup>del/del</sup>* mice (I3KO) used in this study. Blinding or randomization was not applied to mice experiments.</sup>

### Cell culture and flow cytometry

RS4;11, SEM, 70Z/3, and HEK293T cell lines were cultured as previously described [34]. Lin<sup>-</sup> cells were cultured in IMDM with 15% FBS supplemented with SCF, IL-6, FLT3, and TPO. CD11b<sup>+</sup> cells were isolated from splenic tumors for positive selection by MACS (Miltenyi). Blood, BM, thymus, and spleen were collected from mice at indicated time points and staining performed as previously described [22]. Antibodies are provided in Table S1. Flow cytometry was performed on a BD FACS LSRII and analysis using FlowJo software.

### Histopathology

Fixation, sectioning, and analysis were performed as previously described (DSR) [36].

### Competitive repopulation assay and secondary leukemia transplantation

Competitive repopulation experiments are previously described [22]. For leukemia transplantation, BM was collected from WT/MLL-Af4 or I3KO/MLL-Af4 mice that succumbed to leukemia at 10–14 weeks post transplantation and injected into 8-week-old immunocompetent CD45.1<sup>+</sup> female mice.

### RNA-seq

Single-end, strand-specific RNA sequencing was performed on Illumina HiSeq3000 for Lin<sup>-</sup> and CD11b<sup>+</sup> samples, 15–20 million reads/sample (UCLA Technology Center for Genomics & Bioinformatics). Analysis is previously described [22]. RNA-seq reads were mapped to the mouse

genome assembly mm10 using STAR version X. Repeat sequences were masked using Bowtie 2 [40] and RepeatMasker [41]. Differentially expressed genes (DEGs) were identified using DESeq2 [42] (CD11b<sup>+</sup>) and fdrtool [43] (Lin<sup>-</sup>). Multiple testing correction used the Benjamini–Hochberg method. Significant DEGs have adjusted *P* value < 0.1 and log<sub>2</sub>FC > 1. Data collection and parsing were completed with bash and python2.7. Statistical analyses were performed using R version 3.5.1. Enrichment analyses were completed with Metascape [44] and gene set enrichment analysis (GSEA) using GSEAPreranked after *n*-value calculation [45–47].

### Alternative splicing estimation

Mixture of Isoforms (MISO) Bayesian inference model v0.5.4 with mm10 “exon-centric annotation” quantified alternative splicing events [48]. Percent spliced in (PSI) was quantified for each event by number of read counts supporting both events and unique reads to each isoform. Delta PSI was calculated by subtracting from WT. Significant differential events had delta PSI > 0.1, Bayes factor ≥ 10, and sum of exclusion and inclusion reads ≥ 10.

### Enhanced crosslinking-immunoprecipitation (eCLIP)

eCLIP was completed on a minimum of two biological replicates with two technical replicates and size matched input (smlInput) samples (Eclipse BioInnovations). Overall, 5 × 10<sup>5</sup> cells were UV crosslinked (245 nm, 400 mJoules/cm<sup>2</sup>), RNase I treated, and immunoprecipitated with anti-IGF2BP3 antibody (MBL RNO09P) coupled to magnetic Protein G beads. Paired-end RNA-seq was performed on Illumina HiSeq4000 (UCSF Genomics Core Facility). Peaks were called using CLIPper [49] and filtered on smlInput (FS1). HOMER [50] annotatePeaks.pl and findMotifs.pl provided peak genomic locations and motif enrichment. Background for peaks within DEGs was simulated using bedtools [51] and shuffled 1000 times.

### Statistics

Data represent mean ± SD for continuous numerical data, unless otherwise noted in figure legends. One-way ANOVA followed by Bonferroni’s multiple comparisons test (>2 groups) or two-tailed Student’s *t* tests were performed using GraphPad Prism software.

## RESULTS

### IGF2BP3 is integrated into the MLL-AF4 transcriptional program

To understand the overlap of transcriptional and posttranscriptional regulation in MLL-rearranged leukemia, we compared IGF2BP3-regulated targets with a published MLL-Af4 ChIP-Seq dataset [22, 32]. Transcripts modulated by IGF2BP3 were significantly enriched for MLL-Af4-bound genes (Fig. 1a; Supplementary Fig. 1a). Interestingly, IGF2BP3 itself was a direct transcriptional target of MLL-Af4, with binding sites within the first intron and promoter region (Supplementary Fig. 1b) [32]. To confirm, we performed ChIP-PCR assays on RS4;11 and SEM, human MLL-AF4 translocated B-ALL cell lines, and determined that the first intron of *IGF2BP3* is strongly bound by MLL-AF4 (Fig. 1b; Supplementary Fig. 1c). This MLL-AF4 binding was abrogated when SEM cells were treated with the DOT1L inhibitor, EPZ5676, and the bromodomain inhibitor, IBET-151 (Fig. 1c; Supplementary Fig. 1d) [52]. Furthermore, we observed an MLL-AF4-dose-dependent increase in luciferase reporter activity, using the promoter region upstream of the IGF2BP3 transcription start site (Supplementary Fig. 1e). In the murine pre-B 70Z/3 cell line and primary murine BM cells, transduction with retroviral MLL-Af4 [32] caused an ~64-fold upregulation of *Igf2bp3* mRNA (Fig. 1d, e). Concordantly, IGF2BP3 protein was upregulated in MLL-Af4-transduced primary BM cells (Fig. 1f). Furthermore, enforced expression of another MLL fusion protein, MLL-AF9, and other non-MLL leukemia drivers, including AML1-ETO, MYC, and NRAS in primary HSPCs, show that the upregulation of *Igf2bp3* is specific to MLL-Af4 (Supplementary Fig. 1f). These findings of *Igf2bp3* specificity are in line with those that we and others have previously reported, as well as in publicly available datasets

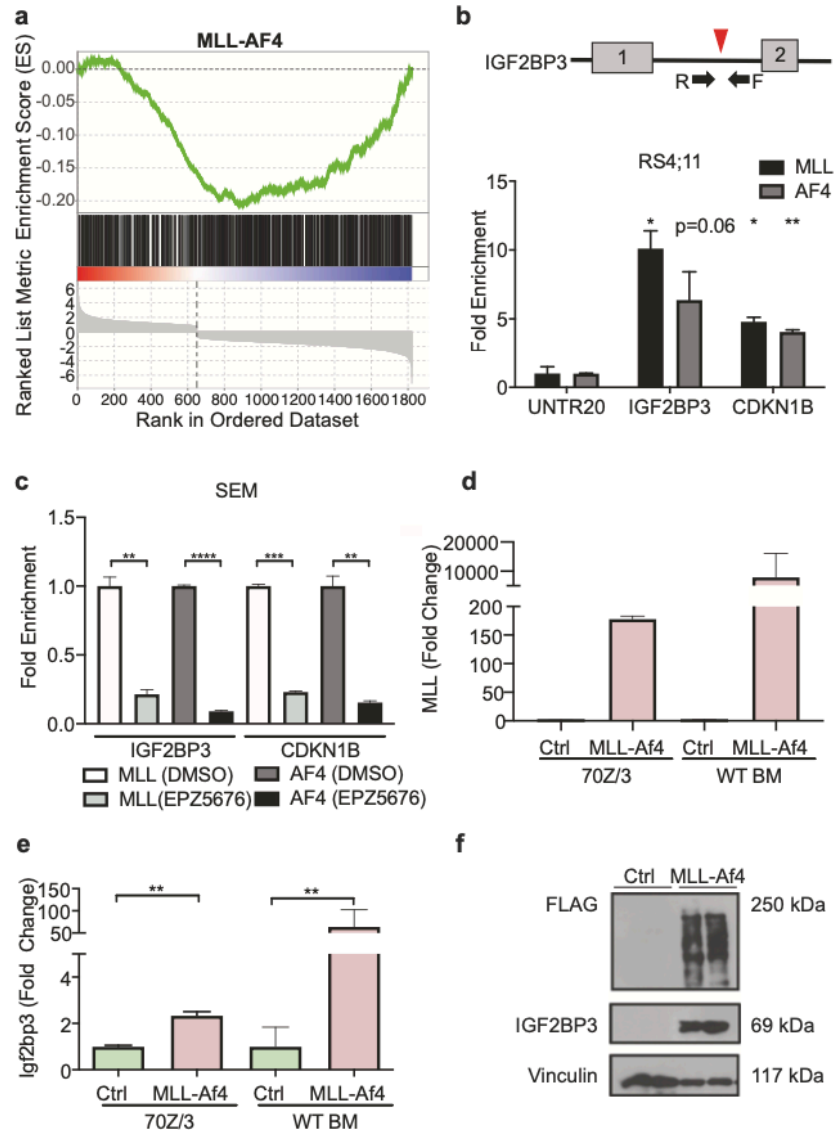


**Fig. 1** MLL-AF4 transcriptionally induces IGF2BP3. **a** GSEA of differentially expressed genes from IGF2BP3 depleted RS4;11 cells shows significant negative enrichment with MLL-AF4 ChIP targets (nominal  $P$  value: 0.001, FDR: 0.001, Normalized ES:  $-1.54$ ). **b** Schematic of MLL-AF4 binding site in intron 1 of IGF2BP3 (top). ChIP-qPCR shows fold enrichment for IGF2BP3 and CDKN1B with MLL and AF4 IP in RS4;11. Normalized to UNTR20, an untranscribed region ( $t$  test; \* $P < 0.05$ , \*\* $P < 0.01$ ). **c** Fold enrichment from ChIP-qPCR of SEM cells show reduced binding of MLL-AF4 to IGF2BP3 with treatment of the DOT1L inhibitor, EPZ5676. Normalized to DMSO. ( $t$  test; \*\* $P < 0.01$ , \*\*\*\* $P < 0.0001$ ). **d** Expression of MLL through RT-qPCR of 70Z/3 transduced with either control (Ctrl) or MLL-Af4 vector selected with G418 and MLL expression at the RNA level in the BM of WT recipients transplanted with Ctrl or MLL-Af4 HSPCs. **e** Induction of *Igf2bp3* at the RNA level in selected 70Z/3 with MLL-Af4 and in the BM of WT recipients transplanted with Ctrl or MLL-Af4 HSPCs (bottom) ( $t$  test; \*\* $P < 0.01$ ). **f** Induction of IGF2BP3 at the protein level in BM from mice transplanted with MLL-Af4-transduced WT donor HSPCs.

[22, 26, 53]. Interestingly, induced expression of structurally and functionally related paralogs *Igf2bp1* and *Igf2bp2* was noted with enforced expression of non-MLL-Af4 oncogenic drivers, again in concordance with observations in human leukemia (Supplementary Fig. 1g, h) [22, 26, 54]. Taken together, these findings demonstrate that MLL-Af4 specifically drives the expression of *Igf2bp3* in vivo.

**Normal hematopoiesis is maintained in *Igf2bp3* KO mice**  
To test the in vivo requirement for IGF2BP3 in leukemogenesis, we generated an *Igf2bp3* KO (I3KO) mouse. We initially generated a floxed *Igf2bp3* allele (*f/f*; Supplementary Fig. 2a) using CRISPR-Cas9. In the course of mating these mice with *Vav1-Cre* mice, we serendipitously generated a germline knockout allele (del), which we isolated and characterized (Supplementary Fig. 2b). This has

been previously reported in the Vav1-Cre mouse strain, which displays “leaky” Cre expression resulting in germline deletion [37–39]. Mendelian inheritance was confirmed for the isolated germline del allele, although distribution of genotypes was marginally skewed (Table S2). Deletion of *Igf2bp3* was confirmed at the DNA, RNA, and protein level (Supplementary Fig. 2c–e). These *Igf2bp3*<sup>del/del</sup> (I3KO) mice were used in this study. Immunophenotyping of I3KO mice showed no significant differences in numbers of HSPCs in the BM compared to WT (Supplementary Fig. 2f). I3KO mice showed similar numbers of myeloid-lineage progenitors (CMPs, GMPs, and MEPs) (Supplementary Fig. 2g), normal B-cell development [55] (Supplementary Fig. 2h), and normal numbers of mature B lymphoid, T lymphoid, and myeloid lineages in the BM and spleen (Supplementary Fig. 2i, j). Hence, I3KO mice demonstrate preserved normal, steady-state adult hematopoiesis.

#### **Igf2bp3 deletion increases the latency of MLL-Af4 leukemia and survival of mice**

Next, we queried MLL-Af4-mediated leukemogenesis in I3KO mice, utilizing BMT (Supplementary Fig. 3a). Retroviral MLL-Af4 transduction was equivalent between WT and I3KO donor BM, based on DNA copy number (Supplementary Fig. 3b) and western blot analysis (Supplementary Fig. 3c). Following transplantation of transduced HSPCs, *Igf2bp3* loss significantly increased both leukemia-free and overall survival of MLL-Af4 mice (Fig. 2a, b). The median survival of I3KO/MLL-Af4 mice was greater than 157 days, compared to 103 days for control mice. White blood cell (WBC) and myeloid cell counts in I3KO/MLL-Af4 mice were significantly reduced, compared with the control mice (Fig. 2c; Supplementary Fig. 3d). On average, I3KO/MLL-Af4 mice became overtly leukemic much later than the control mice peripheral blood (112 versus 70 days) (Fig. 2c). Concordantly, peripheral blood smears showed reduced circulating blasts in I3KO/MLL-Af4 mice (Supplementary Fig. 3e). Together, these findings indicated that *Igf2bp3* is required for efficient MLL-Af4-mediated leukemogenesis.

#### **Igf2bp3 modulates disease severity in MLL-Af4-driven leukemia**

The MLL-Af4 model utilized here causes a highly penetrant, aggressive form of leukemia in mice. In timed experiments, I3KO/MLL-Af4 transplanted mice showed a highly significant, approximately fourfold reduction in spleen weights at 14 weeks post transplant compared to WT/MLL-Af4 mice (Fig. 2d). I3KO/MLL-Af4 mice showed reduced infiltration of the spleen and liver by leukemic cells, which obliterated normal tissue architecture in WT/MLL-Af4 mice (Fig. 2e). In line with this, I3KO/MLL-Af4 transplanted mice showed a significant reduction in CD11b+ cells, which were less proliferative (CD11b+Ki67+), both in the spleen (~30-fold) and BM (~2.5-fold) at 14 weeks (Fig. 2f, g; Supplementary Fig. 3f, g). Thus, *Igf2bp3* deletion significantly reduces tumor burden and attenuates disease severity in MLL-Af4 transplanted mice.

#### **Igf2bp3 is required for LIC function in vitro**

Several studies highlight the importance of LICs in both human and mouse leukemia. In the MLL-Af4 model, LICs show expression of CD11b and c-Kit [17, 32, 56]. Given our findings of delayed initiation and decreased disease severity, we characterized these LICs (CD11b+c-Kit+) in I3KO/MLL-Af4 transplanted mice, finding a significant tenfold decrease in numbers in the spleen and fivefold decrease in the BM at 14 weeks (Fig. 3a, b). After confirming deletion of IGF2BP3 at the protein level in immortalized HSPCs (Lin–) from WT/MLL-Af4 and I3KO/MLL-Af4 mice, we turned to endpoint colony-forming unit assays (CFU) to characterize MLL-Af4 LIC dependence on IGF2BP3 (Fig. 3c). Deletion of *Igf2bp3* resulted in an approximately twofold reduction in total colonies and a significant decrease in CFU-GM progenitors (Fig. 3d). To confirm this, we utilized an orthogonal method for CRISPR-Cas9-mediated

*Igf2bp3* deletion. Briefly, Lin– cells from Cas9-GFP mice were transduced with MSCV-MLL-Af4 virus. After selection, MLL-Af4 Cas9-GFP Lin– cells were transduced with a retroviral vector containing either a NT sgRNA or sgRNA targeting *Igf2bp3* (I3sg) (Fig. 3e). Importantly, *Igf2bp3* is deleted after MLL-Af4 transformation, a distinction from the prior method (Fig. 3f, g). Deletion of *Igf2bp3* led to a significant reduction in total colony numbers and various colony morphologies (Fig. 3h). The differences in overall colony-forming capacity between the two systems are likely the result of utilizing different methodologies, but in both systems, *Igf2bp3* deficiency led to decreased colony formation.

#### **Igf2bp3 is necessary for the function of MLL-Af4 LICs in vivo**

Since *Igf2bp3* deletion reduces LIC numbers and impairs LIC function, we next determined if *Igf2bp3* affects LIC capability to initiate MLL-Af4 leukemia in vivo. First, to investigate baseline HSC function in I3KO mice, we completed competitive repopulation BMT by transplanting lethally irradiated CD45.1 recipient mice with 50% of WT or I3KO CD45.2 donor BM and 50% CD45.1 donor BM. We found no defect in engraftment over time in I3KO recipients (Supplementary Fig. 4a). Moreover, we determined no differences in multilineage hematopoietic reconstitution ability of I3KO donor cells, as immature lineages in the BM and mature lineages in the periphery were intact (Supplementary Fig. 4b–h). With no baseline differences in reconstitution by normal HSPCs, we investigated if *Igf2bp3* impacted the number of effective LICs in secondary transplantation. Equal numbers ( $10^6$ ,  $10^5$ , and  $10^4$ ) of leukemic BM cells from WT and I3KO mice were transplanted into immunocompetent CD45.1 mice. At 4 weeks post transplantation, mice that received  $10^6$  I3KO/MLL-Af4 cells had significantly reduced donor CD45.2+ engraftment (Fig. 4a). With  $10^5$  and  $10^4$  cells, we no longer observed measurable leukemic burden in recipient mice (Fig. 4a), suggesting that LIC active cell frequency in I3KO/MLL-Af4 mice is lost between  $10^6$  and  $10^5$  cells (Fig. 4a) [57]. WBC and splenic weights were significantly decreased in I3KO/MLL-Af4 transplanted mice (Fig. 4b–d). Histologically, leukemic infiltration was absent in the spleen and liver of  $10^5$  I3KO/MLL-Af4 transplanted mice (Fig. 4e). Thus, *Igf2bp3* deletion results in significant reduction in reconstitution of MLL-Af4 transplanted mice, suggesting that *Igf2bp3* is necessary for the self-renewal capability of LICs in vivo.

#### **IGF2BP3 supports oncogenic gene expression networks in LIC-enriched and bulk leukemia cells**

To identify differentially expressed transcripts, we sequenced RNA from WT/MLL-Af4 and I3KO/MLL-Af4 Lin– and CD11b+ bulk leukemia cells after confirming expression of MLL and *Igf2bp3* (Fig. 3c; Supplementary Fig. 5a–e). Differential expression analysis by DESeq2 revealed 208 upregulated and 418 downregulated transcripts in CD11b+ cells, and 189 upregulated and 172 downregulated transcripts in Lin– cells (Fig. 5a, b; Tables S3 and 4) [42]. We identified a significant enrichment in transcripts associated with the KEGG term transcriptional misregulation in cancer in both datasets, using Metascape for enrichment analyses [44] (Fig. 5c, d). Interestingly, discrete oncogenic signaling pathways were enriched in Lin– (PI3K/AKT) and CD11b+ cells (GTPase, MAPK pathway) (Fig. 5c, d). This was confirmed by GSEA, with significant enrichment for the Hallmark KRAS pathway in CD11b+ cells (Supplementary Fig. 5f) and GO Oxidative phosphorylation in Lin– cells (Supplementary Fig. 5g). To validate the RNA-seq data in Lin– cells, we focused on enriched differentially regulated genes including *Csf2rb*, *Notch1*, *Cd69*, and *Hoxa* cluster of transcripts, including *Hoxa9*, *Hoxa10*, and *Hoxa7*. We observed a significant decrease in steady-state mRNA levels for these transcripts in I3KO/MLL-Af4 Lin– cells by RT-qPCR (Fig. 5e). In I3KO/MLL-Af4 CD11b+ cells, we confirmed that transcripts encoding *Ccnd1*, *Maf*, *Mafb*, *Itga6*, *Klf4*, and *Akt3* were decreased (Fig. 5f). Furthermore, we determined that there was a significant

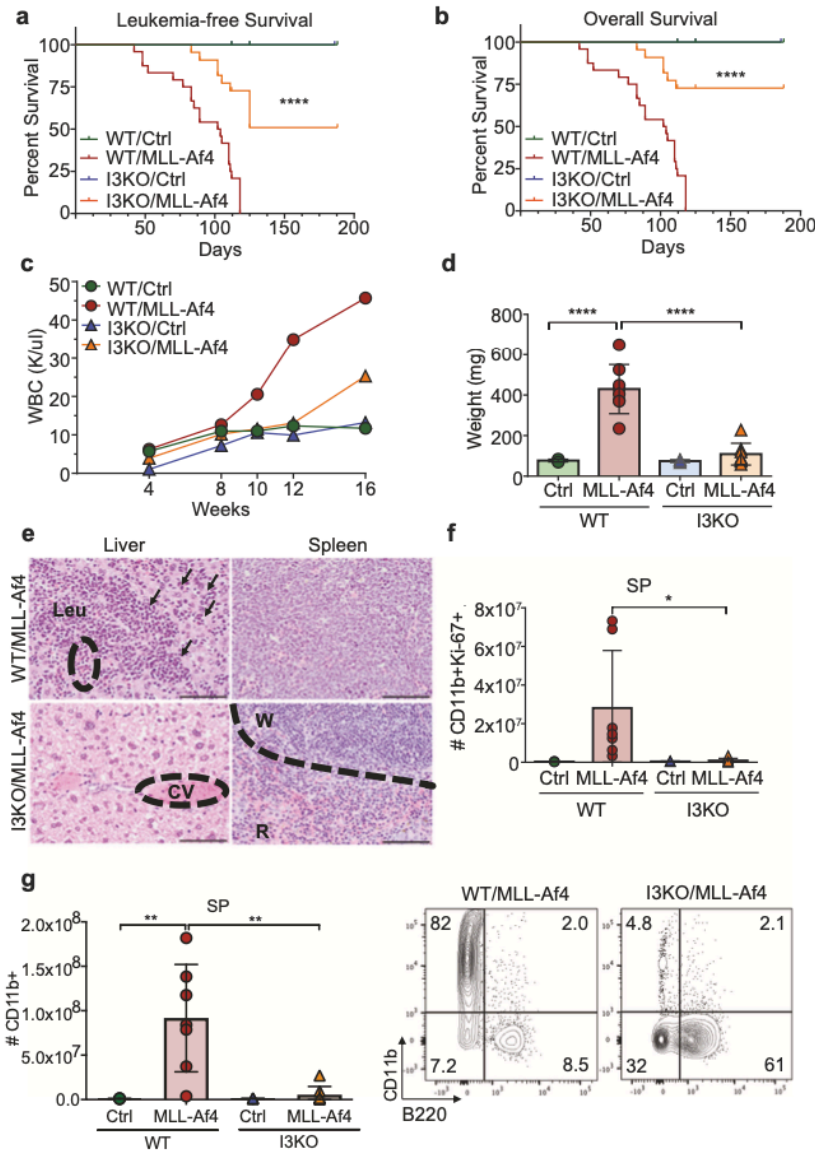


**Fig. 2** *Igf2bp3* deletion delays leukemogenesis and reduces disease severity. **a** Leukemia-free survival of mice transplanted with control (Ctrl) or MLL-Af4-transduced HSPCs from WT or *Igf2bp3* KO mice (Kaplan–Meier method with log-rank test; \*\*\*\* $P < 0.0001$ ). **b** Overall survival of mice transplanted with Ctrl or MLL-Af4-transduced HSPCs from WT or I3KO mice ( $n = 12$  WT/Ctrl,  $n = 24$  WT/MLL-Af4,  $n = 7$  I3KO/Ctrl,  $n = 22$  I3KO/MLL-Af4; Kaplan–Meier method with log-rank test; \*\*\*\* $P < 0.0001$ ). **c** Time course of WBC in the PB of mice transplanted with Ctrl or MLL-Af4-transduced HSPCs from WT or I3KO mice (data represented as means of three experiments;  $n = 4$  Ctrl,  $n = 8$  MLL-Af4 per experiment). **d** Spleen weights of mice transplanted with Ctrl or MLL-Af4-transduced HSPCs from WT or I3KO mice at 14 weeks ( $n = 4$  Ctrl,  $n = 8$  MLL-Af4; one-way ANOVA followed by Bonferroni’s multiple comparisons test; \*\*\*\* $P < 0.0001$ ). **e** H&E staining of liver and spleen of mice transplanted with mice transplanted with MLL-Af4-transduced HSPCs from WT or I3KO mice at 14 weeks. Scale bar: 100 μm; CV central vein; W white pulp; R red pulp; Leu leukemia; arrows showing infiltration. **f** Quantitation of CD11b<sup>+</sup>Ki67<sup>+</sup> cells in the spleen at 14 weeks post transplantation ( $n = 4$  Ctrl,  $n = 8$  MLL-Af4; one-way ANOVA followed by Bonferroni’s multiple comparisons test; \* $P < 0.05$ ). **g** (Left) Number of CD11b<sup>+</sup> in the SP of recipient mice that received Ctrl or MLL-Af4-transduced HSPCs from WT or I3KO mice at 14 weeks (one-way ANOVA followed by Bonferroni’s multiple comparisons test; \*\* $P < 0.01$ ). (Right) Corresponding representative FACS plots showing CD11b<sup>+</sup> and B220<sup>+</sup> cells in the SP.

decrease in Ras GTPase activity in I3KO cells by ELISA assay (Fig. 5g). Together, these data demonstrate that IGF2BP3 plays a major role in amplifying the expression of many cancer-related genes in Lin<sup>-</sup> and CD11b<sup>+</sup> cells.

#### eCLIP analysis reveals a putative role for IGF2BP3 in precursor mRNA (pre-mRNA) splicing

To determine how IGF2BP3 modulates gene expression in MLL-Af4 leukemia, we performed eCLIP-seq (Fig. 5a, b; Tables S3 and 4;

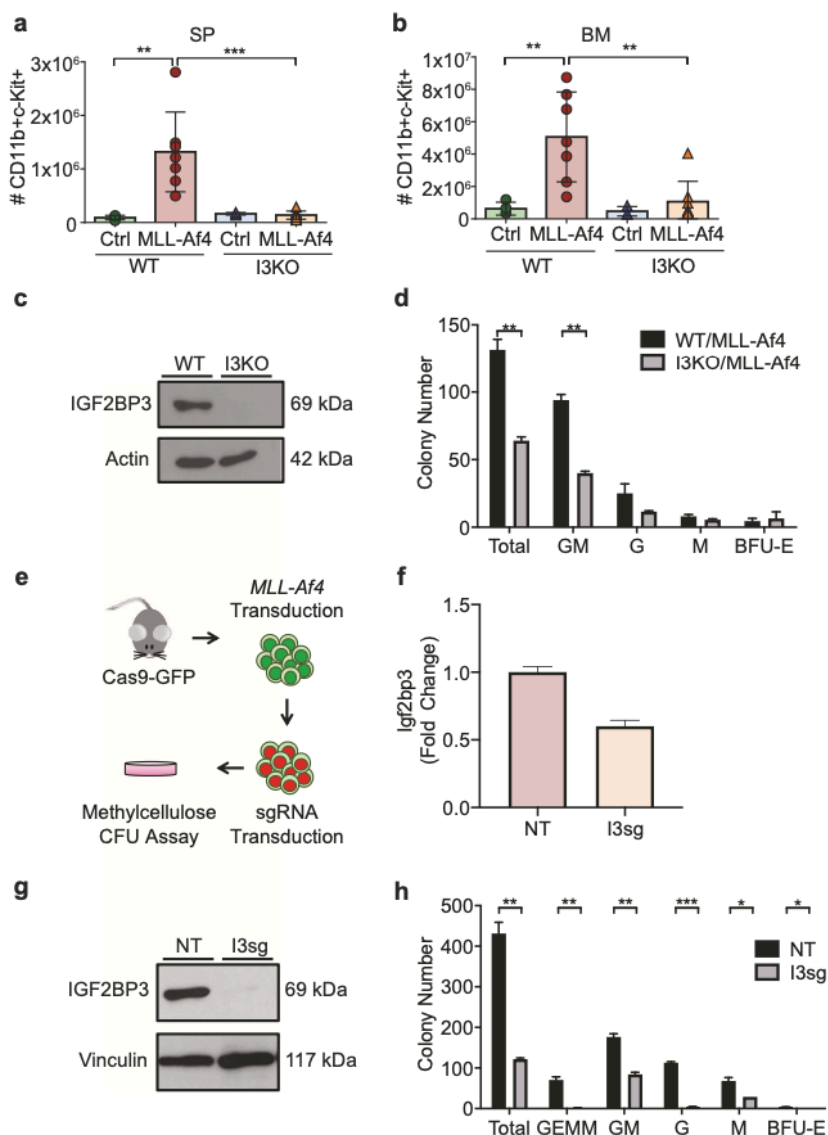


**Fig. 3** *Igf2bp3* is required for LIC function in endpoint colony formation assays. **a** Quantification of CD11b+c-Kit+ cells in the spleen of recipient mice at 14 weeks post transplantation ( $n = 4$  Ctrl,  $n = 8$  MLL-Af4; one-way ANOVA followed by Bonferroni's multiple comparisons test;  $**P < 0.01$ ). **b** Quantitation of CD11b+c-Kit+ cells in the BM 14 weeks post transplantation ( $n = 4$  Ctrl,  $n = 8$  MLL-Af4; one-way ANOVA followed by Bonferroni's multiple comparisons test;  $**P < 0.01$ ,  $***P < 0.001$ ). **c** Expression of IGF2BP3 of in WT/MLL-Af4 and I3KO/MLL-Af4 immortalized Lin<sup>-</sup> cells at the protein level. **d** Colony formation assay of WT/MLL-Af4 and I3KO/MLL-Af4 immortalized Lin<sup>-</sup> cells ( $t$  test;  $**P < 0.01$ ). **e** Schematic of collection of Cas9-GFP MLL-Af4 Lin<sup>-</sup> cells and CRISPR-Cas9-mediated deletion of *Igf2bp3*. **f** Expression of *Igf2bp3* in Cas9-GFP MLL-Af4 Lin<sup>-</sup> cells in nontargeting (NT) and *Igf2bp3* deleted (I3sg) cells by RT-qPCR. **g** Expression of IGF2BP3 in NT and I3sg Cas9-GFP MLL-Af4 Lin<sup>-</sup> cells at the protein level. **h** Colony formation assay of NT and I3sg deleted Cas9-GFP MLL-Af4 Lin<sup>-</sup> cells ( $t$  test;  $*P < 0.05$ ,  $**P < 0.01$ ,  $***P < 0.001$ ).

Supplementary Fig. 6a). We found that a significant fraction of the differentially expressed mRNAs are bound by IGF2BP3 (Supplementary Fig. 6b). Motif analysis confirmed an enrichment of CA-rich elements (Supplementary Fig. 6c) [58]. Although the majority of peaks were present within introns, we observed cell type-specific differences in the locations of exonic IGF2BP3 binding sites (Fig. 6a). The eCLIP data revealed numerous peaks within pre-

mRNA in both Lin<sup>-</sup> and CD11b+ cells, suggesting a potential role in splicing regulation. To characterize this observation, we utilized MISO analysis to identify differentially spliced transcripts [48]. Across both cell lines, we identified hundreds of transcripts with IGF2BP3-dependent changes in alternative splicing, including 97 differential splicing events in Lin<sup>-</sup> and 261 splicing events in CD11b+ cells (Supplementary Fig. 6d). After merging all replicate

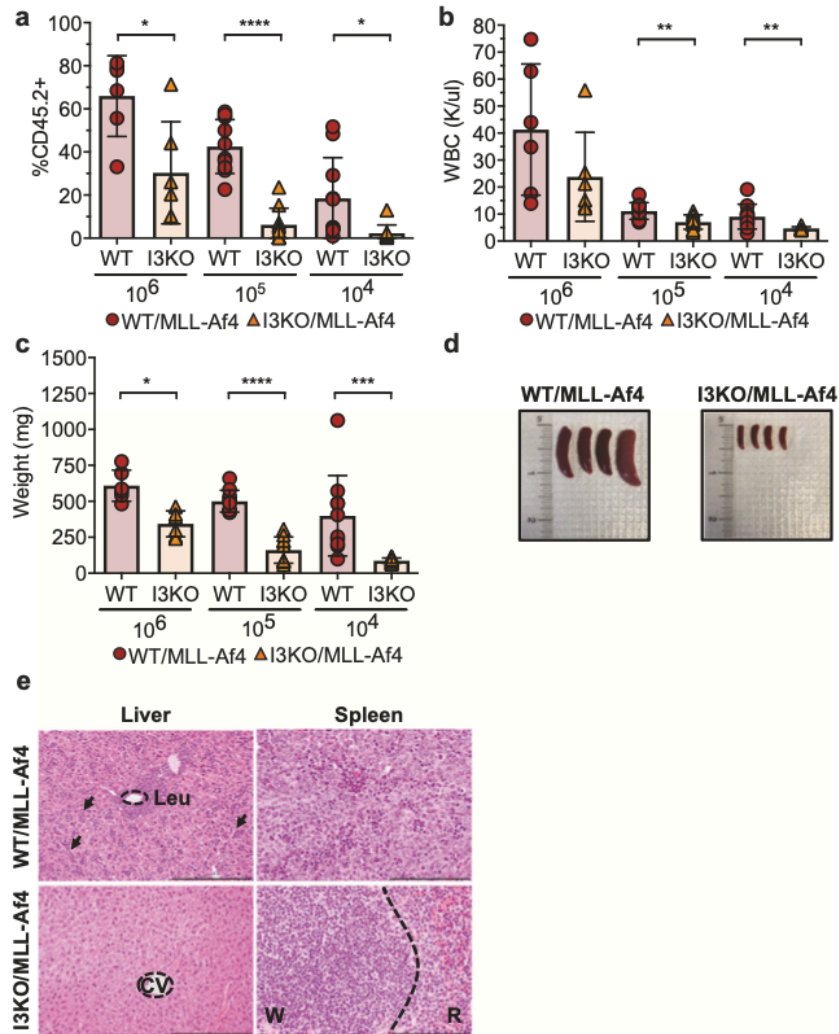


**Fig. 4** *Igf2bp3* deletion is necessary for MLL-Af4 leukemia-initiating cells to reconstitute mice in vivo. **a** Percentage of CD45.2+ in the peripheral blood of secondary transplanted mice from leukemic WT/MLL-Af4 or I3KO/MLL-Af4 donor mice at 10<sup>6</sup>, 10<sup>5</sup>, and 10<sup>4</sup> BM cells at 4 weeks post transplantation (For all panels in this figure:  $n = 6$  recipient mice per genotype for 10<sup>6</sup> cells and  $n = 10$  recipient mice per genotype for 10<sup>5</sup> and 10<sup>4</sup> cells;  $t$  test; \* $P < 0.05$ , \*\*\* $P < 0.001$ , \*\*\*\* $P < 0.0001$ ). **b** WBC from PB of secondary transplanted mice from WT/MLL-Af4 or I3KO/MLL-Af4 BM 3–4 weeks post transplant ( $t$  test; \*\* $P < 0.01$ ). **c** Splenic weights of secondary transplanted mice at 4–5 weeks ( $t$  test; \* $P < 0.05$ , \*\*\* $P < 0.001$ , \*\*\*\* $P < 0.0001$ ). **d** Images of splenic tumors in secondary mice transplanted with 10,000 BM cells from WT/MLL-Af4 mice (left) or I3KO/MLL-Af4 mice (right) at 5 weeks. **e** H&E staining of liver and spleen of secondary transplant recipients that received 10<sup>5</sup> cells at 4 weeks. Scale bar: liver, 200  $\mu$ m; spleen, 100  $\mu$ m; CV central vein, W white pulp, R red pulp, Leu leukemia; arrows showing infiltration.

eCLIP data for each cell type, we determined the position of eCLIP peaks relative to splice sites for splicing events identified by MISO (Fig. 6b). Most event types exhibited both increases and decreases in PSI, whereas intron retention (RI) events showed a consistent reduction in splicing in the I3KO/MLL-Af4 cells (Fig. 6c). A significant fraction of alternatively spliced transcripts contained IGF2BP3 binding sites in proximity of the splicing event (Supplementary Fig. 6e), strongest near the 3' splice site (3'ss), with additional signal near the 5' splice site. This pattern was observed for each distinct splicing event class that MISO identified, with retained introns exhibiting the strongest bias towards the 3'ss (Supplementary Fig. 6f). Notably, this positional

bias in the data was noted for differentially expressed MLL-Af4 target genes, such as *Hoxa9*, *Hoxa7*, and *Cd69* (Fig. 6d). To understand the impact on isoform-specific expression, RT-qPCR primers were designed to nonspecifically detect multiple isoforms or to specifically detect alternatively spliced isoforms (shorter isoforms) and full-length isoforms. As an example, reductions in both isoforms (full-length *Hoxa9* and truncated *Hoxa9T* [59]), as well as in the total level of *Hoxa9*, were observed in I3KO cells (Fig. 6e). Similar reductions were observed in all isoforms for *Hoxa7* and *Cd69* (Fig. 6e). Furthermore, there was an alteration in the ratio of the alternative to full-length isoform for all three genes (Fig. 6f), highlighting an effect on alternative splicing. Hence, the

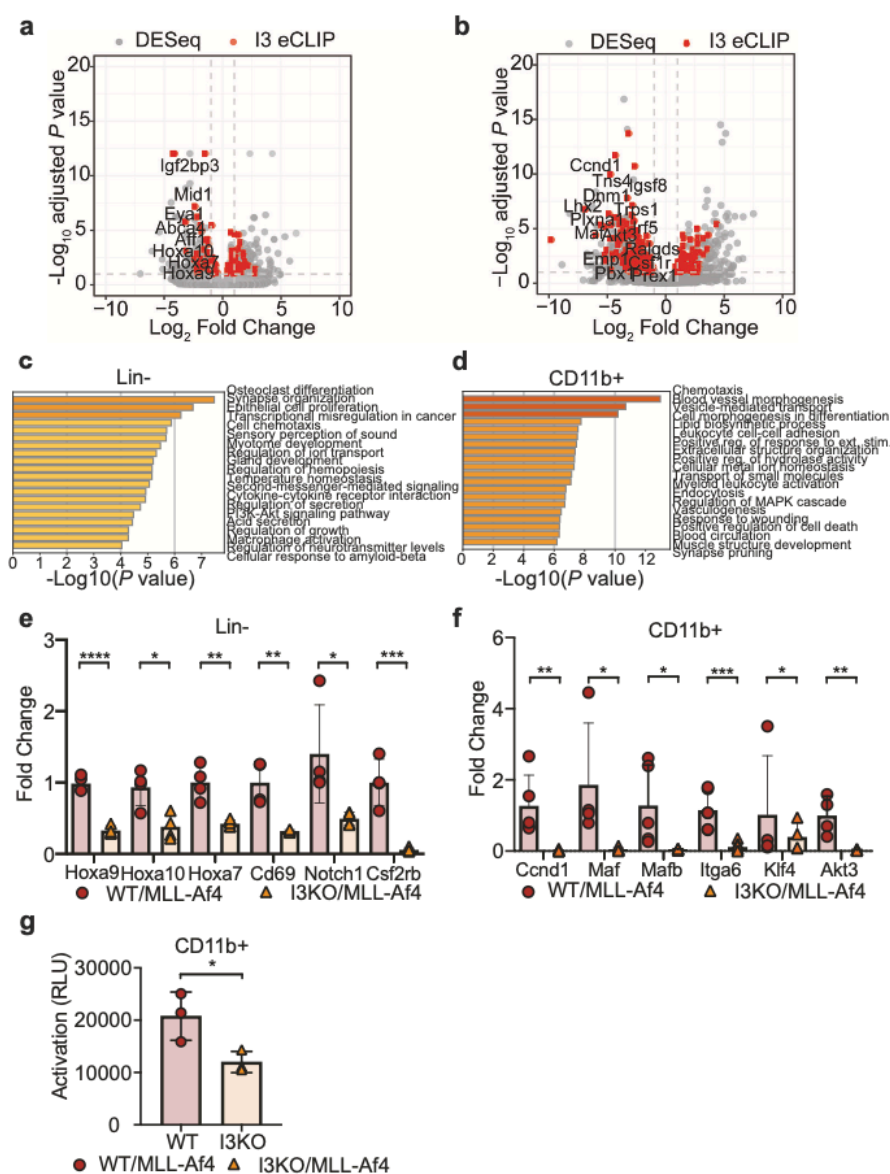


**Fig. 5** IGF2BP3 enhances MLL-Af4-mediated leukemogenesis through targeting transcripts within leukemogenic and Ras signaling pathways. **a** Volcano plot of differentially expressed genes determined using DESeq analysis on RNA-seq samples from WT/MLL-Af4 or I3KO/MLL-Af4 Lin<sup>-</sup> cells. Dotted lines represent one-fold change in expression (vertical lines) and adjusted  $P < 0.1$  cutoff (horizontal line). IGF2BP3 eCLIP-seq targets are highlighted in red. **b** Volcano plot of differentially expressed transcripts determined using DESeq analysis on RNA-seq samples from WT/MLL-Af4 or I3KO/MLL-Af4 CD11b<sup>+</sup> cells. Dotted lines represent one-fold change in expression (vertical lines) and adjusted  $P < 0.1$  cutoff (horizontal line). IGF2BP3 eCLIP-seq targets are highlighted in red. **c** GO Biological Processes and KEGG pathway enrichment determined utilizing the Metascape enrichment analysis webtool on MLL-Af4 Lin<sup>-</sup> IGF2BP3 DESeq dataset with an adjusted  $P < 0.05$  cutoff. **d** GO biological processes and KEGG pathway enrichment determined utilizing the Metascape enrichment analysis webtool on MLL-Af4 CD11b<sup>+</sup> IGF2BP3 DESeq dataset with an adjusted  $P < 0.05$  cutoff. Bar graphs are ranked by  $P$  value and overlap of terms within gene list. **e** Expression of leukemogenic target genes in WT/MLL-Af4 and I3KO/MLL-Af4 Lin<sup>-</sup> cells by RT-qPCR ( $n = 4$ ;  $t$  test; \* $P < 0.05$ , \*\* $P < 0.01$ , \*\*\*\* $P < 0.0001$ ). **f** Expression of Ras signaling pathway genes in WT/MLL-Af4 and I3KO/MLL-Af4 CD11b<sup>+</sup> cells by RT-qPCR ( $n = 4$ ;  $t$  test; \* $P < 0.05$ , \*\* $P < 0.01$ , \*\*\* $P < 0.001$ ). **g** Ras GTPase activity by ELISA in WT/MLL-Af4 and I3KO/MLL-Af4 CD11b<sup>+</sup> cells ( $n = 3$ ;  $t$  test; \* $P < 0.05$ ).

net effect of IGF2BP3 may be multipronged—with a strong impact on steady-state mRNA levels and an additional impact on splicing—in leukemia stem and progenitor cells.

## DISCUSSION

Here, we have shown the central importance of the RBP IGF2BP3 in MLL-Af4-driven leukemia. MLL-Af4-driven leukemogenesis is characterized by massive transcriptional dysregulation [8]. We

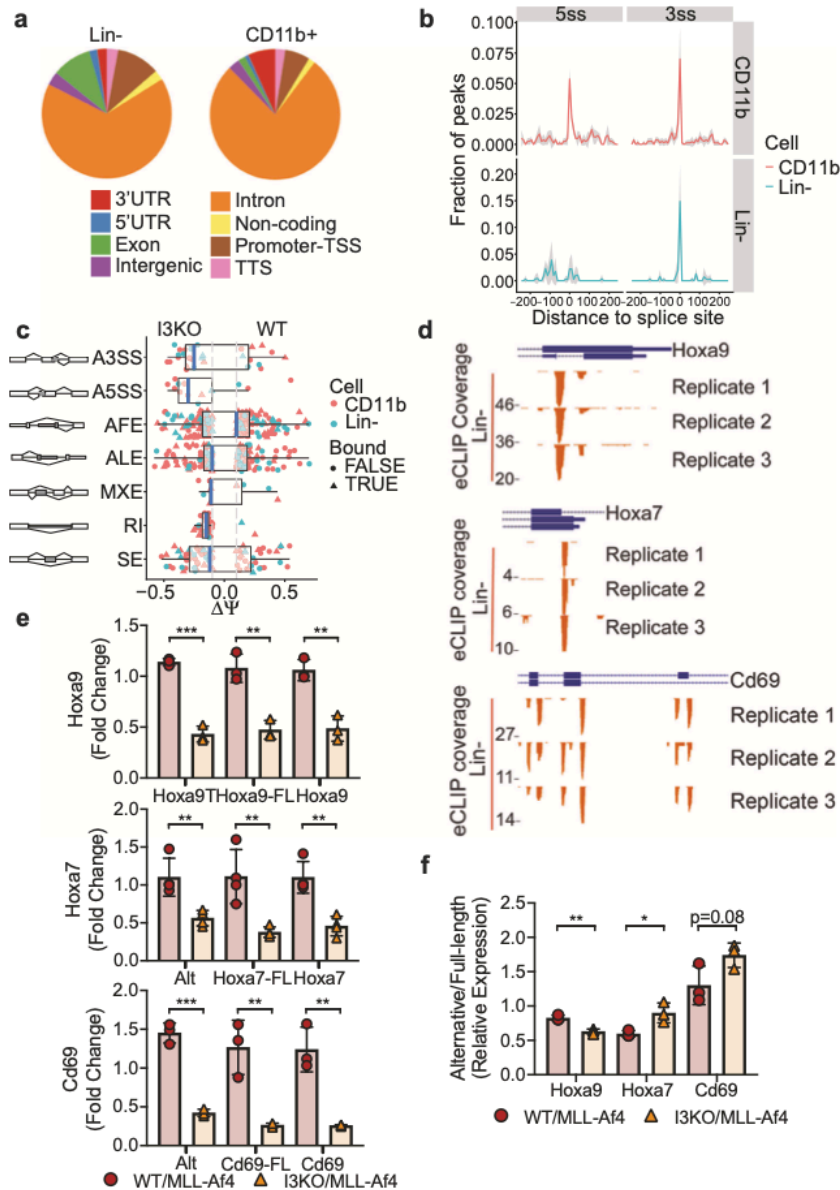


**Fig. 6** eCLIP analysis reveals IGF2BP3 function in regulating alternative pre-mRNA splicing. **a** Genomic locations of IGF2BP3 eCLIP peaks in WT/MLL-Af4 Lin<sup>-</sup> cells and CD11b<sup>+</sup> cells. Cell type differences in location of exonic peaks were noted: in CD11b<sup>+</sup> cells, a greater proportion of exonic peaks were found in 3'UTRs, whereas a greater proportion of peaks mapped to internal exons in Lin<sup>-</sup> cells. **b** Histogram showing normalized IGF2BP3 eCLIP peak counts and distance from IGF2BP3 eCLIP peak of 5' (5ss) and 3' (3ss) splice sites in WT/MLL-Af4 CD11b<sup>+</sup> (top) cells and Lin<sup>-</sup> cells (bottom). **c** Distribution of types of alternative splicing patterns for WT/MLL-Af4 or I3KO/MLL-Af4 Lin<sup>-</sup> and CD11b<sup>+</sup> cells using MISO analysis. Delta psi values plotted indicate difference in isoforms. The event types included are the following, with abbreviations: A3SS alternative 3' splice sites, A5SS alternative 5' splice sites, AFE alternative first exons, ALE alternative last exons, MXE mutually exclusive exons, RI retained introns, SE skipped exons, Bound IGF2BP3 eCLIP target. **d** UCSC Genome Browser snapshots of the Hoxa9, Hoxa7, and Cd69 loci. Each panel shows the exon-intron structure of the gene and unique read coverage from three eCLIP biological replicates from WT/MLL-Af4 Lin<sup>-</sup> cells. The maximum number of reads at each position is indicated to the left of each histogram. **e** Expression of Hoxa9, Hoxa7, and Cd69 splice variants in WT/MLL-Af4 and I3KO/MLL-Af4 Lin<sup>-</sup> cells by RT-qPCR utilizing primers which detect only its respective alternative splice isoforms (Hoxa9T, Alt), full-length isoforms (-FL), and both isoforms ( $n = 3-4$ ; t test; \*\* $P < 0.01$ , \*\*\* $P < 0.001$ ). **f** Relative expression ratio of alternative splice isoform to full-length isoform (alternative/full-length) in WT/MLL-Af4 and I3KO/MLL-Af4 Lin<sup>-</sup> cells by RT-qPCR ( $n = 3$ ; t test; \* $P < 0.05$ , \*\* $P < 0.01$ ).



confirm here that *Igf2bp3* is a direct transcriptional target MLL-AF4. Interestingly, we determined that IGF2BP3 itself seems to positively regulate MLL-AF4 transcriptional targets. Together, these data suggest that IGF2BP3 and MLL-AF4 form a novel posttranscriptional feed-forward loop, enhancing leukemogenic gene expression. It is not clear if IGF2BP3 may play a role in other leukemia subtypes given its relatively restricted pattern of expression in MLL-translocated leukemia. However, IGF2BP3 overexpression is noted in a wide range of cancer types—with different oncogenic transcriptional programs—and further work is needed to define whether this paradigm may be operant in other hematologic and nonhematologic cancer.

Our prior work showed that IGF2BP3 is required for B-ALL cell survival and overexpression in BM of mice leads to a pathologic expansion of HSPCs [22]. Here, we found that deletion of *Igf2bp3* in MLL-Af4 leukemia caused a striking delay in leukemia development and significantly increased the survival of MLL-Af4 mice. Furthermore, *Igf2bp3* deficiency greatly attenuated the aggressiveness of leukemic disease. Given that MLL-Af4 drives an AML in mice [32], our current work suggests that IGF2BP3 is a powerful modulator of the leukemic phenotype in the myeloid lineage, in addition to the previously observed effects in human B-ALL cells. The lineage of the leukemia induced by MLL-Af4 in mice may be a limitation of the study, as we cannot conclude an *in vivo* function for *Igf2bp3* in murine B-ALL. However, Lin et al. showed that there were important pathogenetic similarities between the MLL-Af4-induced pro-B-ALL and AML in mice [32]. In this light, MLL-AF4 leukemia in humans often shows lineage infidelity and plasticity, which has led to difficulties with targeted therapy [2, 60, 61]. We propose that IGF2BP3 may prove to be a valuable therapeutic target in MLL-AF4 leukemia, given its function in the pathogenesis of this unique molecular subtype of acute leukemia.

In this study, *Igf2bp3* regulated the numbers and function of LICs. Importantly, the effect of *Igf2bp3* deletion was restricted to LICs and did not significantly impact normal HSC function. Deletion of *Igf2bp3* led to an MLL-Af4 LIC disadvantage *in vivo* and *in vitro*. LICs have been defined as cells that can self-renew and have the capability to produce downstream bulk leukemia cells, and their persistence is thought to contribute to relapse after treatment in several different leukemia subtypes [62]. However, the details of human LICs in MLL-AF4 leukemia are less well known [28, 63]. The role of IGF2BP3 in such cells and in relapse of leukemia is of great interest and a future direction for our work.

Previously, we discovered IGF2BP3 interacts primarily with the 3'UTR of target transcripts via iCLIP-seq [22]. Unexpectedly in this study, we determined IGF2BP3 targets transcripts within intronic regions and splice sites in addition to the 3'UTR. These findings may result from utilizing the improved eCLIP technique and the implementation of the technique on primary cells instead of cell lines. Of note, a recent study showed IGF2BP3 may regulate alternative splicing of PKM in lung cancer [64]. We also found IGF2BP3-dependent dynamic splicing events, including retained introns, alternative 3'ss, and skipped exons. Intron retention has been reported to be a mechanism of transcriptome diversification in cancer and, specifically, leukemia [65, 66]. Moreover, studies have highlighted the importance of splicing to mRNA export, and that splicing factor mutations, such as those in U2AF1, result in translational misregulation in myeloid malignancy [67, 68]. Our unexpected, novel discovery, together with our prior work, shows that IGF2BP3 likely regulates specific mRNA operons and functions at multiple posttranscriptional levels, as has been described for other RBPs [69].

As an RBP, IGF2BP3 function is intimately connected to the underlying transcriptional program—IGF2BP3 can only act on specifically induced transcripts in the cell type where it is expressed. Hence, the unique gene sets that are bound and

regulated by IGF2BP3 in Lin<sup>−</sup> and CD11b<sup>+</sup> cells are not entirely unexpected, given that transcription changes as LICs differentiate into bulk leukemic cells. This is similar to miRNAs, which posttranscriptionally regulate distinct gene expression programs in distinct cell types [70]. The significant enrichment of IGF2BP3-bound mRNAs in differentially regulated and differentially spliced transcripts confirms a direct regulatory effect. However, further work is required to confirm functional relationships between the specific transcripts that are regulated and the phenotypic effects driven by IGF2BP3.

IGF2BP3 differentially regulated transcripts included MLL-AF4 target genes *Hoxa9*, *Hoxa10*, *Hoxa7*, and *Cd69* [32]. *HOXA9*, *HOXA10*, and *HOXA7* are induced by MLL-AF4 and *HOXA9* is required for MLL-rearranged leukemia survival [71]. We determined significant downregulation of both alternatively spliced and full-length isoforms for *Hoxa9*, *Hoxa7*, and *Cd69*. The relationship between leukemogenesis and splicing regulation is complex—while *Hoxa9T*, the homeodomain-less splice variant, is not sufficient for transformation alone, it is required with full-length *Hoxa9* for leukemogenic transformation [59, 72]. Thus, *Igf2bp3* may act through alteration of splicing regulation and upregulation of MLL-Af4 target leukemogenic genes to promote leukemogenesis and impact MLL-Af4 LIC function. Importantly, *Igf2bp3* is not required for steady-state hematopoiesis, in contrast to *HOXA9*, and may represent a more attractive therapeutic target.

In addition, we found that IGF2BP3 targets and modulates the expression of many transcripts within the Ras signaling pathway and its downstream effector pathways. RAS proteins control numerous cellular processes such as proliferation and survival and are amongst the most commonly mutated genes in cancer [73]. Interestingly, while MLL-AF4 leukemia has a paucity of additional mutations, the mutations that are present are found in the RAS signaling pathway [74]. In addition, MEK inhibitors have shown selective activity against MLL-rearranged leukemia cell lines and primary samples [75]. Hence, IGF2BP3 regulates multiple pathways known to be important in MLL-AF4 leukemia.

Here, we determined *Igf2bp3* is required for the efficient initiation of MLL-Af4-driven leukemia and function of LICs. Mechanistically, IGF2BP3 binds to hundreds of transcripts and modulates their expression through posttranscriptional mechanisms including regulation of steady-state mRNA levels and pre-mRNA splicing. We describe a novel positional bias for IGF2BP3 binding in leukemic cells isolated from an *in vivo* model, a notable advance in the field. In summary, IGF2BP3 is an amplifier of leukemogenesis by targeting and regulating the leukemic transcriptome initiated by MLL-AF4, thereby controlling multiple critical downstream effector pathways required for disease initiation and severity. Our findings highlight IGF2BP3 as a necessary regulator of MLL-AF4 leukemia and a potential therapeutic target for this disease.

#### DATA AVAILABILITY

Data have been deposited onto the NCBI Gene Expression Omnibus repository (GSE156115).

#### REFERENCES

- Krivtsov AV, Armstrong SA. MLL translocations, histone modifications and leukaemia stem-cell development. *Nat Rev Cancer*. 2007;7:823–33.
- Rayes A, McMasters RL, O'Brien MM. Lineage switch in MLL-rearranged infant leukemia following CD19-directed therapy. *Pediatr Blood Cancer*. 2016;63:1113–5.
- Pui C-H, Carroll WL, Meshinchi S, Arceci RJ. Biology, risk stratification, and therapy of pediatric acute leukemias: an update. *J Clin Oncol*. 2011;29:551–65.
- Jude CD, Climer L, Xu D, Artinger E, Fisher JK, Ernst P. Unique and independent roles for MLL in adult hematopoietic stem cells and progenitors. *Cell Stem Cell*. 2007;1:324–37.

5. Milne TA, Briggs SD, Brock HW, Martin ME, Gibbs D, Allis CD, et al. MLL targets SET domain methyltransferase activity to Hox gene promoters. *Mol Cell*. 2002;10:1107–17.
6. Nakamura T, Mori T, Tada S, Krajewski W, Rozovskaia T, Wassell R, et al. ALL-1 is a histone methyltransferase that assembles a supercomplex of proteins involved in transcriptional regulation. *Mol Cell*. 2002;10:1119–28.
7. McMahon KA, Hiew SYL, Hadjur S, Veiga-Fernandes H, Menzel U, Price AJ, et al. MLL has a critical role in fetal and adult hematopoietic stem cell self-renewal. *Cell Stem Cell*. 2007;1:338–45.
8. Smith E, Lin C, Shilatfard A. The super elongation complex (SEC) and MLL in development and disease. *Genes Dev*. 2011;25:661–72.
9. Hess JL. MLL: a histone methyltransferase disrupted in leukemia. *Trends Mol Med*. 2004;10:500–7.
10. Marschalek R. Mechanisms of leukemogenesis by MLL fusion proteins. *Br J Haematol*. 2011;152:141–54.
11. Takahashi S, Yokoyama A. The molecular functions of common and atypical MLL fusion protein complexes. *Biochim Biophys Acta*. 2020;1863:194548.
12. Yokoyama A. Transcriptional activation by MLL fusion proteins in leukemogenesis. *Exp Hematol*. 2017;46:21–30.
13. Slany RK. The molecular biology of mixed lineage leukemia. *Haematologica*. 2009;94:984–93.
14. Krivtsov AV, Hoshii T, Armstrong SA. Mixed-lineage leukemia fusions and chromatin in leukemia. *Cold Spring Harb Perspect Med*. 2017;7:a026658.
15. Meyer C, Burmeister T, Gröger D, Tsaur G, Fechina L, Renneville A, et al. The MLL recombinome of acute leukemias in 2017. *Leukemia*. 2018;32:273–84.
16. Krivtsov AV, Feng Z, Lemieux ME, Faber J, Vempati S, Sinha AU, et al. H3K79 methylation profiles define murine and human MLL-AF4 leukemias. *Cancer Cell*. 2008;14:355–68.
17. Somerville TCP, Matheny CJ, Spencer GJ, Iwasaki M, Rinn JL, Witten DM, et al. Hierarchical maintenance of MLL myeloid leukemia stem cells employs a transcriptional program shared with embryonic rather than adult stem cells. *Cell Stem Cell*. 2009;4:129–40.
18. Guenther MG, Lawton LN, Rozovskaia T, Frampton GM, Levine SS, Volkert TL, et al. Aberrant chromatin at genes encoding stem cell regulators in human mixed-lineage leukemia. *Genes Dev*. 2008;22:3403–8.
19. Wallace JA, Kagele DA, Eiring AM, Kim CN, Hu R, Runtsch MC, et al. miR-155 promotes FLT3-ITD-induced myeloproliferative disease through inhibition of the interferon response. *Blood*. 2017;129:3074–86.
20. Elcheva IA, Spiegelman VS. Targeting RNA-binding proteins in acute and chronic leukemia. *Leukemia*. 2021;35:360–76.
21. Park S-M, Gönen M, Vu L, Minuesa G, Tivnan P, Barlowe TS, et al. Musashi2 sustains the mixed-lineage leukemia-driven stem cell regulatory program. *J Clin Invest*. 2015;125:1286–98.
22. Palanichamy JK, Tran TM, Howard JM, Contreras JR, Fernando TR, Sterne-Weiler T, et al. RNA-binding protein IGF2BP3 targeting of oncogenic transcripts promotes hematopoietic progenitor proliferation. *J Clin Invest*. 2016;126:1495–511.
23. Mueller F, Bommer M, Lacher U, Ruhland C, Stagge V, Adler G, et al. KOC is a novel molecular indicator of malignancy. *Br J Cancer*. 2003;88:699–701.
24. Schaeffer DF, Owen DR, Lim HJ, Buczkowski AK, Chung SW, Scudamore CH, et al. Insulin-like growth factor 2 mRNA binding protein 3 (IGF2BP3) overexpression in pancreatic ductal adenocarcinoma correlates with poor survival. *BMC Cancer*. 2010;10:59.
25. Lochhead P, Imamura Y, Morikawa T, Kuchiba A, Yamauchi M, Liao X, et al. Insulin-like growth factor 2 messenger RNA binding protein 3 (IGF2BP3) is a marker of unfavourable prognosis in colorectal cancer. *Eur J Cancer*. 2012;48:3405–13.
26. Stoskus M, Gineikiene E, Valcekiene V, Valatkaite B, Pileckyte R, Griskevicius L. Identification of characteristic IGF2BP3 expression patterns in distinct B-ALL entities. *Blood Cells Mol Dis*. 2011;46:321–6.
27. Chen W, Li Q, Hudson WA, Kumar A, Kirchhof N, Kersey JH. A murine MLL-AF4 knock-in model results in lymphoid and myeloid deregulation and hematologic malignancy. *Blood*. 2006;108:669–77.
28. Metzler M, Forster A, Pannell R, Arends MJ, Daser A, Lobato MN, et al. A conditional model of MLL-AF4 B-cell tumorigenesis using inverter technology. *Oncogene*. 2006;25:3093–103.
29. Bursen A, Schwabe K, Ruster B, Henschler R, Ruthardt M, Dingermann T, et al. The AF4-MLL fusion protein is capable of inducing ALL in mice without requirement of MLL-AF4. *Blood*. 2010;115:3570–9.
30. Tamai H, Miyake K, Takatori M, Miyake N, Yamaguchi H, Dan K, et al. Activated K-Ras protein accelerates human MLL/AF4-induced leukemo-lymphomogenicity in a transgenic mouse model. *Leukemia*. 2011;25:888–91.
31. Montes R, Ayllon V, Gutierrez-Aranda I, Prat I, Hernandez-Lamas MC, Ponce L, et al. Enforced expression of MLL-AF4 fusion in cord blood CD34+ cells enhances the hematopoietic repopulating cell function and clonogenic potential but is not sufficient to initiate leukemia. *Blood*. 2011;117:4746–58.
32. Lin S, Luo Roger T, Ptasinska A, Kerry J, Assi Salam A, Wunderlich M, et al. Instructive role of MLL-fusion proteins revealed by a model of t(4;11) pro-B acute lymphoblastic leukemia. *Cancer Cell*. 2016;30:737–49.
33. Janardhan HP, Milstone ZJ, Shin M, Lawson ND, Kearney JF Jr., Trivedi CM. Hdac3 regulates lymphovenous and lymphatic valve formation. *J Clin Invest*. 2017;127:4193–206.
34. Fernando TR, Contreras JR, Zampini M, Rodriguez-Malave NI, Alberti MO, Angiano J, et al. The lncRNA CAS15 regulates SOX4 expression in RUNX1-rearranged acute leukemia. *Mol Cancer*. 2017;16:126.
35. Kumar A, Hellen J, Tuong Tiffany M, Tran Tasha L, Lin D, Casero MO, et al. Focused CRISPR-Cas9 genetic screening reveals USO1 as a vulnerability in B-cell acute lymphoblastic leukemia. *Scientific Reports* 2021;11. <https://doi.org/10.1038/s41598-021-92448-w>.
36. O'Connell RM, Balazs AB, Rao DS, Kivork C, Yang L, Baltimore D. Lentiviral vector delivery of human interleukin-7 (hIL-7) to human immune system (HIS) mice expands T lymphocyte populations. *PLoS ONE*. 2010;5:e12009.
37. de Boer J, Williams A, Skavdis G, Harker N, Coles M, Tolaini M, et al. Transgenic mice with hematopoietic and lymphoid specific expression of Cre. *Eur J Immunol*. 2003;33:314–25.
38. Heffner CS, Herbert Pratt C, Babiuk RP, Sharma Y, Rockwood SF, Donahue LR, et al. Supporting conditional mouse mutagenesis with a comprehensive cre characterization resource. *Nat Commun*. 2012;3:1218.
39. Joseph C, Quach Julie M, Walkley Carl R, Lane Steven W, Lo Celso C, Purton, et al. Deciphering hematopoietic stem cells in their niches: a critical appraisal of genetic models, lineage tracing, and imaging strategies. *Cell Stem Cell*. 2013;13:520–33.
40. Langmead B, Salzberg SL. Fast gapped-read alignment with Bowtie 2. *Nat Methods*. 2012;9:357–9.
41. Tarailo-Graovac M, Chen N. Using RepeatMasker to identify repetitive elements in genomic sequences. *Curr Protoc Bioinform*. 2009;25:1–4.
42. Love MI, Huber W, Anders S. Moderated estimation of fold change and dispersion for RNA-seq data with DESeq2. *Genome Biol*. 2014;15:550.
43. Strimmer K. fdrtool: a versatile R package for estimating local and tail area-based false discovery rates. *Bioinformatics*. 2008;24:1461–2.
44. Zhou Y, Zhou B, Pache L, Chang M, Khodabakhshi AH, Tanaseichuk O, et al. Metascape provides a biologist-oriented resource for the analysis of systems-level datasets. *Nat Commun*. 2019;10:1523.
45. Mootha VK, Lindgren CM, Eriksson K-F, Subramanian A, Sihag S, Lehar J, et al. PGC-1 $\alpha$ -responsive genes involved in oxidative phosphorylation are coordinately downregulated in human diabetes. *Nat Genet*. 2003;34:267–73.
46. Subramanian A, Tamayo P, Mootha VK, Mukherjee S, Ebert BL, Gillette MA, et al. Gene set enrichment analysis: a knowledge-based approach for interpreting genome-wide expression profiles. *Proc Natl Acad Sci USA*. 2005;102:15545.
47. Xiao Y, Hsiao T-H, Suresh U, Chen H-IH, Wu X, Wolf SE, et al. A novel significance score for gene selection and ranking. *Bioinformatics*. 2014;30:801–7.
48. Katz Y, Wang ET, Airolidi EM, Burge CB. Analysis and design of RNA sequencing experiments for identifying isoform regulation. *Nat Methods*. 2010;7:1009–15.
49. Lovci MT, Ghanem D, Marr H, Arnold J, Gee S, Parra M, et al. Rbfox proteins regulate alternative mRNA splicing through evolutionarily conserved RNA bridges. *Nat Struct Mol Biol*. 2013;20:1434–42.
50. Heinz S, Benner C, Spann N, Bertolino E, Lin YC, Laslo P, et al. Simple combinations of lineage-determining transcription factors prime cis-regulatory elements required for macrophage and B cell identities. *Mol Cell*. 2010;38:576–89.
51. Quinlan AR, Hall IM. BEDTools: a flexible suite of utilities for comparing genomic features. *Bioinformatics*. 2010;26:841–2.
52. Dawson MA, Prinjha RK, Dittmann A, Giotopoulos G, Bantscheff M, Chan W-I, et al. Inhibition of BET recruitment to chromatin as an effective treatment for MLL-fusion leukaemia. *Nature*. 2011;478:529–33.
53. Haferlach T, Kohlmann A, Wiczorek L, Basso G, Kronnie GT, Béné M-C, et al. Clinical utility of microarray-based gene expression profiling in the diagnosis and subclassification of leukemia: report from the International Microarray Innovations in Leukemia Study Group. *J Clin Oncol*. 2010;28:2529–37.
54. Elcheva IA, Wood T, Chiarolanzio K, Chim B, Wong M, Singh V, et al. RNA-binding protein IGF2BP1 maintains leukemia stem cell properties by regulating HOXB4, MYB, and ALDH1A1. *Leukemia*. 2020;34:1354–63.
55. Hardy RR, Hayakawa KB. Cell development pathways. *Annu Rev Immunol*. 2001;19:595–621.
56. Somerville TCP, Cleary ML. Identification and characterization of leukemia stem cells in murine MLL-AF9 acute myeloid leukemia. *Cancer Cell*. 2006;10:257–68.
57. Brien CA, Kreso A, Jamieson CHM. Cancer stem cells and self-renewal. *Clin Cancer Res*. 2010;16:3113.
58. Schneider T, Hung L-H, Aziz M, Wilmen A, Thaum S, Wagner J, et al. Combinatorial recognition of clustered RNA elements by the multidomain RNA-binding protein IMP3. *Nat Commun*. 2019;10:2266.

59. Stadler CR, Vegi N, Mulaw MA, Edmaier KE, Rawat VPS, Dolnik A, et al. The leukemogenicity of Hoxa9 depends on alternative splicing. *Leukemia*. 2014;28:1838–43.
60. Gardner R, Wu D, Cherian S, Fang M, Hanafi LA, Finney O, et al. Acquisition of a CD19-negative myeloid phenotype allows immune escape of MLL-rearranged B-ALL from CD19 CAR-T-cell therapy. *Blood*. 2016;127:2406–10.
61. Haddox CL, Mangaonkar AA, Chen D, Shi M, He R, Oliveira JL, et al. Blinatumomab-induced lineage switch of B-ALL with t(4:11)(q21;q23) KMT2A/AFF1 into an aggressive AML: pre- and post-switch phenotypic, cytogenetic and molecular analysis. *Blood Cancer J*. 2017;7:e607.
62. Magee Jeffrey A, Piskounova E, Morrison Sean J. Cancer stem cells: impact, heterogeneity, and uncertainty. *Cancer Cell*. 2012;21:283–96.
63. Bardini M, Woll PS, Corral L, Luc S, Wittmann L, Ma Z, et al. Clonal variegation and dynamic competition of leukemia-initiating cells in infant acute lymphoblastic leukemia with MLL rearrangement. *Leukemia*. 2015;29:38–50.
64. Xueqing H, Jun Z, Yueqiang J, Xin L, Liya H, Yuanyuan F, et al. IGF2BP3 may contribute to lung tumorigenesis by regulating the alternative splicing of PKM. *Front Bioeng Biotechnol*. 2020;8:679.
65. Dvinge H, Bradley RK. Widespread intron retention diversifies most cancer transcriptomes. *Genome Med*. 2015;7:45.
66. Wang E, Lu SX, Pastore A, Chen X, Imig J, Chun-Wei Lee S, et al. Targeting an RNA-binding protein network in acute myeloid leukemia. *Cancer Cell*. 2019;35:369–84.
67. Akef A, Lee ES, Palazzo AF. Splicing promotes the nuclear export of  $\beta$ -globin mRNA by overcoming nuclear retention elements. *RNA*. 2015;21:1908–20.
68. Akef A, McGraw K, Cappell SD, Larson DR. Ribosome biogenesis is a downstream effector of the oncogenic U2AF1-S34F mutation. *PLoS Biol*. 2020;18:e3000920.
69. Keene JD. RNA regulons: coordination of post-transcriptional events. *Nat Rev Genet*. 2007;8:533–43.
70. Lechman Eric R, Gentner B, Ng Stanley WK, Schoof Erwin M, van Galen P, Kennedy James A, et al. miR-126 regulates distinct self-renewal outcomes in normal and malignant hematopoietic stem cells. *Cancer Cell*. 2016;29:214–28.
71. Faber J, Krivtsov AV, Stubbs MC, Wright R, Davis TN, van den Heuvel-Eibrink M, et al. HOXA9 is required for survival in human MLL-rearranged acute leukemias. *Blood*. 2009;113:2375–85.
72. He M, Chen P, Arnovitz S, Li Y, Huang H, Neilly MB, et al. Two isoforms of HOXA9 function differently but work synergistically in human MLL-rearranged leukemia. *Blood Cells Mol Dis*. 2012;49:102–6.
73. Downward J. Targeting RAS signalling pathways in cancer therapy. *Nat Rev Cancer*. 2003;3:11–22.
74. Andersson AK, Ma J, Wang J, Chen X, Gedman AL, Dang J, et al. The landscape of somatic mutations in infant MLL-rearranged acute lymphoblastic leukemias. *Nat Genet*. 2015;47:330.
75. Lavallée V-P, Baccelli I, Krosli J, Wilhelm B, Barabé F, Gendron P, et al. The transcriptomic landscape and directed chemical interrogation of MLL-rearranged acute myeloid leukemias. *Nat Genet*. 2015;47:1030–7.

## ACKNOWLEDGEMENTS

This work was supported by the Tumor Cell Biology Training Grant NIH T32 CA009056 (TMT), Tumor Immunology Training Grant NIH T32 CA009120 (TLL), NIH/NIGMS R35 GM130361 (JRS), NIH/NCI R01 CA166450 (DSR), NIH/NCI R21 CA197441 (DSR), American Society of Hematology Bridge Grant (DSR), UCLA Jonsson Comprehensive Cancer Center Seed Grant (DSR), and STOPCancer/Barbara and Gary Luboff Mitzvah Fund Seed Grant (DSR). Flow cytometry was performed in the Eli and Edythe Broad Center of Regenerative Medicine and Stem Cell Research UCLA Flow Cytometry Core Resource and the UCLA JCCC/CFAR Flow Cytometry Core Facility that is supported by

NIH AI-28697, P30CA016042, the JCCC, the UCLA AIDS Institute, and the David Geffen School of Medicine at UCLA. The authors acknowledge the support of the Chao Family Comprehensive Cancer Center Transgenic Mouse Facility (TMF) Shared Resource, supported by the National Cancer Institute of the National Institutes of Health under award number P30CA062203. The content is solely the responsibility of the authors and does not necessarily represent the official views of the National Institutes of Health. The authors would like to thank Jon Neumann (TMF), Michael O. Alberti, and Jorge Contreras for their expertise and helpful discussions.

## AUTHOR CONTRIBUTIONS

TMT, JSB, NN, JP, JMD, TLL, JKP, AKJ, MP, and JK performed experiments. TMT, JP, and SK analyzed results and made the figures. OS provided experimental resource. TMT and DSR designed the research and wrote the paper. TMT, JSB, NN, JP, TLL, JKP, OS, JK, JRS, and DSR reviewed and edited the paper.

## COMPETING INTERESTS

The authors declare no competing interests.

## ETHICS APPROVAL AND CONSENT TO PARTICIPATE

All mouse experimental procedures were conducted with the approval of the UCLA Chancellor's Animal Research Committee.

## ADDITIONAL INFORMATION

**Supplementary information** The online version contains supplementary material available at <https://doi.org/10.1038/s41375-021-01346-7>.

**Correspondence** and requests for materials should be addressed to D.S.R.

**Reprints and permission information** is available at <http://www.nature.com/reprints>

**Publisher's note** Springer Nature remains neutral with regard to jurisdictional claims in published maps and institutional affiliations.



**Open Access** This article is licensed under a Creative Commons Attribution 4.0 International License, which permits use, sharing, adaptation, distribution and reproduction in any medium or format, as long as you give appropriate credit to the original author(s) and the source, provide a link to the Creative Commons license, and indicate if changes were made. The images or other third party material in this article are included in the article's Creative Commons license, unless indicated otherwise in a credit line to the material. If material is not included in the article's Creative Commons license and your intended use is not permitted by statutory regulation or exceeds the permitted use, you will need to obtain permission directly from the copyright holder. To view a copy of this license, visit <http://creativecommons.org/licenses/by/4.0/>.

© The Author(s) 2021

APPENDIX II:

“Focused CRISPR-Cas9 genetic screening reveals USO1 as a vulnerability in B-cell acute lymphoblastic leukemia” (reprint)



OPEN

# Focused CRISPR-Cas9 genetic screening reveals *USO1* as a vulnerability in B-cell acute lymphoblastic leukemia

Amit Kumar Jaiswal<sup>1</sup>, Hellen Truong<sup>1</sup>, Tiffany M. Tran<sup>1,2</sup>, Tasha L. Lin<sup>3</sup>, David Casero<sup>4</sup>, Michael O. Alberti<sup>5</sup> & Dinesh S. Rao<sup>1,6,7</sup>✉

Post-transcriptional gene regulation, including that by RNA binding proteins (RBPs), has recently been described as an important mechanism in cancer. We had previously identified a set of RBPs that were highly dysregulated in B-cell acute lymphoblastic leukemia (B-ALL) with *MLL* translocations, which carry a poor prognosis. Here, we sought to functionally characterize these dysregulated RBP genes by performing a focused CRISPR dropout screen in B-ALL cell lines, finding dependencies on several genes including *EIF3E*, *EPRS* and *USO1*. Validating our findings, CRISPR/Cas9-mediated disruption of *USO1* in *MLL*-translocated B-ALL cells reduced cell growth, promoted cell death, and altered the cell cycle. Transcriptomic analysis of *USO1*-deficient cells revealed alterations in pathways related to mTOR signaling, RNA metabolism, and targets of MYC. In addition, *USO1*-regulated genes from these experimental samples were significantly and concordantly correlated with *USO1* expression in primary samples collected from B-ALL patients. Lastly, we found that loss of *Uso1* inhibited colony formation of *MLL*-transformed in primary bone marrow cells from *Cas9-EGFP* mice. Together, our findings demonstrate an approach to performing focused sub-genomic CRISPR screens and highlight a putative RBP vulnerability in *MLL*-translocated B-ALL, thus identifying potential therapeutic targets in this disease.

B-ALL is the most common type of leukemia in the pediatric population, and is characterized by a number of recurrent chromosomal rearrangements<sup>1–4</sup>. Among these, the t(4;11) *MLL-AF4* (*KMT2A-AFF1*) translocation gives rise to a highly aggressive form of B-ALL<sup>5,6</sup>. Patients with *MLL*-rearranged B-ALL have a dismal prognosis, with 5-year event-free survival rates hovering at 33.6% for infants<sup>7</sup> and 50% for older children and adults<sup>8</sup>. Most of these patients are resistant to conventional treatment with chemotherapy and steroids<sup>9</sup>, with bone marrow transplantation being the only curative therapeutic alternative<sup>10</sup>. Although recent developments such as CAR-T therapy<sup>11</sup> and anti-CD19 based therapy such as Blinatumomab<sup>12</sup> have raised hope for such patients<sup>13</sup>, antigen escape and lineage infidelity in *MLL*-translocated leukemia have proved problematic<sup>14</sup>. Therefore, there is an urgent need to better characterize potential therapeutic targets with high specificity.

The *MLL-AF4* translocation engenders a unique transcriptional profile, as the fusion protein juxtaposes a histone methyltransferase (*MLL*, also known as *KMT2A*) with a protein that is involved in transcriptional regulation (*AF4*, or *AFF1*). Recently our lab carried out a study examining the expression of RBPs in B-ALL<sup>15</sup>, including both known and predicted RBPs<sup>16</sup>. In our analysis, we identified 36 RBPs that are highly upregulated in *MLL-AF4* translocated B-ALL<sup>15</sup>. To study the importance of these genes in B-ALL, we implemented the powerful gene editing technique, CRISPR/Cas9, to perform a rapid and medium-throughput assessment of gene function. Genome wide CRISPR/Cas9 screens on AML cell lines have identified multiple gene targets critical for cell proliferation and survival<sup>17</sup>, but similar studies have not been performed in *MLL-AF4* translocated B-ALL.

<sup>1</sup>Department of Pathology and Laboratory Medicine, David Geffen School of Medicine At UCLA, Los Angeles, CA 90095, USA. <sup>2</sup>Molecular, Cellular and Integrative Physiology Graduate Program, UCLA, Los Angeles, USA. <sup>3</sup>Department of Internal Medicine, Division of Hematology/Oncology, UCLA, Los Angeles, USA. <sup>4</sup>F. Widjaja Foundation Inflammatory Bowel and Immunobiology Research Institute, Cedars Sinai Medical Center, Los Angeles, CA 90048, USA. <sup>5</sup>Department of Pathology, Washington University, St. Louis, USA. <sup>6</sup>Jonsson Comprehensive Cancer Center, UCLA, Los Angeles, USA. <sup>7</sup>Broad Stem Cell Research Center, UCLA, Los Angeles, USA. ✉email: drao@mednet.ucla.edu

In the present study, we performed a sub-genomic CRISPR/Cas9 dropout screen using 36 highly upregulated RBPs in primary human B-ALL and identified several novel vulnerabilities that included three putative RBPs. Of these, *USO1*, a putative RBP and a known regulator of vesicular transport, was identified as a *MLL-AF4* target gene. CRISPR/Cas9-mediated disruption of *USO1* significantly altered cell growth and the cell cycle in B-ALL cell lines; as well as inhibited the colony forming potential of *MLL*-transformed primary murine bone marrow cells. *USO1* depletion regulated the expression of genes related to mTOR signaling, metabolism of RNA, and MYC targets. Together, our studies provide a comprehensive rubric to functionally evaluate putative targets identified from expression profiling, and the identification of a novel potential target in *MLL*-rearranged leukemia.

## Results

**CRISPR/Cas9 screen identifies potential vulnerabilities in *MLL-AF4* leukemic cell growth.** Previously, we identified 36 putative RBPs that were significantly dysregulated in primary human *MLL*-rearranged B-ALL<sup>15</sup>. To directly query the functional relevance of RBP dysregulation in *MLL*-rearranged B-ALL, we performed a sub-genomic CRISPR screen (Fig. 1A). The library consisted of sgRNAs targeting 36 RBP genes, 12 “positive control” genes, representing known vulnerabilities in *MLL*-translocated leukemia<sup>17</sup>, and 28 non-targeting (NT) sgRNAs. The screen was designed using a two-vector lentiviral system. First, B-ALL cells with and without *MLL-AF4* translocation (SEM and NALM6, respectively) were stably transduced with a *Cas9-P2A-EGFP* transgene, followed by FACS sorting of the transduced cells based on GFP positivity. Next, *Cas9-GFP*<sup>+</sup> SEM and NALM6 cells were transduced at a MOI of < 0.3 with the pooled sgRNA lentiviral library, comprised of 268 unique sgRNAs. Cells were subsequently FACS sorted 48 h following transduction for GFP and tRF double positivity (Fig. 1B).  $2 \times 10^6$  cells were sorted, of which  $10^6$  cells were used to isolate genomic DNA for the reference (REF) libraries and the remainder were cultured to maintain 3700× coverage until collection of genomic DNA for the depletion (DEP) libraries following 28 days in culture. Experimental replicates of REF and DEP libraries showed a high degree of concordance in abundance of both individual sgRNAs and for total sgRNAs per gene (Supplementary Fig. 1D & 1E). In addition, the SEM and NALM6 REF libraries showed overall similar rates of individual gRNA incorporation, as measured by the abundance of each gRNA in each of the cell lines and biological replicates (Supplementary Fig. 1F). As expected, a majority of “positive control” genes, including *BCL2*, *COA5*, *CDK6*, and *MYC*, were significantly downregulated in the DEP libraries in both NALM6 and SEM cells. This is not surprising as many of these are known oncogenic genes, particularly in B-ALL. Non-targeting or “negative control” sgRNAs were consistently unchanged between the REF and DEP libraries (Fig. 1C, D). Comparing the results across cell lines, we found that sgRNAs targeting three genes, *USO1*, *EIF3E* and *EPRS* were significantly depleted in SEM cells ( $p < 0.001$ ), when compared to NALM6 cells (Fig. 1E). Interestingly, sgRNA dropout in general was more readily observed in SEM cells than in NALM6 cells, potentially due to the fact that these genes were selected based on high expression in patient B-ALL samples with *MLL-AF4* translocation. Of these three genes, *USO1* had previously been detected in a genome-wide CRISPR screen as a vulnerability in MV-4-11 cells, which also harbor the *MLL-AF4* fusion gene<sup>17</sup>.

***USO1* is directly regulated by *MLL-AF4*.** *USO1*, *EPRS* and *EIF3E* expression was assessed in, SEM, RS4;11 (another *MLL-AF4* translocated cell line), and NALM6 (Supplementary Fig. 2A & 2B). To query their regulation by the *MLL-AF4* fusion protein, we analyzed their expression following inhibition with I-BET151<sup>18</sup>, a BRD4 BET domain inhibitor, MI-503 menin-MLL1 inhibitor<sup>19</sup> and EPZ5676, a DOT1L inhibitor<sup>20</sup>, all known to inhibit *MLL*-dependent gene expression regulation. With increasing doses of I-BET151, MI-503 and EPZ5676 there was a decrease in the *USO1* mRNA expression level in SEM (Fig. 2A), and RS4;11 cells (Fig. 2B), but not in NALM6 cells (Fig. 2C as well as Supplementary Fig. 2C, 2D & 2E), suggesting that *USO1* expression is *MLL-AF4* dependent. A consistent reduction in *EIF3E* and *EPRS* was not observed in the *MLL* translocated cell lines. We further queried the *MLL* dependence of *USO1* by over-expressing the *MLL-AF4* transgene<sup>21</sup> in murine bone marrow cells. Western Blot and RT-qPCR analysis showed upregulation of MLL1 and *USO1* in *MLL-AF4* transduced cells compared to control cells (Fig. 2D and Supplementary Fig. 2F). Using publicly available data<sup>21</sup>, we found that the *USO1* and *EIF3E* genes demonstrated multiple *MLL-AF4* binding sites within the 5'UTR, the first exon, and the first intron (Fig. 2E and Supplementary Fig. 2G). In contrast, the *EPRS* gene did not show strong *MLL-AF4* binding sites (Supplementary Fig. 2H). *EIF3e* and *EPRS* were previously reported to be “common essential genes”, per the depmap portal<sup>22</sup>, whereas *USO1* was not such a gene, suggesting its potential utility as a novel clinical target. To confirm our findings of *USO1* dependence on *MLL-AF4*, we designed chromatin immunoprecipitation (ChIP) experiments, designing primers for the regulatory regions of *USO1* including the 5' UTR within the first exon. We found significant enrichment of the *USO1* regulatory regions in both the MLL1 and AF4 pull-downs (Fig. 2F). Treatment of the cells with I-BET151 inhibited the association of both MLL1 and AF4 with the promoter region of *USO1* (Fig. 2G). Together, these findings indicate that *USO1* is a direct target of the *MLL-AF4* transcriptional program.

***USO1* depletion alters B-ALL cell proliferation, survival and cell cycle.** *USO1* expression is upregulated in several types of cancer including B-ALL with *MLL-AF4* translocations<sup>23–25</sup>. To characterize the functional role of *USO1* in B-ALL suggested by our CRISPR screen, we utilized the previously mentioned two-vector lentivirus system to transduce SEM cells with three different lentiviral constructs containing sgRNAs that target different regions of the *USO1* gene (Fig. 3A, B). We found that two sgRNAs (sg2 and sg3) caused a significant downregulation of *USO1* protein and mRNA expression by approximately 80% in SEM cells (Fig. 3C, D). Cas9-mediated frameshift mutation in *USO1* was confirmed using TIDE assay<sup>26</sup> (Supplementary Fig. 3A). The lack of complete ablation was a reproducible finding in all cell lines we tested, as multiple single-cell cloning experiments failed to produce cells with complete knockout and multiple bulk cultures experiments showed

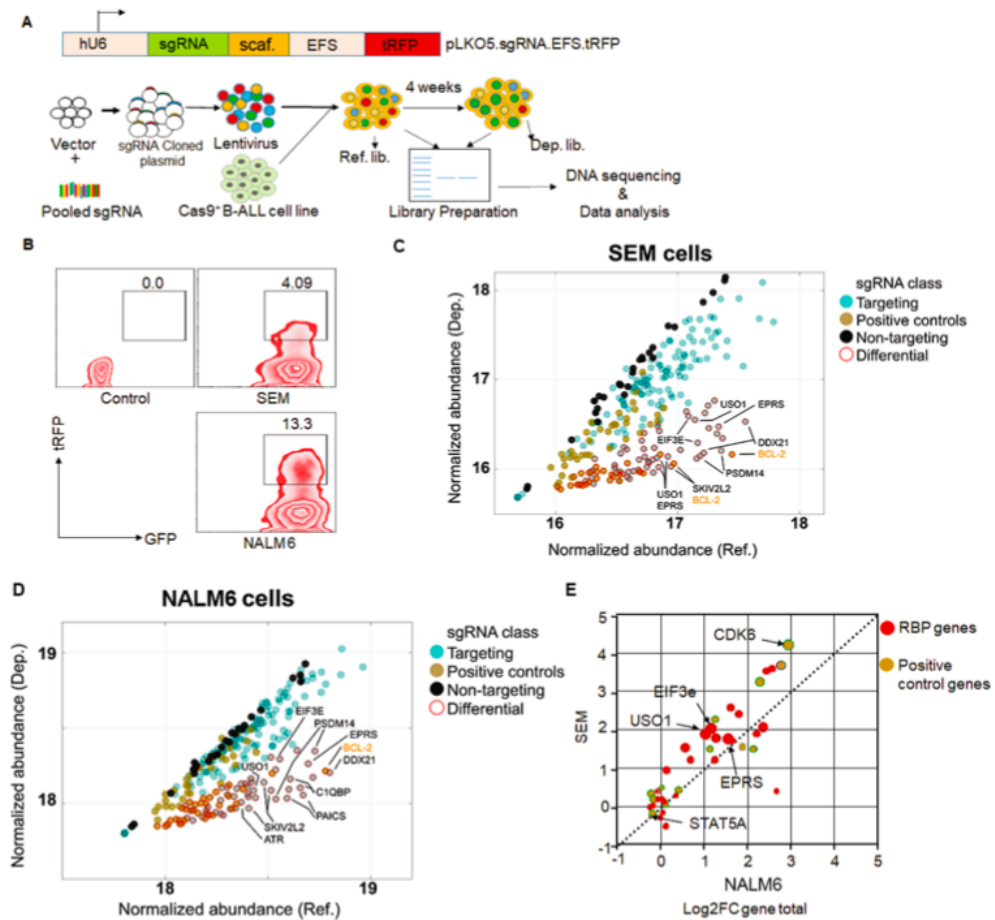


**Figure 1.** Sub-genomic CRISPR screen identifies functionally important genes in *MLL-AF4*-translocated B-ALL. (A) Schematic of sub-genomic CRISPR screen. (B) FACS contour plots reflecting sorting strategy based on high expression of Cas9 (GFP) and pooled guide RNA library (tRFP) in B-ALL cell lines. (C, D) Variance-stabilized normalized abundance for individual sgRNAs in Reference (Ref; x-axis) and Depletion (Dep; y-axis) libraries in SEM (C) and NALM6 (D) cell lines. Dots are colored by sgRNA class (dark yellow: positive controls; black: non-targeting with negative controls; teal: targeting sgRNAs). Dots highlighted with a red border were classified as differentially abundant (Log<sub>2</sub> fold change [Log<sub>2</sub>FC] > 1, Wald adjusted p value < 0.001). Genes with three or more differential sgRNAs are highlighted in the inset and colored by class. (E) Differential expression of sgRNAs aggregated by gene (Log<sub>2</sub>FC gene total), in NALM6 (x-axis) vs SEM (y-axis) cell lines. Dots in the upper left represent genes with a higher fold-change in SEM cells, while those on the lower right represent genes with a higher fold-change in NALM6 cells. Dots are colored by sgRNA class and sized according to the number of individual sgRNAs that showed significant differential representation in the Dep libraries.

retained partial expression of <25%. Nonetheless, we observed that bulk *USO1*-depleted SEM cells from sg2 and sg3 showed reduced proliferation by MTS assay (Fig. 3E). Since sg3 showed near-total ablation of *USO1* protein expression, we later used sg3 to target *USO1* in RS4;11 cells (Supplementary Fig. 3B & 3C), finding downregulation, but not complete depletion, of *USO1* protein. Propidium Iodide (PI) based cell cycle analysis on *USO1*-depleted cells showed an increased percentage of cells in the G<sub>0</sub>/G<sub>1</sub> stage, suggesting cell cycle arrest, and more cells in Sub-G<sub>0</sub>/G<sub>1</sub>, suggesting increased apoptosis (Fig. 3F, G). Increased cell death was also observed in the *USO1*-depleted cells by Annexin V staining (Fig. 3H, I). Interestingly, *USO1*-depleted cells treated with I-BET151 also showed increased cell cycle arrest and apoptosis (Supplementary Fig. 3D–3G), suggesting an additive effect with this inhibitor of BRD4. To confirm our findings in an orthogonal system, we introduced siRNAs targeting *USO1* using nucleofection. In these short-term assays, we found that there was partial reduction of *USO1* mRNA, as expected with siRNA-mediated knockdown (Supplementary Fig. 4A) and increased Annexin V staining (Supplementary Fig. 4B, C). There were also increased cells in Sub-G<sub>0</sub>/G<sub>1</sub> and a modest reduction in cell proliferation as measured by the MTS assay (Supplementary Fig. 4E, F). Together, these observations confirm the importance of *USO1* in regulation of cell cycle and survival of B-ALL cells.

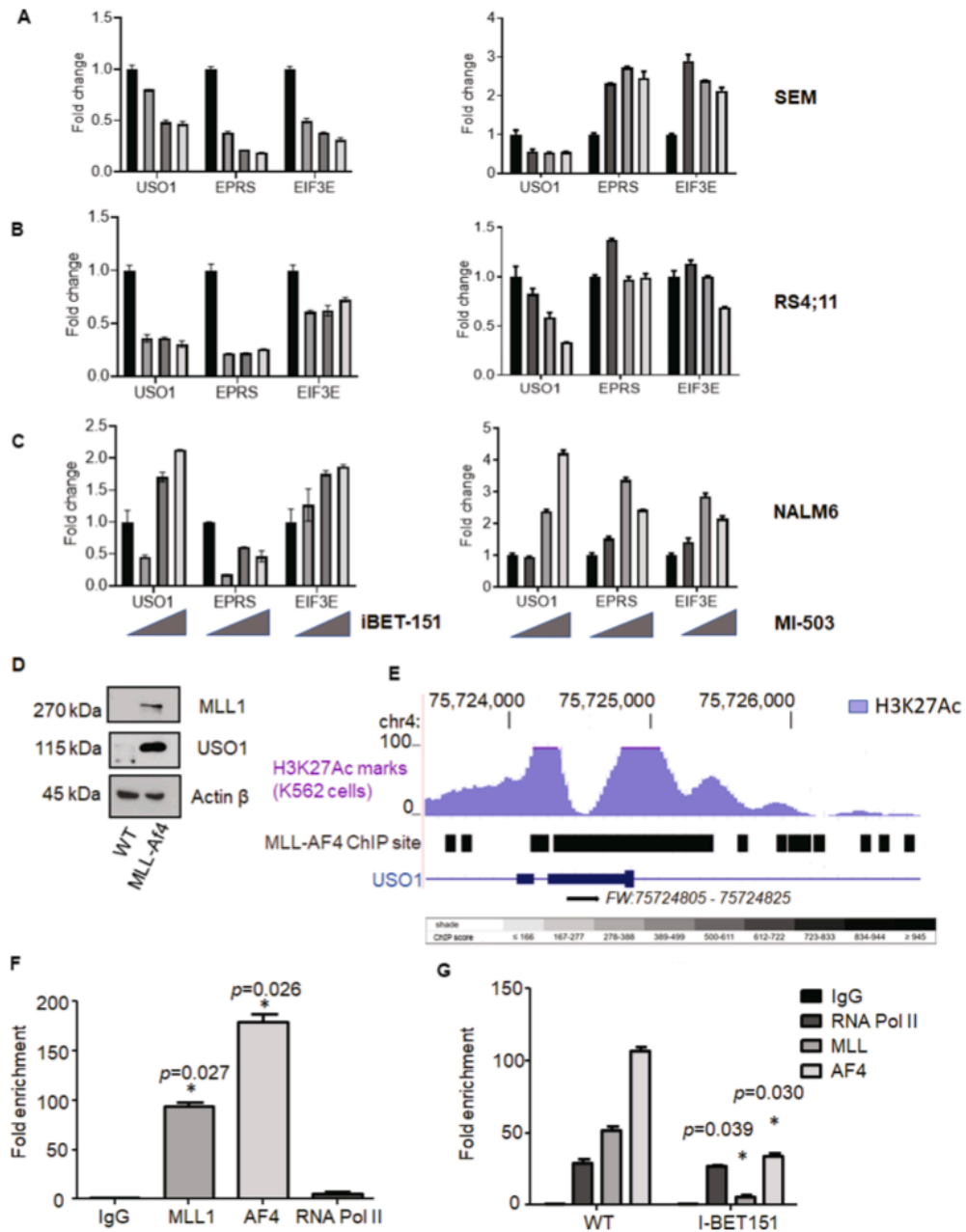


**Figure 2.** Dependence of RBP gene expression on MLL-AF4 translocation. (A–C) Effect of I-BET 151 and MI-503 treatment on mRNA expression levels of *USO1*, *EPRS* and *EIF3E*, measured by RT-qPCR, in SEM (A), RS4;11 (B), and NALM6 (C). The cells were treated with increasing concentrations of I-BET151 (DMSO only, 0.5, 1 and 2 μM) or with increasing concentrations of the menin inhibitor, MI-503 (DMSO only, 0.12, 0.25, and 0.5 μM). RT-qPCR was performed with an optimized set of primers, normalized to 18S, and then represented as fold-change from vehicle-treated control. D. Western blot analysis of murine bone marrow cells with and without transduction with MLL-Af4 (WT versus MLL-Af4), for MLL1 (top), USO1 (middle) and β-actin (lower). (E) UCSC genome browser shot of the *USO1* locus showing the MLL-AF4 ChIP site(s), as identified from the ChIP-Seq data from Lin et al.<sup>21</sup>, in a gene expression regulatory region; Courtesy: UCSC Genome Browser. Shown are the H3K27Ac track in hematopoietic K562 cells (Blue), and MLL-AF4 binding sites represented as a grayscale score, with black indicating the highest score/highest number of reads from the dataset. (F) Chromatin immunoprecipitation with indicated antibodies (MLL1, AF4, and RNA Pol II), followed by qPCR (ChIP-qPCR) analysis for quantitation of bound *USO1* promoter/regulatory region to MLL1 and AF4 pulldown samples. Shown is the fold-enrichment for qPCR of the *USO1* regulatory site over background (t test; \* $P < 0.05$ ) (G) SEM cells treated with 1 μM of I-BET151 for 48 h. and subjected to ChIP qPCR with MLL1 and AF4 antibodies as in (F) (t test; \* $P < 0.05$ ).



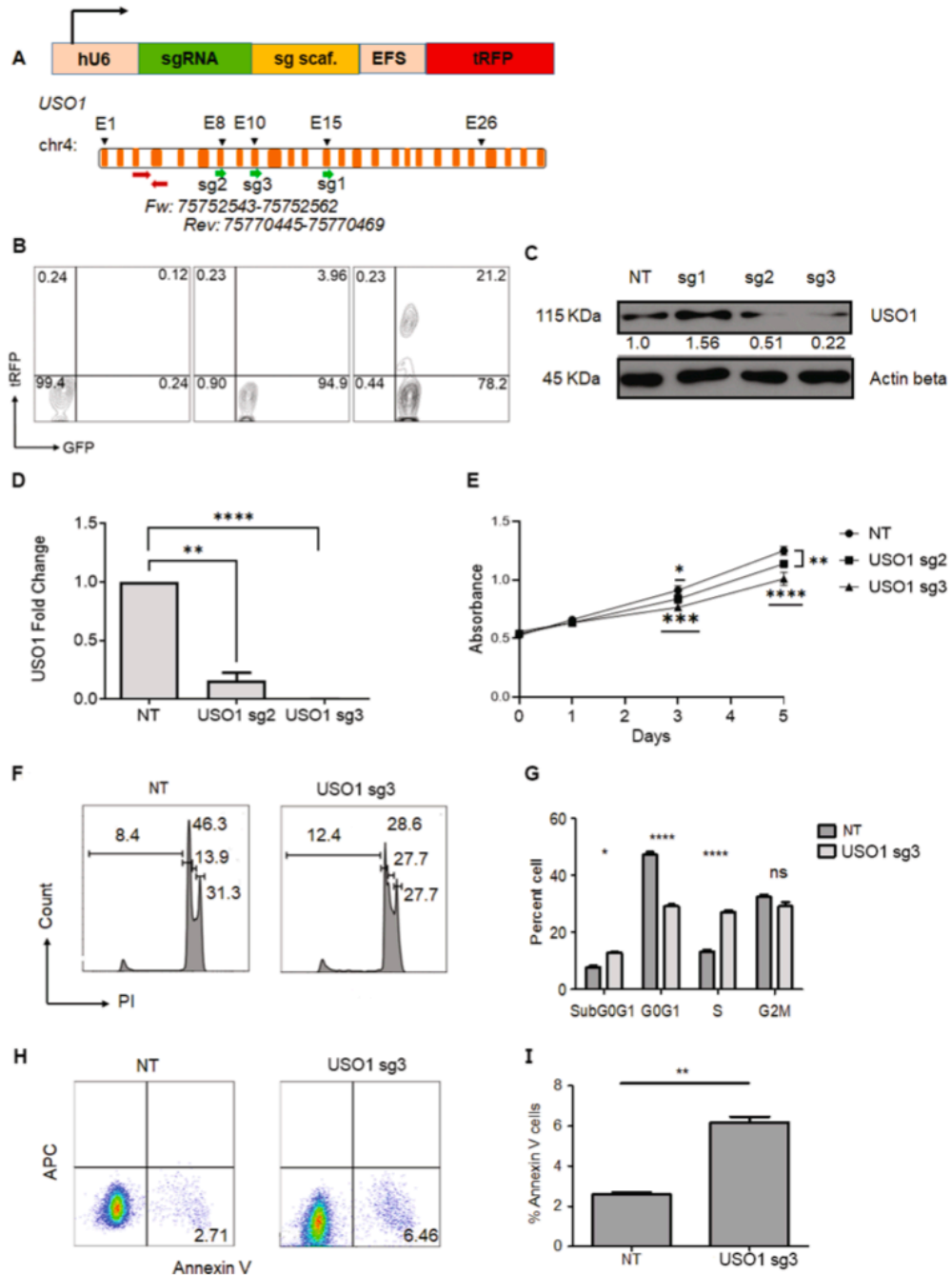


**Figure 3.** Depletion of *USO1* leads to decreased cell growth, cell cycle arrest and increased apoptosis. (A) Schematic representation of the pLKO5.sgRNA.EFS.tRFP lentiviral vector. Abbreviations, hU6, human U6 promoter; sgRNA, short guide RNA; sg scaf, sgRNA scaffold; tRFP, turbo red fluorescent protein. (B) Sample FACS plots of SEM cells transduced sequentially with Cas9 vector and sgRNA containing vector. Left, non-transduced SEM cells; middle, transduced with pLentiCas9-GFP; right, cells transduced with both pLenti-Cas9-GFP and pLKO5 vector containing *USO1*-targeting sgRNA. (C) Western blot for *USO1* in SEM cells following CRISPR/Cas9-mediated disruption of the *USO1* gene using three different sgRNAs (sg1-3) and NT, non-targeting sgRNAs. (D) RT-qPCR measurement of *USO1* in control (NT) and *USO1* (sg2 & sg3) SEM cells (t test; \*\* $P < 0.01$ ; \*\*\*\* $P < 0.0001$ ). (E) MTS assay to study the cell growth of *USO1*-depleted cells (sg2 & sg3), measured as Absorbance at 490 nm (t test; \*\* $P < 0.01$ ; \*\*\* $P < 0.001$ ). (F, G) Cell cycle analysis using propidium iodide (PI) staining of control cells and *USO1*-depleted cells (F) and quantitation of cells from cell cycle analysis (Two-way Anova with Bonferroni correction; \* $P < 0.05$ ; \*\*\*\* $P < 0.0001$ ). (H, I) FACS plots of Annexin V positivity in control versus *USO1*-depleted cells (H), Quantitation of cells with Annexin V positivity (t test; \*\* $P < 0.01$ ) (I).

**USO1 impacts pathways related to cellular proliferation and RNA homeostasis.** To evaluate the effect of *USO1* depletion on the overall gene expression pattern in B-ALL cells, we performed RNA-Seq on SEM cells that were depleted of *USO1* by CRISPR/Cas9 (three biological replicates per condition). Following differential expression analysis of *USO1*-depleted and control cells, we utilized the Metascape algorithm and Gene set enrichment analysis (GSEA) to assess pathway enrichment<sup>27,28</sup>. We found that significantly downregulated pathways included MTOR, ERB2, and Hallmark Hypoxia, while upregulated terms included Metabolism of RNA and Hallmark MYC targets (Fig. 4A and Supplementary Fig. 5A). Analysis of Gene Ontology -Molecular Function gene sets revealed positive enrichment of several gene sets related to RNA homeostasis in the *USO1*-depleted cells (Supplementary Fig. 5B). Selected examples of up- and down regulated genes ( $\log_2FC > 1.5$  and  $Padj. \text{ value} < 0.01$ ), from the enriched pathway identified by GSEA are highlighted in the Volcano plot for RNA-seq data (Fig. 4B). RT-qPCR was used to confirm these same significantly upregulated (*TFR3*, *MRPS12*, and *PSMD1*) (Fig. 4C) and downregulated genes (*BAP1P2*, *ABCA1* and *BTAFL1*) (Fig. 4D) in *USO1*-depleted SEM cells. This led us to hypothesize that there were alterations in expression and activation of MTOR in *USO1*-depleted cells using western blotting. We observed there was a mild downregulation of p-MTOR (Ser2481) in the *USO1*-depleted cells (Fig. 4E). Hence, it appears that *USO1* regulates several pathways that are known to play a role in cell survival and cell death<sup>29</sup>.

To assess whether the gene expression changes caused by *USO1*-depletion had any clinical relevance, we turned to the Target Phase II Acute lymphoblastic leukemia dataset, accessed via the cBioPortal interface<sup>30,31</sup>. We calculated correlation coefficients between *USO1* and 24,278 genes detected by RNA-seq in 203 samples from 154 patients. Using a cut-off  $q$  value of 0.001, we then overlapped genes up- or down-regulated in *USO1*-depleted with genes that had either a positive or negative correlation coefficient. We found a highly significant overlap between genes that were positively correlated with *USO1* across the B-ALL samples and downregulated in *USO1*-depleted cells (Hypergeometric test;  $p < 0.0001$ ), but not in genes that were upregulated in *USO1*-depleted cells (non-significant  $p$  value) (Fig. 4F, Supplementary 5C & 5D). This suggests that *USO1* regulates gene expression in patient samples of B-ALL. As concrete examples, differentially expressed genes confirmed by RT-qPCR (Fig. 4C, D) showed a direct correlation with *USO1* expression in the ALL dataset from cBioPortal (Supplementary Fig. 6A–6D). These findings strongly suggest that *USO1* plays a role in gene regulation in human B-ALL.

**USO1 inhibits the MLL-AF4-driven leukemogenesis in primary murine bone marrow cells.** Having demonstrated that *USO1* is required for the survival and growth of *MLL-AF4*<sup>+</sup> cells in culture, we wanted to determine if *USO1* was required in an experimentally induced primary cell model of *MLL-AF4*-driven leukemia. Briefly,  $Lin^-$  cells from the bone marrow of *Cas9-EGFP* mice<sup>32</sup> were transduced with *MLL-Af4* retrovirus<sup>33</sup> (Fig. 5A) and selected with G418. We confirmed expression of the *MLL-Af4* transgene, finding overexpression by RT-qPCR and western blot analysis (Fig. 5B). As expected, we observed rapid proliferation and expansion of the  $Lin^- Cas9^{MLL-Af4}$  cells. In order to deplete *Uso1* from these cells, we designed and cloned three *Uso1* murine specific sgRNAs (*msg2* and *msg3*) into our internally designed MSCV.EFs.mCherry retroviral vector. To determine their effectiveness, we sorted  $GFP^+ mCherry^- 70Z/3$  cells transduced with the MSCV retroviruses, briefly expanded them in culture, and then queried *USO1* expression. Western blot and RT-qPCR demonstrated that *msg2* and *msg3* both resulted in significant reduction of *USO1* protein and mRNA expression (Fig. 5C, D). *Uso1*-depleted 70Z/3 cells also had reduced cell growth by MTS assay which correlated with the different levels of *USO1* depletion for *msg2* and *msg3* (Fig. 5E). From these data, the *msg3* retrovirus was selected for transduction of  $Lin^- Cas9^{MLL-Af4}$  cells. After sorting  $GFP^+ mCherry^+$  transduced  $Lin^- Cas9^{MLL-Af4}$  cells (Fig. 5F), *USO1*-depletion was confirmed by western blot, in which protein expression was reduced to 26% (Fig. 5G), and the cells were subsequently used in a colony formation assay. Functionally, *USO1*-depletion resulted in significantly fewer colonies in  $Lin^- Cas9^{MLL-Af4}$  cells compared to NT control cells at 12 days. This change was maintained at several different starting numbers of  $Lin^- Cas9^{MLL-Af4}$  cells (Fig. 5H). Hence, the function of *USO1* is preserved in not only in human B-ALL cell lines but also in primary murine *MLL-Af4* transduced cells.

## Discussion

The molecular mechanism of *MLL-AF4* driven leukemogenesis remains incompletely understood, and this subtype of B-ALL is highly aggressive<sup>5,7</sup>. Although there are several fusion partners for *MLL* in acute leukemia, downstream transcriptional dysregulation is a common feature<sup>15,34,35</sup>. In this study, we sought to understand whether overexpression of putative RBPs, which we identified previously, contributes to the pathogenesis of *MLL-AF4*<sup>+</sup> B-ALL<sup>15</sup>. We performed a focused sub-genomic CRISPR/Cas9 dropout screen to specifically address whether these putative RBPs had a functional role in leukemia cell growth. Indeed, we identified three genes (*EIF3E*, *EPRS*, and *USO1*) that appeared to be required in the *MLL-AF4*<sup>+</sup> cell line, SEM. These genes showed slightly higher rates of dropout in SEM cells than in NALM6 cells. Of these, *USO1* expression showed a dependence on *MLL-AF4*, whereas *EIF3E* and *EPRS* did not show the same dependence and were previously reported to be “common essential genes”, per the depmap portal<sup>22</sup>. Follow-up studies confirmed a role for *USO1*, both in cell lines and in a model of *MLL-AF4* driven leukemia in primary murine bone marrow cells. RNA sequencing revealed that *USO1* regulates numerous pathways, including mTOR, MYC targets, as well as elements of RNA homeostasis.

One of the challenges of genomic-scale CRISPR screens is that genes with a small average effect size on the phenotype of interest can be quite difficult to identify and can frequently be “drowned out” by genes with a larger effect size<sup>36</sup>. As we were particularly interested in the role that RBPs play in B-ALL, and their effect size in cell lines is unknown, we chose to perform a sub-genomic essentiality screen targeting a pre-defined set of RBPs known to be highly expressed in B-ALL. Therefore, under the hypothesis that a significant proportion of the

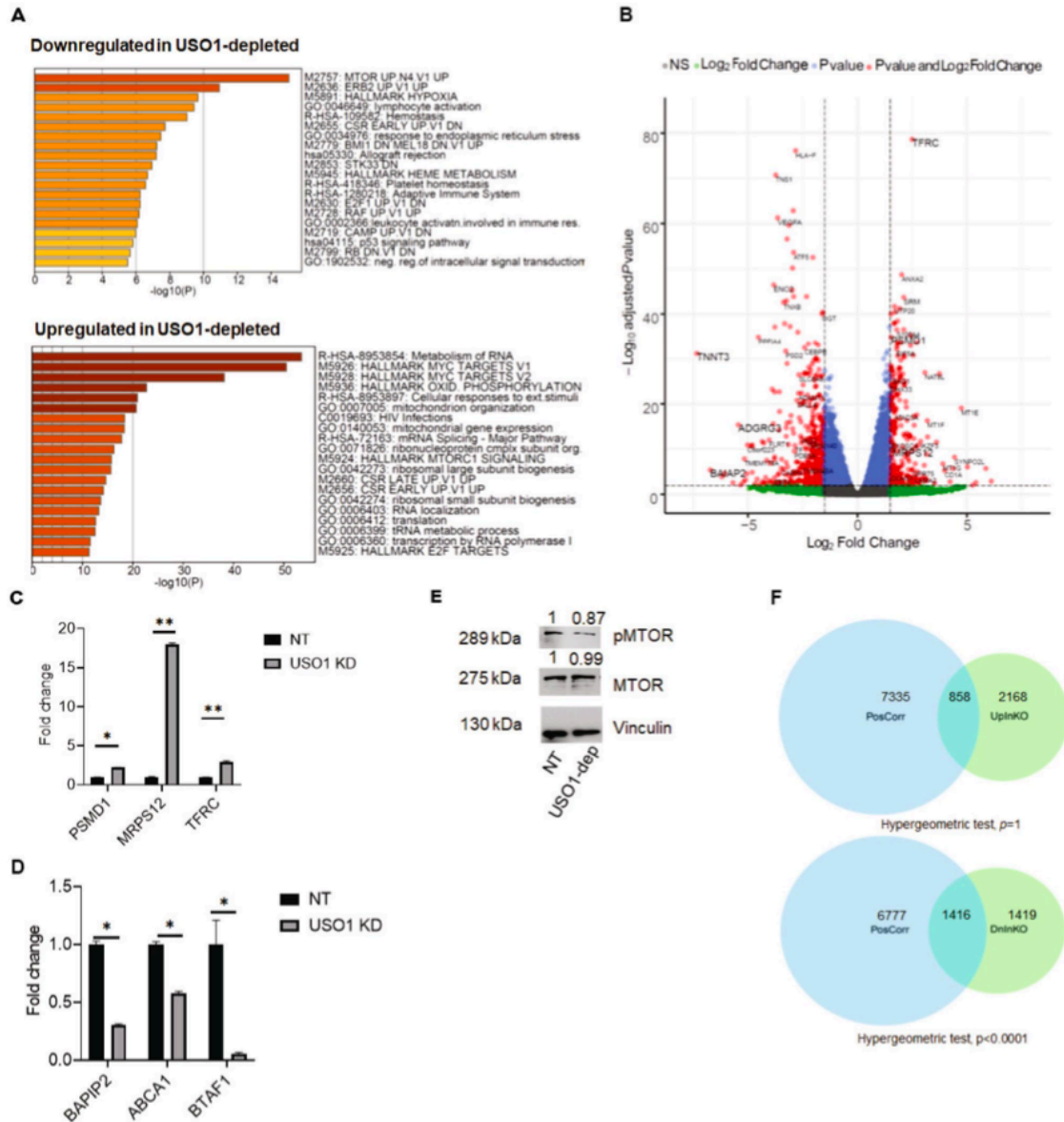


**Figure 4.** USO1 depletion significantly affects gene expression and pathways related to cell survival and proliferation. (A) Enrichment plots generated by the Metascape gene list enrichment analysis webtool on for the RNA-seq data from *USO1*-depleted versus NT control SEM cells. The top and bottom panels show pathways that are downregulated and upregulated in *USO1*-depleted SEM cells, respectively. (B) Volcano plot representing differentially expressed genes ( $Padj < 0.01$  and  $Log_2FC > 1.5$ ) with several examples highlighted from the pathways enriched in (A). (C, D) RT-qPCR validation of differentially expressed genes identified in (B) (t test;  $*P < 0.05$ ;  $**P < 0.01$ ) (E) Western blot showing mildly reduced expression of p-MTOR (Ser2481) expression in *USO1*-depleted cells, compared to NT control, while MTOR remains unchanged. (F) Venn diagrams showing the number of shared genes between *USO1*-positively correlated genes in Target-Phase II ALL dataset with the genes that are significantly upregulated (top) or downregulated (bottom) in *USO1*-depleted SEM cells. A hypergeometric test was utilized to compare the overlaps between the datasets using a genome size of 24,278 genes. Total and shared number of genes are indicated.

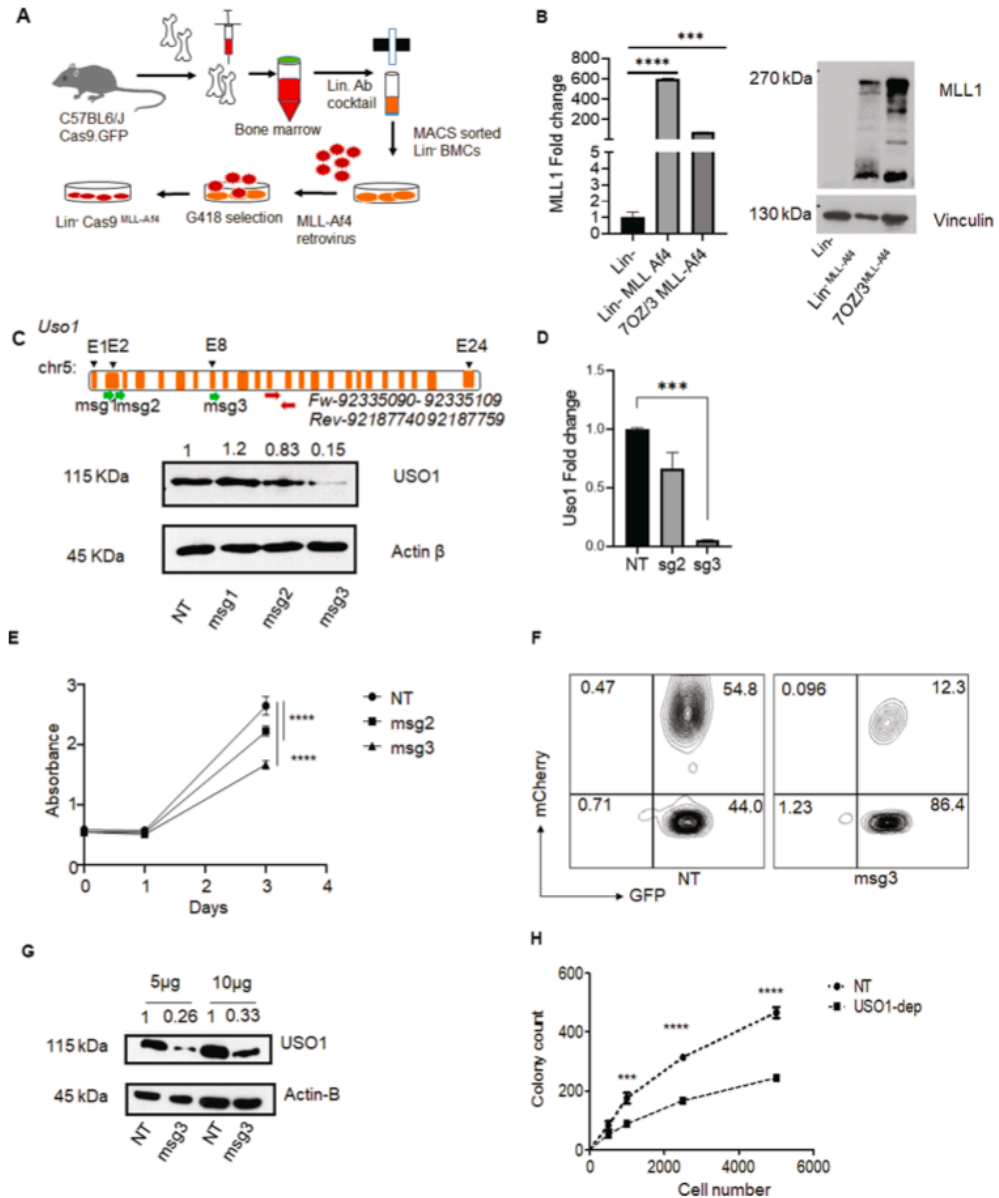


**Figure 5.** USO1 depletion in transformed bone marrow cells shows reduced proliferation and colony forming potential. **(A)** Schematic of an in vitro model system to transform Lin<sup>-</sup> bone marrow cells from *Cas9-egfp* mice using overexpression of *MLL-Af4* transgene in. **(B)** Analysis of overexpression of *MLL-Af4* by RT-qPCR and western blot in retrovirally transduced Lin<sup>-</sup> Cas9<sup>MLL-Af4</sup> cells, Lin<sup>-</sup> Cas9 cells were used as negative control and 70Z/3 cells transduced with *MLL-Af4* were used as positive control. RT qPCR was performed with an optimized set of primers, normalized to L32, and represented as fold-change from an internal control for each experiment. Western Blotting was performed with an antibody to MLL1. Vinculin was used as a high molecular weight loading control. **(C)** Upper panel, schematic of murine *Usol* depletion experiments, showing location of sgRNAs relative to the gene, and RT-qPCR primer location. Bottom panel, western blot analysis of 70Z/3 cells transduced with three different sgRNAs targeting *Usol* (msg1-3) cloned in the MSCV.sgRNA.mCherry.v1 vector. **(D)** RT-qPCR analysis of *Usol* depletion in 70Z/3 cells. **(E)** MTS assay (Absorbance at 490 nm) to measure proliferation in *Usol*-depleted 70Z/3 cells compared to NT control cells. **(F)** FACS plot showing gating schema to sort the Lin<sup>-</sup> Cas9<sup>MLL-Af4</sup> GFP<sup>+</sup> mCherry<sup>+</sup> population following transduction with the *Usol* msg3 vector. **(G)** Western blot was used to confirm the reduction in USO1 expression in sorted Lin<sup>-</sup> Cas9<sup>MLL-Af4</sup> cells. **(H)** Colony formation assay using Lin<sup>-</sup> Cas9<sup>MLL-Af4</sup> cells in methylcellulose assay as described in methods with titration of input cell number (t test, \*\*\* $P < 0.001$ ; \*\*\*\* $P < 0.0001$ ).

sgRNAs would have a negative effect on cell viability, our design included a substantial number of both positive and negative control sgRNAs in order to properly model the null effect distribution and compare the effect size of functional RBPs to that of known essential genes. Secondly, the use of a non-*MLL-AF4* control cell line allowed us to identify those proteins whose expression might be most important in *MLL-AF4* leukemia. Supporting the idea that such specific effects may not be seen in genome scale studies, *USO1* dropout was detected in one prior genome-scale analysis, whereas it was not observed in two other genome scale studies that queried vulnerabilities in *MLL*-translocated leukemia<sup>17,37,38</sup>. Thus, our approach to perform this type of CRISPR/Cas9 screen may help inform the design of future forward genetic screens.

Our group is interested in understanding RNA binding proteins in B-ALL, and we recently described the functional role of *IGF2BP3* in pathologic expansions of cells within the hematopoietic system and its requirement for survival and growth in B-ALL cell lines<sup>15</sup>. Here, we focused on *USO1*, based on its identification in this screen as well as a prior study in MV-4-11 AML cells that had identified *USO1* as a factor required for AML survival<sup>17</sup>. A recent study reported a *KMT2A(MLL)-USO1* fusion gene in a secondary AML, hinting at a further connection between *MLL*-driven leukemia and *USO1*<sup>39</sup>. More generally, *USO1* has been shown to be of functional importance in cancer<sup>23–25</sup>. *USO1* was recently reported to have RNA-binding function in studies utilizing high-throughput biochemical techniques<sup>16,40,41</sup>, despite a canonical role in the regulation of vesicular transport<sup>42,43</sup>. Adding to these prior descriptions of *USO1* function, we validated *USO1* as a *MLL-AF4*-induced gene, and found that it was functionally required in cell lines and in primary bone marrow for *MLL-AF4* dependent phenotypes. This work firmly establishes the significance of this protein in acute leukemia, which was not previously appreciated.

Recent studies in multiple myeloma have shown that *USO1*-deficient cells showed reduced cell proliferation and increased apoptosis via regulation of Erk pathway activity<sup>24</sup>. Transcriptome analysis of *USO1*-depleted SEM cells in our study demonstrated a mixed picture, with the downregulation of certain cancer and cell growth-related pathways, including *mTOR* and *ERB2*, but concurrent downregulation of RNA metabolism and *MYC* targets. Curiously, there was also upregulation of the *mTORC1* hallmark pathway in *USO1*-depleted cells (as opposed to downregulation of *mTOR* generally), perhaps indicating a specific effect on *mTORC2*. Nonetheless, we observed decreased phospho-*mTOR*, which is consistent with the effect seen on cell growth and cell cycle. Additionally, our data suggests that *USO1* is associated with other molecular functions of gene regulation, such as RNA homeostasis. Interestingly, the pathways noted to be deregulated show similarity to those deregulated upon inhibition of the RNA demethylase *FTO*<sup>44</sup>. It is important to note, however, that we have not characterized its function as a RBP. It is tempting to speculate that *USO1* is a bifunctional protein with roles in vesicular transport and RNA binding, perhaps in a manner similar to *YBX1*<sup>45</sup>. *YBX1* appears to bind to and sort microRNAs, specifically, miR-223, into exosomes. By regulating this process, *YBX1* can impact cellular homeostasis. Hence, further work to assess the molecular role of *USO1* as a putative RBP in *MLL-AF4* translocated leukemia is warranted.

Overall, our study successfully queried the functional relevance of a set of genes identified from primary patient samples using expression profiling. Here, we provide a rubric for how to functionally analyze a prioritized list of genes in leukemogenesis, or in other pathogenetic processes. In addition, we establish a role for the putative RBP, *USO1*, in leukemogenesis. Given the broader range of cancer types that show *USO1* dysregulation, our work may have implications beyond those in B-ALL. Furthermore, understanding how non-canonical RBP may participate in leukemogenesis may open up new avenues in developing novel strategies for the diagnosis, prognosis, and treatment of B-ALL.

## Methods

**Cell lines and cell culture.** All the cell lines involved in the study were maintained at 37 °C in a humidified incubator at 5% CO<sub>2</sub>. RS4;11 (ATCC CRL-1873), NALM6 (ATCC CRL-3273) were cultured in RPMI 1640 supplemented with 10% FBS. 70Z/3 (ATCC TIB 158) cells were cultured in RPMI 1640 supplemented with 10% FBS and 0.05 mM 2-mercaptoethanol. SEM cells (DMZ-ACC 546), MV-4-11 (ATCC CRL-9591) were cultured in Iscove's Modified Dulbecco's Medium (IMDM) supplemented with 10% FBS. Mouse bone marrow derived Lineage (Lin<sup>-</sup>) cells were cultured in IMDM media supplemented with 15% FBS, 20 ng/mL mTPO, 20 ng/FLT3 ligand and 50 ng/mL mSCF.

**Sub-genomic CRISPR screen.** A sub-genomic CRISPR/Cas9 screen was designed to target 36 RBP genes and 12 “positive control genes”, and included 28 negative control (or non-targeting) single guide RNAs (sgRNAs). The positive control genes, representing known vulnerabilities in *MLL*-translocated acute leukemia, were selected from top 100 genes dysregulated in Genome wide CRISPR screen in MV-4-11 cells<sup>17</sup>. These genes are expected to “drop out” in a CRISPR screen of *MLL*-translocated leukemia, but it is not known whether they are specific for *MLL*-translocated leukemia. This design was adapted to provide enough non-targeting controls in the context of a sub-genomic screen, where a significant proportion of targeting sgRNAs may be expected to change. Five sgRNAs were designed for each RBP or positive control genes, using sgRNA design tools from Broad Institute<sup>46</sup>. pLKO5.sgRNA.EFS.tRFP is a lentiviral vector, which contains EF-1 alpha binding sequence (EFS) upstream of tRFP, was obtained from Addgene (#57,823)<sup>47</sup>. The 268 pooled sgRNA were then cloned into pLKO5.sgRNA.EFS.tRFP lentiviral vector using standard protocols<sup>17</sup>. Prior to CRISPR/Cas9 screening, B-ALL cell lines with *MLL-AF4* translocation (SEM)<sup>33</sup> and without *MLL-AF4* translocation (NALM6)<sup>48</sup> were stably transduced with pLentiCas9-GFP<sup>49</sup> lentivirus and sorted on GFP positivity, with subsequent confirmation of Cas9 expression (Supplementary Fig. 1A). pLKO5.sgRNA.EFS.tRFP lentiviral pool titers were calculated from SEM and NALM6 cell transduction. For experiments, bulk GFP<sup>+</sup> SEM and NALM6 cells were infected at <0.3 MOI and 2 × 10<sup>6</sup> cells GFP<sup>+</sup> tRFP<sup>+</sup> were sorted by FACS after 48 h of infection (Supplementary Fig. 1B). Genomic DNA (gDNA) isolated from 10<sup>6</sup> cells was used for construction of the Reference (REF) library sample, and

the other  $10^6$  cells were cultured and expanded. Cells were split every five days and  $10^6$  cells were reseeded for culture<sup>50</sup> to maintain a sgRNA representation of 3700X. Following 28 days of culture, cells were harvested and gDNA was isolated for the Depletion (DEP) library sample preparation.

**Library preparation, DNA sequencing, and analysis.** Sequencing libraries were prepared from both the Reference (REF) and Depleted (DEP) genomic DNA (gDNA) samples obtained at days 0 and 28 of CRISPR screen experiment, respectively<sup>17,50</sup>. Libraries were prepared from 200 ng of input DNA, by using Q5 high-fidelity DNA polymerase (#M0492S, NEB) and Illumina adapted primers to amplify the sgRNA target region from the gDNA, as previously described<sup>17</sup> (Supplementary Fig. 1C). The purified PCR product was quantified using Qubit and quality control was done using Bioanalyzer and sequenced on HiSeq 3000 at the Technology Center for Genomic and Bioinformatics at UCLA. Adapter sequences were removed using in-house scripts. Candidate reads (those containing a valid primer sequence and with a minimum length of 20 bp after trimming) were aligned to the sgRNA library using bowtie v0.12.8<sup>51</sup> with a maximum tolerance of one mismatch. Counts tables for both individual sgRNAs and gene-level summaries were compiled from non-ambiguous hits for both the Reference and Depletion libraries in each experiment and for each cell line. Count tables were processed with DESeq2<sup>48</sup> to obtain variance-stabilized normalized abundance and rank sgRNAs and genes based on differential abundance (moderated fold change and adjusted Wald test p value).

**Cell line treatment with transcription inhibitors.** B-ALL cell lines were plated at  $0.5 \times 10^6$  cells/mL density 24 h before treatment, and harvested 48 h after initiating treatment with the chemical inhibitor. I-BET151, a BRD4 inhibitor was reconstituted in DMSO (10 mM), was diluted in complete media and added to the cells at a concentration of 0.5  $\mu$ M, 1.0  $\mu$ M and 2.0  $\mu$ M. MI-503, a menin-MLL inhibitor, was used to treat the cells at 0.12  $\mu$ M, 0.25  $\mu$ M and 0.5  $\mu$ M. EPZ5676, a DOT1L inhibitor, was used to treat cells at a concentration of 0.5  $\mu$ M of EPZ5676.

**Cell proliferation, cell cycle and apoptosis assays.** Cell proliferation assay was performed using standard MTS assay protocol. 5000 cells were plated in 100  $\mu$ L volume of media in a single well of 96-well tissue culture plates. Cells were harvested at different time points of day 0, day1, day 3 and day 5. MTS reagent mix was prepared by adding 100  $\mu$ L of PMS solution (0.21 mg/mL) to 1 ml of MTS reagent (0.33 mg/mL) and 20  $\mu$ L reagent mix was added to each well. The plate was incubated at 37 °C for 2 h and absorbance was taken at 490 nm in a microplate reader.

Cell cycle analysis was performed using propidium iodide (PI). Cells were harvested and washed in PBS and fixed in 70% ethanol overnight at -20 °C. Fixed cells were washed with PBS and centrifuged at 2500 rpm. PI solution (2 mg/10 mL) was diluted in PBS and added with 0.2 mg/mL of DNase free RNase A. Nearly, 300  $\mu$ L of the PI solution was added to each tube and incubated at RT for 2 h. The stained samples were analyzed by flow cytometer.

Annexin V staining was performed to study the apoptosis in the cells using standard protocol. Briefly, cells treated with inhibitors/siRNAs were harvested and washed in PBS before resuspending in binding buffer ( $10^6$  mL). 100  $\mu$ L of cell suspension was stained with 0.5  $\mu$ L of Annexin V antibody conjugated to Pacific blue and incubated at RT for 30 min. After incubation, 300  $\mu$ L of binding buffer was added to the sample and analyzed by flow cytometer.

**siRNA knockdown of cell lines.** siRNA transfection was performed using standard Nucleofection program provided by the manufacturer. SEM cells were Nucleofected using the 4D Nucleofector System (Lonza, Cologne, Germany). Cells were washed with phosphate-buffered saline and then resuspended in nucleofection solution (SF Cell Line 4D-Nucleofector X Kit, Lonza, Cologne, Germany), at a final concentration of  $2 \times 10^6$  cells/100  $\mu$ L reaction. Cells were nucleofected with 30 pmol of control siRNA, USO1 siRNA1, or USO1 siRNA 4, in 100  $\mu$ L cuvettes using program CV-104. Immediately after nucleofection, 500  $\mu$ L of pre-warmed, antibiotic-free media was added to the cuvette and incubated for 10 min at RT. After incubation cells were transferred to a 12 well plate containing 1.5 mL of media. Nucleofected cells were maintained at 37 °C and 5% CO<sub>2</sub> prior to harvesting for analysis.

**RT-qPCR assays.** Previous protocols were adapted for RT-qPCR, based on our prior work<sup>15</sup>. A full list of RT-qPCR primers is presented in Table S2. For normalization, we utilized RT-qPCR primers for 18S (human) and L32 (mouse).

**Western Blotting.** Western Blotting was performed as previously described<sup>15</sup>. The blots were developed and imaged on ECL film or on a Bio-Rad Chemidoc digital imager using Super signal West Pico PLUS chemiluminescent reagent. EPRS (#A303-957A), EIF3E (#A302-984A), USO1 (#A304-513A) antibodies were purchased from Bethyl laboratories. USO1 (13,509-1-AP) antibody to detect mouse USO1 was purchased from Proteintech. MTOR (#2972 s) and Phospho-MTOR (Ser2481) (#2971) antibodies were procured from Cell Signaling Technology. Vinculin (Santa Cruz Biotechnology, # sc-73614) and Anti- $\beta$ -Actin (Sigma Aldrich, #A1978) were used for loading controls.

**Chromatin immunoprecipitation (ChIP).** SEM cells were cultured with and without I-BET151 (Sigma Aldrich, # SML0666) and DMSO for 48 h at 37 °C<sup>52</sup>. ChIP was performed using EZ-Magna ChIP kit (Millipore,

# 17–408) with MLL1 antibody (Bethyl laboratories, #A300-374A) and AF4 antibody (Abcam, #ab31812). The purified DNA was used as input for qPCR and binding was quantitated as previously described<sup>52</sup>.

**Immortalization of Lin<sup>-</sup> bone marrow cells.** All mice used in this study were obtained from Jackson Labs and were genotyped according to JAX protocols and maintained in the UCLA Division of Laboratory Animal Medicine. Bone marrow cells from C57BL6/J *Cas9-EGFP* mice<sup>53</sup> (Jackson Laboratories, # 026,179) were isolated by flushing the bones from the mice and creating a single cell suspension. Cells were incubated with a lineage antibody cocktail and depleted for Lineage<sup>+</sup> cells using MACS technology (Miltenyi Biotech). Lin<sup>-</sup> cells were spin-infected and transduced with *MLL-Af4* retroviral preparation<sup>33</sup>. The MSCV-MLL-flag-Af4 plasmid was the kind gift via MTA by Dr. Michael Thirman (University of Chicago, Department of Medicine). After four rounds of transduction, cells were selected in 400 µg/mL G418 supplemented media for 7 days.

**MSCV sgRNA vectors.** We generated a novel MSCV vector that can overexpress an individual sgRNA in addition to an mCherry reporter. In brief, the MSCV.mU6.sgRNA-EFs.mCherry.v1 retroviral vector was constructed by replacing a 2.1 kb EGFP-PGK.Puro fragment from the pMGP vector with a 2.7 kb sequence containing mU6.BbsI-stuffer-BbsI-scaffold-spacer-EFs.mCherry via BglII/Clal digest. The sgRNA scaffold and EF-1α short (EFs) promoter elements were derived from the pLentiCRISPRv2 vector. The mU6 promoter was designed from the GenBank sequence NC\_000076.6 (nt 79,908,880–79,909,195). A silent mutation was incorporated into the mCherry reporter element to remove an internal BbsI restriction site. The 1.2 kb stuffer sequence was derived from portions of the 1.8 kb firefly luciferase gene. The sgRNA sequences targeting mouse were designed as above and directionally cloned between the mU6 promoter and sgRNA scaffold sequence via BbsI. Detailed methods and vector maps are available upon request.

**Colony forming unit assay.** A colony forming unit assay was performed to study the effect of *USO1*-depletion on the colony forming potential of Lin<sup>-</sup>Cas9<sup>MLL-Af4</sup> cells. The assay was performed using the Methocult colony forming media (STEMCELL Technologies, #M3434)<sup>54</sup>. Briefly, approximately 5,000 Lin<sup>-</sup>Cas9<sup>MLL-Af4</sup> *USO1* depleted cells were mixed in 3.2 ml of overnight thawed Methocult media and plated in two 35 mm dishes along with the NT controls and cultured for 12 days. After 12 days of culture, individual 35 mm dishes were counted for both total number and morphologic subtypes of colonies formed by *USO1* depletion and NT control cells.

**RNA-Seq library preparation and analysis.** Libraries for RNA-Seq were prepared with Nugen Universal plus mRNA-Seq Kit to generate strand-specific RNA-seq libraries. Sequencing was performed on Illumina HiSeq 3000 SR 1 × 50 bp run. Data quality check was done on Illumina SAV. Demultiplexing was performed with Illumina Bcl2fastq2 v 2.19.1.403 program. The STAR ultrafast universal RNA-seq aligner v2.7.0d<sup>55</sup> was used to align the reads to a genome index that included both the genome sequence (GRC38 human primary assembly) and the exon/intron structure of known human gene models (Gencode v29 genome annotation). Alignment files were used to generate strand-specific, gene-level count summaries with STAR's built-in gene counter. Independent filtering was applied as before<sup>56,57</sup>; genes with less than 6 total counts across all samples, count outliers, or low mappability (< 50 bp) were filtered out for downstream analyses. Expression estimates were computed in units of fragments per kilobase of mappable length and million counts (FPKM). Differential expression analyses between *USO1* depletion and non-targeted controls was performed with DESeq2<sup>27</sup> and genes were ranked based on moderated fold change and adjusted Wald test p value. Functional enrichment for selected genes was performed with Metascape<sup>36</sup>.

**Approvals and Compliance.** This study was carried out in compliance with the ARRIVE guidelines. All animal experiments were carried out in accordance with relevant guidelines governing the use of animals in research. In addition, all experiments involving animals were approved by the University of California, Los Angeles, Chancellor's Animal Research Committee (ARC), which was established for compliance with Public Health Service (PHS) guidelines on animal research.

#### Data availability

All sequencing data have been deposited in the Sequence Read Archive (PRJNA658354). All research materials will be made available in accordance with UCLA policy.

Received: 13 December 2020; Accepted: 10 June 2021

Published online: 23 June 2021

#### References

1. Mullighan, C. G. Molecular genetics of B-precursor acute lymphoblastic leukemia. *J. Clin. Invest.* **122**(10), 3407–3415 (2012).
2. Takeuchi, S. *et al.* TEL is one of the targets for deletion on 12p in many cases of childhood B-lineage acute lymphoblastic leukemia. *Leukemia* **11**(8), 1220–1223 (1997).
3. Luong-Gardiol, N. *et al.* Gamma-catenin-dependent signals maintain BCR-ABL1(+) B cell acute lymphoblastic leukemia. *Cancer Cell* **35**(4), 649–663 (2019).
4. Stong, R. C., Korsmeyer, S. J., Parkin, J. L., Arthur, D. C. & Kersey, J. H. Human acute leukemia cell line with the t(4;11) chromosomal rearrangement exhibits B lineage and monocytic characteristics. *Blood* **65**(1), 21–31 (1985).
5. Dreyer, Z. E. *et al.* Analysis of the role of hematopoietic stem-cell transplantation in infants with acute lymphoblastic leukemia in first remission and MLL gene rearrangements: A report from the Children's Oncology Group. *J. Clin. Oncol.* **29**(2), 214–222 (2011).

6. Behm, F. G. *et al.* Rearrangement of the MLL gene confers a poor prognosis in childhood acute lymphoblastic leukemia, regardless of presenting age. *Blood* **87**(7), 2870–2877 (1996).
7. Hilden, J. M. *et al.* Analysis of prognostic factors of acute lymphoblastic leukemia in infants: Report on CCG 1953 from the Children's Oncology Group. *Blood* **108**(2), 441–451 (2006).
8. Moorman, A. V. *et al.* Prognostic effect of chromosomal abnormalities in childhood B-cell precursor acute lymphoblastic leukaemia: Results from the UK Medical Research Council ALL97/99 randomised trial. *Lancet Oncol.* **11**(5), 429–438 (2010).
9. Witkowski, M. T. *et al.* Conserved IKAROS-regulated genes associated with B-progenitor acute lymphoblastic leukemia outcome. *J. Exp. Med.* **214**(3), 773–791 (2017).
10. Miglino, M. *et al.* Allogeneic bone marrow transplantation (BMT) for adults with acute lymphoblastic leukemia (ALL): Predictive role of minimal residual disease monitoring on relapse. *Bone Marrow Transplant.* **30**(9), 579–585 (2002).
11. Prasad, V. Immunotherapy: Tisagenlecleucel—The first approved CAR-T-cell therapy: implications for payers and policy makers. *Nat. Rev. Clin. Oncol.* **15**(1), 11–12 (2018).
12. Gokbuget, N. *et al.* Blinatumomab for minimal residual disease in adults with B-cell precursor acute lymphoblastic leukemia. *Blood* **131**(14), 1522–1531 (2018).
13. Turtle, C. J. *et al.* CD19 CAR-T cells of defined CD4+:CD8+ composition in adult B cell ALL patients. *J. Clin. Invest.* **126**(6), 2123–2138 (2016).
14. Majzner, R. G. & Mackall, C. L. Tumor antigen escape from CAR T-cell therapy. *Cancer Discov.* **8**(10), 1219–1226 (2018).
15. Palanichamy, J. K. *et al.* RNA-binding protein IGF2BP3 targeting of oncogenic transcripts promotes hematopoietic progenitor proliferation. *J. Clin. Invest.* **126**(4), 1495–1511 (2016).
16. Castello, A. *et al.* Comprehensive identification of RNA-binding domains in human cells. *Mol. Cell.* **63**(4), 696–710 (2016).
17. Wallace, J. *et al.* Genome-wide CRISPR-Cas9 screen identifies microRNAs that regulate myeloid leukemia cell growth. *PLoS ONE* **11**(4), e0153689 (2016).
18. Dawson, M. A. *et al.* Inhibition of BET recruitment to chromatin as an effective treatment for MLL-fusion leukaemia. *Nature* **478**(7370), 529–533 (2011).
19. Borkin, D. *et al.* Pharmacologic inhibition of the Menin-MLL interaction blocks progression of MLL leukemia in vivo. *Cancer Cell* **27**(4), 589–602 (2015).
20. Daigle, S. R. *et al.* Potent inhibition of DOT1L as treatment of MLL-fusion leukemia. *Blood* **122**(6), 1017–1025 (2013).
21. Lin, S. *et al.* Instructive role of MLL-fusion proteins revealed by a model of t(4;11) Pro-B acute lymphoblastic leukemia. *Cancer Cell* **30**(5), 737–749 (2016).
22. Tsherniak, A. *et al.* Defining a cancer dependency map. *Cell* **170**(3), 564–76.e16 (2017).
23. Sui, J. *et al.* Lentivirus-mediated silencing of USO1 inhibits cell proliferation and migration of human colon cancer cells. *Med. Oncol.* **32**(8), 218 (2015).
24. Jin, Y. & Dai, Z. USO1 promotes tumor progression via activating Erk pathway in multiple myeloma cells. *Biomed. Pharmacother.* **78**, 264–271 (2016).
25. Howley, B. V., Link, L. A., Grelet, S., El-Sabban, M. & Howe, P. H. A CREB3-regulated ER-Golgi trafficking signature promotes metastatic progression in breast cancer. *Oncogene* **37**(10), 1308–1325 (2018).
26. Sentmanat, M. E., Peters, S. T., Florian, C. P., Connelly, J. P. & Pruett-Miller, S. M. A survey of validation strategies for CRISPR-Cas9 editing. *Sci. Rep.* **8**(1), 888 (2018).
27. Zhou, Y. *et al.* Metascape provides a biologist-oriented resource for the analysis of systems-level datasets. *Nat. Commun.* **10**(1), 1523 (2019).
28. Subramanian, A. *et al.* Gene set enrichment analysis: A knowledge-based approach for interpreting genome-wide expression profiles. *Proc. Natl. Acad. Sci. USA* **102**(43), 15545–15550 (2005).
29. van Riggelen, J., Yetil, A. & Felsher, D. W. MYC as a regulator of ribosome biogenesis and protein synthesis. *Nat. Rev. Cancer.* **10**(4), 301–309 (2010).
30. Cerami, E. *et al.* The cBio cancer genomics portal: An open platform for exploring multidimensional cancer genomics data. *Cancer Discov.* **2**(5), 401–404 (2012).
31. Gao, J. *et al.* Integrative analysis of complex cancer genomics and clinical profiles using the cBioPortal. *Sci. Signal.* **6**(269), 11 (2013).
32. Platt, R. J. *et al.* CRISPR-Cas9 knockin mice for genome editing and cancer modeling. *Cell* **159**(2), 440–455 (2014).
33. Lin, S., Luo, R. T., Shrestha, M., Thirman, M. J. & Mulloy, J. C. The full transforming capacity of MLL-AF4 is interlinked with lymphoid lineage commitment. *Blood* **130**(7), 903–907 (2017).
34. Xia, Z. B. *et al.* The MLL fusion gene, MLL-AF4, regulates cyclin-dependent kinase inhibitor CDKN1b (p27kip1) expression. *Proc. Natl. Acad. Sci. USA* **102**(39), 14028–14033 (2005).
35. Andersson, A. K. *et al.* The landscape of somatic mutations in infant MLL-rearranged acute lymphoblastic leukemias. *Nat. Genet.* **47**(4), 330–337 (2015).
36. Bodapati, S., Daley, T. P., Lin, X., Zou, J. & Qi, L. S. A benchmark of algorithms for the analysis of pooled CRISPR screens. *Genome Biol.* **21**(1), 62 (2020).
37. Tzelepis, K. *et al.* A CRISPR dropout screen identifies genetic vulnerabilities and therapeutic targets in acute myeloid leukemia. *Cell Rep.* **17**(4), 1193–1205 (2016).
38. Erb, M. A. *et al.* Transcription control by the ENL YEATS domain in acute leukaemia. *Nature* **543**(7644), 270–274 (2017).
39. Jin, W. *et al.* A novel KMT2A–USO1 fusion gene-induced de novo secondary acute myeloid leukaemia in a patient initially diagnosed with acute promyelocytic leukaemia. *Br. J. Haematol.* **192**, e32–e36 (2021).
40. Castello, A. *et al.* Insights into RNA biology from an atlas of mammalian mRNA-binding proteins. *Cell* **149**(6), 1393–1406 (2012).
41. Beckmann, B. M. *et al.* The RNA-binding proteomes from yeast to man harbour conserved enigmRBPs. *Nat. Commun.* **6**, 10127 (2015).
42. Nakamura, N., Lowe, M., Levine, T. P., Rabouille, C. & Warren, G. The vesicle docking protein p115 binds GM130, a cis-Golgi matrix protein, in a mitotically regulated manner. *Cell* **89**(3), 445–455 (1997).
43. Allan, B. B., Moyer, B. D. & Balch, W. E. Rab1 recruitment of p115 into a cis-SNARE complex: Programming budding COPII vesicles for fusion. *Science* **289**(5478), 444–448 (2000).
44. Huang, Y. *et al.* Small-molecule targeting of oncogenic FTO demethylase in acute myeloid leukemia. *Cancer Cell* **35**(4), 677–691 (2019).
45. Shurtleff MJ, Temoche-Diaz MM, Karfilis KV, Ri S, and Schekman R. Y-box protein 1 is required to sort microRNAs into exosomes in cells and in a cell-free reaction. *Elife.* **5**, e19276 (2016).
46. Doench, J. G. *et al.* Optimized sgRNA design to maximize activity and minimize off-target effects of CRISPR-Cas9. *Nat. Biotechnol.* **34**(2), 184–191 (2016).
47. Heckl, D. *et al.* Generation of mouse models of myeloid malignancy with combinatorial genetic lesions using CRISPR-Cas9 genome editing. *Nat. Biotechnol.* **32**(9), 941–946 (2014).
48. Benito, J. M. *et al.* MLL-Rearranged acute lymphoblastic leukemias activate BCL-2 through H3K79 methylation and are sensitive to the BCL-2-specific antagonist ABT-199. *Cell Rep.* **13**(12), 2715–2727 (2015).
49. Wang, S. *et al.* Enhancement of LIN28B-induced hematopoietic reprogramming by IGF2BP3. *Genes Dev.* **33**(15–16), 1048–1068 (2019).
50. Doench, J. G. Am I ready for CRISPR? A user's guide to genetic screens. *Nat. Rev. Genet.* **19**(2), 67–80 (2018).



51. Langmead B. Aligning short sequencing reads with Bowtie. *Curr. Protoc. Bioinform.* 2010; Chapter 11:Unit 11.7.
52. Ptasinska, A. *et al.* Identification of a dynamic core transcriptional network in t(8;21) AML that regulates differentiation block and self-renewal. *Cell Rep.* **8**(6), 1974–1988 (2014).
53. LaFleur, M. W. *et al.* A CRISPR-Cas9 delivery system for in vivo screening of genes in the immune system. *Nat. Commun.* **10**(1), 1668 (2019).
54. McKenzie, M. D. *et al.* Interconversion between tumorigenic and differentiated states in acute myeloid leukemia. *Cell Stem Cell* **25**(2), 258–272 (2019).
55. Dobin, A. *et al.* STAR: Ultrafast universal RNA-seq aligner. *Bioinformatics* **29**(1), 15–21 (2013).
56. Love, M. I., Huber, W. & Anders, S. Moderated estimation of fold change and dispersion for RNA-seq data with DESeq2. *Genome Biol.* **15**(12), 550 (2014).
57. Casero, D. *et al.* Long non-coding RNA profiling of human lymphoid progenitor cells reveals transcriptional divergence of B cell and T cell lineages. *Nat. Immunol.* **16**(12), 1282–1291 (2015).

## Acknowledgements

We thank Drs. Jayanth Palanichamy and Jennifer King for helpful discussions and technical assistance with experiments performed herein. This work was supported by the NIH/NCI R01CA166450 (D.S.R.), NIH/NCI R03CA251845 (D.S.R.), NIH/NIAID R21AI132869 (D.S.R.), Tumor Cell Biology Training Grant T32 CA009056 (T.M.T.), Tumor Immunology Training Grant T32CA009120 (T.L.L.), and a grant from the Margaret E. Early Trust (D.S.R.). Flow cytometry was performed in the Eli and Edythe Broad Center of Regenerative Medicine and Stem Cell Research UCLA Flow Cytometry Core Resource and the UCLA JCCC/CFAR Flow Cytometry Core Facility that is supported by NIH AI-28697, P30CA016042, the JCCC, the UCLA AIDS Institute, and the David Geffen School of Medicine at UCLA. The results published here are in part based upon data generated by the Therapeutically Applicable Research to Generate Effective Treatments (<https://ocg.cancer.gov/programs/target>) initiative, phs000218. The data used for this analysis are available at <https://portal.gdc.cancer.gov/projects>.

## Author contributions

A.K.J.: Experimental Design, Experimentation, Data Analysis and Interpretation, Manuscript Preparation. H.T., T.L.L.: Experimentation, Data Analysis and Interpretation. T.M.T.: Experimentation, Data Analysis and Interpretation, Manuscript Preparation. D.C.: Data Analysis and Interpretation. M.O.A.: Experimentation. D.S.R.: Experimental Design, Data Analysis and Interpretation, Manuscript Preparation, Funding.

## Competing interests

The authors declare no competing interests.

## Additional information

**Supplementary Information** The online version contains supplementary material available at <https://doi.org/10.1038/s41598-021-92448-w>.

**Correspondence** and requests for materials should be addressed to D.S.R.

**Reprints and permissions information** is available at [www.nature.com/reprints](http://www.nature.com/reprints).

**Publisher's note** Springer Nature remains neutral with regard to jurisdictional claims in published maps and institutional affiliations.



**Open Access** This article is licensed under a Creative Commons Attribution 4.0 International License, which permits use, sharing, adaptation, distribution and reproduction in any medium or format, as long as you give appropriate credit to the original author(s) and the source, provide a link to the Creative Commons licence, and indicate if changes were made. The images or other third party material in this article are included in the article's Creative Commons licence, unless indicated otherwise in a credit line to the material. If material is not included in the article's Creative Commons licence and your intended use is not permitted by statutory regulation or exceeds the permitted use, you will need to obtain permission directly from the copyright holder. To view a copy of this licence, visit <http://creativecommons.org/licenses/by/4.0/>.

© The Author(s) 2021